ICRP ref 4851-1931-9834
17 April 2014

Annals of the ICRP

ICRP PUBLICATION 1XX

Radiological Protection in Ion Beam Radiotherapy

Editor-in-Chief
C.H. CLEMENT

Associate Editor
N. HAMADA

Authors
Y. Yonekura, H. Tsujii, J.W. Hopewell, P. Ortiz López, J.-M. Cosset, H. Paganetti, A. Montelius, D. Schardt, B. Jones, T. Nakamura

PUBLISHED FOR

The International Commission on Radiological Protection

by

[SAGE logo]

Please cite this issue as 'ICRP, 201X. Radiological Protection in Ion Beam Radiotherapy. ICRP Publication 1XX, Ann. ICRP 4X(0).'

CONTENTS

ABSTRACT

Radiological Protection in Ion Beam Radiotherapy

ICRP Publication 1XX

Approved by the Commission in Month 201X

Abstract- The goal of external beam radiotherapy is to provide precise dose localisation in the treatment volume of the target with minimal damage to the surrounding normal tissues. Ion beams, such as protons and carbon ions, provide excellent dose distributions due primarily to their finite range, allowing a significant reduction of undesired exposure to normal tissues. Careful treatment planning is required for the given type and localisation of the tumour to be treated in order to maximise the treatment efficiency and minimise the dose to the normal tissues. Radiation exposure in the out-of-field volumes arises from secondary neutrons and photons, particle fragments, and photons from activated materials. These unavoidable doses should be considered from the standpoint of radiological protection of the patient. Radiological protection of medical staff at ion beam therapy facilities requires special attention. Appropriate management and control are required for the therapy equipment and also for the air in the treatment room which can be activated by the particle beam and its secondaries. Radiological protection and safety management should always be in conformity with regulatory requirements. The current regulations for occupational exposures in photon radiotherapy are applicable to ion beam radiotherapy with protons or carbon ions. Ion beam radiotherapy requires, however, a more complex treatment system than conventional radiotherapy, and appropriate training of the staff and suitable quality assurance programme are recommended to avoid possible accidental exposure to the patient, to minimise unnecessary doses to normal tissues and to minimise radiation exposure of staff.

Keywords: Radiotherapy; Ion beam; Proton; Carbon ion

AUTHORS ON BEHALF OF ICRP

Y. Yonekura, H. Tsujii, J.W. Hopewell, P. Ortiz López, J.-M. Cosset, H. Paganetti, A. Montelius, D. Schardt, B. Jones, T. Nakamura

PREFACE

Over the years, the International Commission on Radiological Protection (ICRP), referred below as 'the Commission', has issued many reports providing advice on radiological protection and safety in medicine. *Publication 105* is a general overview of this area (ICRP, 2007d). These reports summarise the general principles of radiological protection, and provide advice on the application of these principles to the various uses of ionising radiation in medicine.

Most of these reports are of a general nature, and the Commission wishes to address some specific situations where difficulties have been observed. It is desirable that reports on such problem areas be written in a style which is accessible to those who may be directly concerned in their daily work, and that every effort is taken to ensure wide circulation of such reports.

Rapid advances in radiotherapy require practical guidance for radiological protection in patients and medical staff. *Publication 86*, published in 2000, dealt with the prevention of accidental exposure of radiotherapy patients. That report provided the lessons learned from real case histories of major accidental exposures, and provided recommendations to prevent such accidental exposure to patients. *Publication 112* followed the same theme with particular emphasis on new technologies in external radiotherapy.

Ion beam radiotherapy is a recently introduced technique which could potentially offer an improved dose conformation to the target volume with better sparing of the surrounding normal tissue structures. Since ion beam radiotherapy requires a more complex treatment system than conventional radiotherapy, appropriate training of the staff and suitable quality assurance programme are recommended to avoid possible accidental exposure to the patient and to keep radiation exposure of staff at a minimum level. The Commission launched a Task Group on Radiological Protection in Ion Beam Radiotherapy in 2012.

The membership of the Task Group was as follows:

Y. Yonekura (Chair)	J.-M. Cosset	J.W. Hopewell
P. Ortiz López	H. Tsujii	

The corresponding members were:

B. Jones	A. Montelius	T. Nakamura
H. Paganetti	D. Schardt	

Committee 3 critical reviewers were:

M.R. Baeza	L.T. Dauer

Main Commission critical reviewers were:

J.D. Boice	H.-G. Menzel

The membership of Committee 3 during the period of preparation of this report was:

(*2009-2013*)

E. Vañó (Chair)	J.-M. Cosset (Sub-chair)	M. Rehani (Secretary)
M.R. Baeza	L.T. Dauer	I. Gusev
J.W. Hopewell	P-L. Khong	P. Ortiz López
S. Mattson	D.L. Miller	K. Åhlström Riklund
H. Ringertz	M. Rosenstein	Y. Yonekura
B. Yue		

(*2013-2017*)

E. Vañó (Chair)	D.L. Miller (Vice-chair)	M. Rehani (Secretary)
K. Applegate	M. Bourguignon	L.T. Dauer
S. Demeter	K. Kang	P-L. Khong
R. Loose	P. Ortiz López	C. Martin
K.Å. Riklund	P. Scalliet	Y. Yonekura
B. Yue		

MAIN POINTS

- **External beam radiotherapy relies on precise dose localisation in the target treatment volume with minimal damage to the surrounding normal tissues. The success of treatment largely depends on the performance and capacity of accelerators, its beam delivery system and the quality of the used treatment planning systems.**
- **The clinical use of ion beams, such as protons and carbon ions, provides precise dose distributions due primarily to their finite range in tissue. Such precise deposition of energy in tumour volumes enables a significant reduction in radiation exposure to uninvolved normal tissues.**
- **The clinical advantage of ion beam radotherapy results from the manner in which protons and carbon ions lose their energy in tissue. Much of their energy is lost near the end of their range in tissue. This peak of energy loss or stopping power is called the Bragg peak. As a result, the absorbed dose in tissue irradiated by (monoenergetic) ions has also a peak at a depth near the end of the range. This is often (strictly incorrectly) called the Bragg peak. This physical phenomenon is exploited in ion beam therapy of cancer to achieve a higher absorbed dose within the tumour than in the surrounding healthy tissues.**
- **The relative biological effectiveness (RBE) values for different ions vary for different endpoints but tend to increase with increments of stopping power or linear energy transfer (LET) up to a maximum value before declining. Clinically used proton beams are low-LET radiations, hence the RBE values are very close to that of high energy X-rays. For a given biological endpoint, carbon ions have higher RBE values than protons and increase with depth and have their maximum near the depth where the Bragg peak occurs.**
- **An ion beam delivery system generally consists of an accelerator, a high energy beam transporter and an irradiation system, where dose is delivered to the patient with either a narrow beam extracted from the accelerator (pencil beam scanning method) or a broadened beam (broad beam method). When ion beams pass through or hit these beam line structures, secondary radiations including neutrons are produced, and some of the particles in the structures can become radioactive and form an autoradioactive component of the beam.**
- **The first step for ion beam radiotherapy, similarly to any medical procedures, is justification. The proper selection of the patient should be based on knowledge of radiation oncology, the specific tumour to be treated and available clinical results to provide the optimal benefit to the patient.**
- **Careful treatment planning is required for optimisation to maximise the efficiency of treatment and minimise the dose to normal tissues, and depends on the treatment method and the targeted tumour. Theoretically, ion beam radiotherapy delivers radiation dose more efficiently to the target volume than conventional radiotherapy while minimising the undesired exposure to normal tissues. Nonetheless, the treatment planning must be sufficiently**

precise to avoid damaging the critical organs or tissues within or near the target.

- **Doses in the out-of-field volumes arise from the secondary neutrons and photons, particle fragments, and photons from activated materials. These undesired but unavoidable doses should be considered from the standpoint of radiological protection. Secondary neutrons are the major contributor to absorbed dose in the areas distant from the treatment volume. The pencil beam scanning method can minimise this type of radiation exposure.**
- **Because of the complexity of ion beam therapy, imaging procedures with ionising radiation are used in treatment planning. While the associated doses are low compared with radiotherapy doses delivered for tumour treatment, they nonetheless increase patient dose.**
- **Appropriate management is required for the therapy equipment and also for the air in the treatment room which is activated. Management should always be in conformity with criteria of the regulatory agency. The current regulations for occupational exposures in photon radiotherapy are applicable to ion beam radiotherapy with protons or carbon ions.**
- **After treatment with ion beams, the patient will be slightly radioactive for a short time. However, radiation exposure to family members of the patients and care takers due to this activation is negligible, and no specific protection procedures are required. By coming into contact with patients immediately after the ion beam radiotherapy, members of the public also can be exposed, but the possible doses are negligible if compared to the the public dose limit. Thus the methods of radiological protection for public exposures in photon radiotherapy facilities are applicable to and adequate for ion beam radiotherapy facilities.**
- **Because ion beam radiotherapy requires a more complex treatment system than conventional radiotherapy, appropriate training of the staff and suitable quality assurance programmes are essential to avoid possible accidental exposure to the patient.**

GLOSSARY

Absorbed dose, *D*

The fundamental dose quantity given by:

$$D = \frac{\mathrm{d}\bar{\varepsilon}}{\mathrm{d}m}$$

Where $\mathrm{d}\bar{\varepsilon}$ is the mean energy imparted to matter of mass d*m* by ionising radiation. The SI unit for absorbed dose is joule per kilogramme (J kg^{-1}), and its special name is gray (Gy).

Activation

Physical phenomenon in which radioactivity is induced in materials irradiated with radiations such as high-energy photons, neutrons and ion beams.

Bragg peak

The Bragg peak is a pronounced peak on the *Bragg curve* which plots the energy loss of ion beams during their passage through matter. For protons and other ions, the peak occurs near the end of their range. In radiation therapy with ions, the term Bragg peak is used for the peak in the curve of absorbed dose against depth in irradiated phantom or patient. Although this is strictly not correct, this usage is applied in this report. (see also Spread-out Bragg Peak).

Broad beam

A beam of radiant energy covering irradiation field entirely in an approximately conical or cylindrical portion of space of relatively large diameter.

Broad beam (algorithm)

One of the dose calculation techniques for the radiotherapy treatment planning. It assumes that any beam incidenting the patient travels straightly on the incident axis through the patient with no lateral blurring. The dose at any point of interest is given only as a function of the corresponding thickness to the point on the beam axis.

Broad beam (irradiation technique)

Incident beam from an accelerator is broadened laterally to cover the target uniformly. The “broad beam” is then shaped by use of collimator to match the irradiation field to the cross section of the target.

Cone-beam computed tomography (CBCT)

An computed tomography (CT) apparatus with divergent cone-like X-ray beam. It is considered beneficial to obtain 3-dimensional volumetric tomographic image in short time.

Deterministic effect

Injury in populations of cells, characterised by a threshold dose and an increase in the severity of the reaction as the dose is increased further. It is also termed tissue reactions. In some cases, deterministic effects are modifiable by post-irradiation procedures including biological response modifiers.

Detriment

The total harm to health experienced by an exposed group and its descendants as a result of the group's exposure to a radiation source. Detriment is a multidimensional concept. Its principal components are the stochastic quantities: probability of attributable fatal cancer, weighted probability of attributable non-fatal cancer, weighted probability of severe heritable effects, and length of life lost if the harm occurs.

Diagnostic reference level

Used in medical imaging with ionising radiation to indicate whether, in routine conditions, the patient dose or administered activity (amount of radioactive material) from a specified procedure is unusually high or low for that procedure.

Dose equivalent, H

The product of D and Q at a point in tissue, where D is the absorbed dose and Q is the quality factor for the specific radiation at this point, thus:

$$H = D \cdot Q$$

The unit of dose equivalent is joule per kilogramme (J kg^{-1}), and its special name is Sievert (Sv).

Effective dose, E

The tissue-weighted sum of the equivalent doses in all specified tissues and organs of the body, given by the expression:

$$E = \sum_{T} w_T \sum_{R} w_R D_{T,R}$$

or

$$E = \sum_{T} w_T \sum_{R} H_T$$

where H_T or $w_R D_{T,R}$ is the equivalent dose in a tissue or organ, T, and w_T is the tissue weighting factor. The unit for the effective dose is the same as for absorbed dose (J kg^{-1}), and its special name is sievert (Sv).

Equivalent dose, H_T

The dose in a tissue or organ T given by:

$$H_T = \sum_{R} w_R D_{T,R}$$

where $D_{T,R}$ is the mean absorbed dose from radiation R in a tissue or organ T, and w_R is the radiation weighting factor. Since w_R is dimensionless, the unit for the equivalent dose is the same as for absorbed dose, J kg^{-1}, and its special name is sievert (Sv).

Fluence, Φ

The quotient of dN by da, where dN is the number of particles incident on a sphere of cross-sectional area da, thus:

$$\Phi = \frac{\mathrm{d}N}{\mathrm{d}a}$$

Lineal energy

The lineal energy, y, is the quotient of ε_s, by $\bar{l}$, where ε_s is the energy imparted to the matter in a given volume by a single energy-deposition event and $\bar{l}$ is the mean chord length of that volume, thus

$$y = \frac{\varepsilon_s}{\bar{l}}$$

The unit of y is given in J m^{-1}, often given in keV μm^{-1}.

Linear energy transfer (LET)

The average linear rate of energy loss of charged particle radiation in a medium, i.e., the radiation energy lost per unit length of path through a material. That is, the quotient of dE by dl where dE is the mean energy lost by a charged particle owing to collisions with electrons in traversing a distance dl in matter.

$$L = \frac{dE}{dl}$$

The unit of L is J m^{-1}, often given in keV μm^{-1}.

MeV/n

Kinetic energy of a particle expressed by a unit of mega-electron volt per nucleon (MeV/n). It reflects the square of the speed v of the particle. Particles sharing the same MeV/n value have the same $\beta=v/c$ (c: light speed).

Organ at risk (OAR)

Organs that might be damaged during exposure to radiation. It most frequently refers to healthy organs located in the radiation field during radiotherapy.

Oxygen enhancement ratio (OER)

The radio of the absorbed dose required to cause the same biological endpoint in hypoxic condition to that in normoxic condition. Hypoxia often appears in the middle of rapidly glowing tumour. OER of X-ray is about three while high-LET radiation tends to show smaller OER down to one, indicating that the high-LET radiation is effective against hypoxic tumour.

Pencil beam

A beam of radiant energy concentrated in an approximately conical or cylindrical portion of space of relatively small diameter.

Pencil beam (algorithm)

One of the dose calculation techniques for radiotherapy treatment planning. It assumes that any beam incidenting the patient is actually a conglomeration of lots of “pencil beams”, and the dose at any point of interest is given as the superposition of all the pencil beams.

Pencil beam (in scanning irradiation technique)

Dose is delivered by superposing “pencil beams” from an accelerator on the target by controlling the beam path three dimensionally.

Quality factor, $Q(L)$

The factor characterising the biological effectiveness of a radiation, based on the ionisation density along the tracks of ion beams in tissue. Q is defined as a

function of the unrestricted linear energy transfer, L_∞ (often denoted as L or LET), of ion beams in water:

$$Q(L) = \begin{cases} 1 & L < 10 \text{ keV}/\mu\text{m} \\ 0.32L - 2.2 & 10 \leqslant L \leqslant 100 \text{ keV}/\mu\text{m} \\ 300/\sqrt{L} & L > 100 \text{ keV}/\mu\text{m} \end{cases}$$

Q has been replaced by the radiation weighting factor in the definition of equivalent dose, but it is still used in calculating the operational dose equivalent quantities used in monitoring.

Radiation detriment

A concept used to quantify the harmful health effects of radiation exposure in different parts of the body. It is defined by the Commission as a function of several factors, including incidence of radiation-related cancer or heritable effects, lethality of these conditions, quality of life, and years of life lost owing to these conditions.

Radiation induced second cancer

Ionising radiation has paradoxical aspects in both beneficial effects of curing cancer and the risk of inducing cancer. Induction of cancer by low to high dose of radiation has been demonstrated by the significant increase in the incidence of cancers among workers handling radioactive substances and among atomic bomb survivors, as well as among survivors after radiotherapy.

Radiation weighting factor, w_R

A dimensionless factor by which the organ or tissue absorbed dose is weighted to reflect the higher biological effectiveness of high-LET radiations compared with low-LET radiations. It is used to derive the equivalent dose from the absorbed dose averaged over a tissue or organ.

Relative biological effectiveness (RBE)

The ratio of a dose of a low-LET reference radiation to a dose of the radiation considered that gives an identical biological effect. RBE values vary with the dose, dose rate, and biological endpoint considered.

Second cancer

A term that is used to describe either a new primary cancer or cancer that has spread from the place in which it started to other parts of the body.

Secondary radiation

Radiation produced by interaction between the primary beam and the matter. In the radiotherapy treatment room, all radiation except for the primary beam is secondary radiation, which is produced by scattering off of objects or leakage through the protective shield.

Spread-out Bragg peak (SOBP)

The extended isoeffect region in depth formed by the optimal stacking of multiple depth dose curves of pristine Bragg peaks of different energies.

Stochastic effect

The induction of malignant disease or heritable effects, for which the probability of an effect occurring, but not its severity, is regarded for the purpose of radiological protection to be increasing with the dose without a threshold.

Time resolved computed tomography (4DCT)

An X-ray CT apparatus capable of rapidly acquiring serial 3-dimensional volumetric image as a function of time. The taken image is often associated with breathing or heartbeat phase.

Tissue reaction

See 'Deterministic effect'

Tissue weighting factor, w_T

The factor by which the equivalent dose in a tissue or organ T is weighted to represent the relative contribution of that tissue or organ to the total health detriment resulting from uniform irradiation of the body (ICRP, 1991b). It is weighted such that:

$$\sum_T w_T = 1$$

Voxel phantom

Computational anthropomorphic phantom based on medical tomographic images where the anatomy is described by small three-dimensional volume elements (voxels) specifying the density and the atomic composition of the various organs and tissues of the human body.

1. INTRODUCTION

(1) Considerable progress has been made in the treatment of patients with radiation in terms of increased applicability and improved therapeutic outcomes. Most notably, high-precision photon beam radiotherapy, such as intensity-modulated radiotherapy (IMRT) and stereotactic radiotherapy (SRT), are used effectively in clinical practice.

(2) The goal of external radiotherapy is precise dose localisation in the treatment volume of the target, with minimal damage to the surrounding normal tissues. Therefore, the success of treatment largely depends on the performance and capacity of accelerators and treatment planning system (TPS), in addition to the accurate delineation of the targeted tumour by the radiation oncologist. This became particularly evident in the 1950's, when it was recognised that high energy photons contributed significantly to the improvement of the treatment outcome. The beginning of modern radiotherapy takes its origins in the 1950's when tele-cobalt machines, high-energy accelerators and linear accelerators were developed and applied to clinical use.

(3) Cancer therapy with ion beams has a history of more than 50 years (Tobias et al., 1956). Ion beam radiotherapy is characterised by the production of the maximum ionisation density at depth in tissue, referred to as the Bragg peak, and thus, in comparison with photon beams, offers an improved dose conformation to the treatment volume with better sparing of the surrounding normal tissue structures. Furthermore, protons and heavier ion beams allow the reduction of the total energy deposited in the patient when compared with photon techniques. This allows, in many cases, dose escalation in the target or a significant reduction in dose to healthy tissue. The latter is of particular importance if the treatment volume is close to critical structures. In addition, ion beams, such as protons and carbon ions, exhibit a strong increase in LET in the Bragg peak as compared with the entrance region. In cancer radiotherapy, these physical and biological properties of ion beams are much more favourable than photon beams (Castro et al., 1985). Consequently, ion beam radiotherapy with protons and carbon ions has gained increasing interest and has expanded rapidly in the last decade.

(4) Ion beam radiotherapy with protons is becoming popular in some countries, and carbon ion radiotherapy has also been introduced in medical care. Approximately ten years ago, there were nearly 20 ion beam radiotherapy facilities in the world[1]. Now the number has doubled and many new facilities are being built or planned. Potential demand is anticipated to exceed the projected increased number of facilities.

(5) High-energy radiation is necessary for ion beam radiotherapy. The treatment facility generally requires a large scale accelerator installed in the building with appropriate shielding. There are specific issues in radiological protection to operate such a treatment facility.

(6) A result of the worldwide development and the spread of high-precision radiotherapy has been the increased opportunity to treat benign diseases and malignant cancers in young patients. The therapeutic outcome has also been improved for locally advanced cancers that were not curable with conventional

[1]Referred from PTCOG website: http://ptcog.web.psi.ch/

methods. Many of these patients now survive for longer periods, and thus, more attention should be paid to any late occurring radiation effects.

(7) In the past, radiation oncologists focused mainly on curing cancers with little consideration of second cancer or radiotherapy related caardiovascular disease. Recently, the situation has changed; while high-precision photon radiotherapy methods are superior in the dose distribution they deliver to a tumour, a large volume of surrounding normal tissues may be exposed to increased low and medium levels of dose (NCRP, 2011). Ion beam radiotherapy with protons or carbon ions largely contributes to localise dose to tumour, and the extra dose received in surrounding normal tissues is reduced. However, the possible risk of high LET radiation in the surrounding normal tissue may be of more general concern even though the absolute dose level is reduced.

(8) This document reviews the present status and problems of the use of ion beam radiotherapy from the viewpoints of radiological protection and safety, and provides practical guidance for the effective and safe use of ion beams for medical treatment for benign and malignant disease.

2. OUTLINE OF ION BEAM RADIOTHERAPY

2.1. Clinical target of ion beam radiotherapy

(9) The introduction of new technologies in radiotherapy aims to improve treatment outcome by means of a dose distribution which conforms more strictly to the tumour volume and treatment volume (ICRP *Publication 112*, 2009). Ion beams are considered to have the optimum properties in dose localisation. The selection of the patients suitable for ion beam radiotherapy is the first step in the treatment. Benefits of ion beam therapy can be achieved in patients with solid cancer with defined borders. This noninvasive treatment does not require surgery to remove the cancer, making it ideal for inoperable tumours. Proton beam radiotherapy may offer clinical advantages compared with conventional photon radiotherapy for many cancers, mainly as a result of a more favourable distribution of radiation dose (Lundkvist et al., 2005).

(10) Ion beams heavier than protons have additional advantage of enhanced biological effects, which increases with depth, reaching the maximum at the end of the beam's range. These unique properties have led to the use of heavy ion beams, such as helium, carbon and neon ions, for cancer radiotherapy. The carbon ions enable the treatment of various tumours which are resistant to conventional photon radiotherapy or chemotherapy (Chauvel et al., 1995). The clinical benefits of carbon ion radiotherapy have been demonstrated in non-squamous cell tumour types, including sarcoma, malignant melanoma, adenocarcinoma, adenoid cystic carcinoma and chordoma (Tsujii et al., 2012).

(11) Some studies suggest that new technology has not yet resulted in a substantial improvement in the long-term outcome for most patients (Soarers et al., 2005), and there is a need for systematic evaluation of the benefits, considering the total cost of the method (Allen et al., 2012; Lievens and Pijls-Johannesma, 2013).

2.2. General treatment processes

2.2.1. Features of ion beams

(12) Ion beams, as indicated above, are characterised by dose concentration at depth in tissue and an enhanced biological effectiveness. The clinical advantage results from a steeply rising absorbed dose, or Bragg peak, and a rapid falloff in dose after the peak. Therefore, by targeting the lesion within the Bragg peak, a superior dose concentration is achieved. This superiority is similar for both proton and carbon ion beams.

(13) The RBE values vary for different endpoints for most cells and tissues, but tend to increase in parallel with increment of LET up to a maximum value before declining. Clinically used proton beams are low LET radiations, hence the RBE values are very close to that of high energy X-rays. The International Commission on Radiation Units and Measurements (ICRU) has recommended 1.10 as a generic RBE for proton beams (ICRU, 2007). This is based on the available evidence indicating that the magnitude of RBE variation with treatment parameters is small relative to possibly realistic RBEs. There is some concern about the use of a generic RBE value due to the limited range of data, particularly for lack of human cell types, and future clarification is needed. For carbon ions, the LET increases with depth in

tissue, reaching a maximum at the end of a particles range. Carbon ions have higher RBE values than protons but the variation with depth in tissue and energy is not well defined.

(14) The available data indicate that the oxygen enhancement ratio (OER, the ratio of doses to produce a defined response under hypoxic conditions to that for aerobic conditions) is reduced using high LET radiation, and that the high LET radiation less influences the variation in radio-sensitivity with respect to a phase in the cell division cycle. To treat cancers with ion beams, it is essential to have the knowledge and technology to utilise these characteristic features of the beams.

2.2.2. Imaging

(15) Imaging technology plays a crucial role for precise localisation of the target volume in radiotherapy. In the case of ion beam radiotherapy, the state-of-the-art diagnostic imaging with X-ray computed tomography (CT), magnetic resonance imaging (MRI), and positron emission tomography (PET) is indispensable in the entire procedures of treatment planning. For example, in treatment planning, CT gives patient density information to calculate dose distribution and design the shape of the SOBP to conform to the target volume. Recently, the PET-CT system has become available to provide the valuable diagnostic information for treatment planning. It is a common procedure in ion beam radiotherapy to use X-ray exposures for patient positioning.

2.2.3. High-precision beam delivery system

(16) In order to appreciate the advantage of dose distribution, ion beams are spread to conform to the target by passive scattering, pencil beam scanning and wobbling or uniform scanning. Thus, the high precision beam delivery system is achieved to cover the target with the designed spread beam with millimetre accuracy. In tha past, the most commonly employed method was passive beam scattering, including single and double scattering. For the treatment of a target volume moving with respiration, the respiratory gated irradiation method has been used in passive scattering method.

2.2.4. Procedures for ion beam radiotherapy

(17) Procedures for ion beam radiotherapy are described below. These include patient immobilisation, planning CT, treatment planning, patient positioning and beam delivery.

Patient immobilisation

(18) Rotating gantries have become available for proton radiotherapy (Slater et al., 1995), while fixed horizontal or vertical beams are mainly used in most carbon ion therapy facilities. In the case of fixed beam lines, different beam directions can only be achieved by the combination of patient's positions with or without rotating the patient. Normally, ion beam radiotherapy is fractionated over several weeks. It is crucial for radiotherapy to repeat the beam delivery with high precision over the period. Initially, it is important to examine diagnostic images to determine the treatment sites and available beam directions. In some cases, physiological factors, for example, bladder filling is actively controlled in prostate cancer patients. For immobilisation, cares should be taken not only for the patients' comfort but also for

the possible influence on the beam delivery. Precision, ease of manufacture/use/disposal, safety and cost should be included in the consideration as well. In many facilities, vacuum bags, bite blocks, individual cradles and thermoplastics are used.

Planning CT

(19) Treatment planning for ion beam radiotherapy is performed using CT images, which must be taken under the same condition as used for treatment. Namely, the patients must be immobilised on the treatment couch under the same breathing condition as for treatment. This sometimes requires respiratory gating for both CT scanning and subsequent beam delivery. The planning CT images provide patient density information for dose calculation. The use of contrast agents are thus normally avoided in planning CT scans.

Treatment planning

(20) The clinical target volume (CTV) and organs at risk (OAR) are first defined on the planning CT images. In practice, additional diagnostic images, such as contrast-enhanced or breath-hold CT, MR images and PET images, are often helpful for delineation of the target, if they are taken under treatment conditions (Hosokawa et al., 1995). The planning target volume (PTV) is then determined, which in addition considers physiological changes between planning CT and treatment, organ motion (ICRU, 1993b, 1999; Osaka et al., 1997) and setup errors. The ion beams are designed to deliver the prescribed dose uniformly to the PTV, for which beam parameters are chosen or varied to obtain an optimum dose distribution for the prescription (ICRU, 2007).

Patient positioning

(21) For high-precision ion beam radiotherapy, the patient position is usually aligned and verified with orthogonal X-ray radiographs in comparison with digital radiographs reconstructed from planning CT images. The reference planning images can be substituted by the equivalent X-ray images, which are taken prior to the first treatment. Bony structures and fiducial markers, implanted near the site before the planning CT, are often used as reference points in patient positioning.

Beam delivery

(22) After the patient is immobilised and positioned, the ion beams are delivered as planned for a period of seconds or minutes. During the beam delivery, the patient and active devices are visually or electrically monitored for interlock in case of any emergency. The beam is stopped when the prescribed dose is administered, for which the dose monitor output has to be calibrated prior to treatment. Due to the complexity of ion beam delivery systems, the dose monitor calibration may require specific control measurement on a beam-by-beam basis.

2.3. Introduction of the beam delivery system and irradiation method

(23) An ion beam delivery system generally consists of an accelerator system, a high energy beam transport system and an irradiation system. In most cases, synchrotron, cyclotron or synchro-cyclotron is used to accelerate particles. A high-energy ion beam is delivered through a beam transport system to an irradiation system. The narrow pristine beam extracted from the accelerator, which is called a

669 'pencil beam', is not ready for use in treatment except for the beam scanning method.
670 The irradiation system broadens 'the pencil beam' for the target volume. This
671 method is called the 'broad beam method' and is classified as the 'passive method'
672 (Fig. 2.1).
673 (24) A layer stacking method is a more advanced broad beam method, using a
674 multi-leaf collimator (MLC), resulting in higher relative dose being delivered to the
675 target volume than the standard broad beam method (Kanai et al., 1983; Futami et
676 al., 1999). In a scanning method pencil beams are scanned over a target tumour,
677 three-dimensionally, without expanding the pencil beam, unlike the conventional
678 broad beam method (Fig. 2.2). The layer stacking and scanning methods are
679 classified as the 'active method'.
680
681

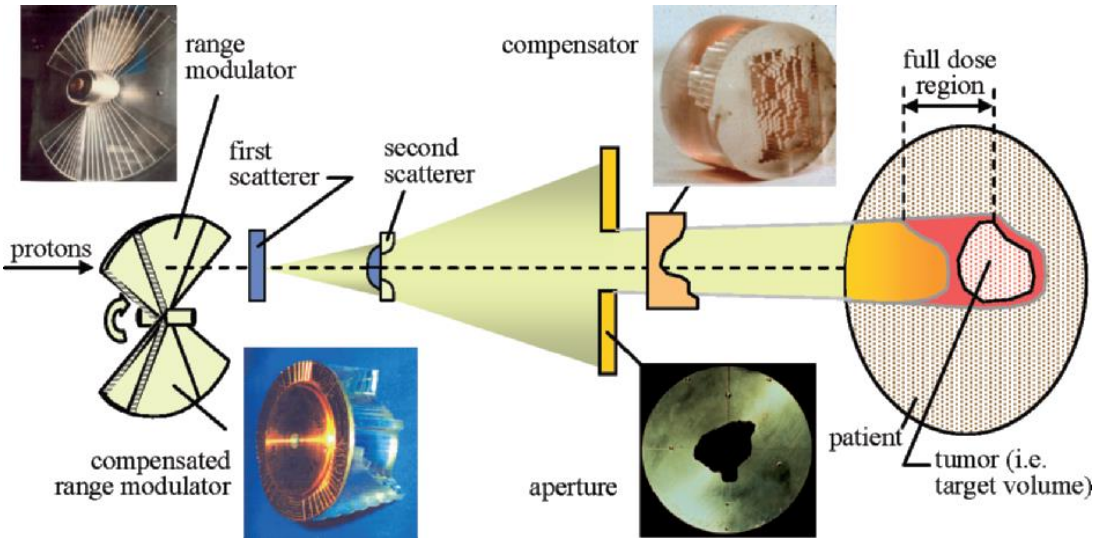

682
683
684 Fig. 2.1. Broad beam system with passive scattering for proton beam therapy. Reprinted
685 from Goiten, 2008. (Permission needed)
686
687

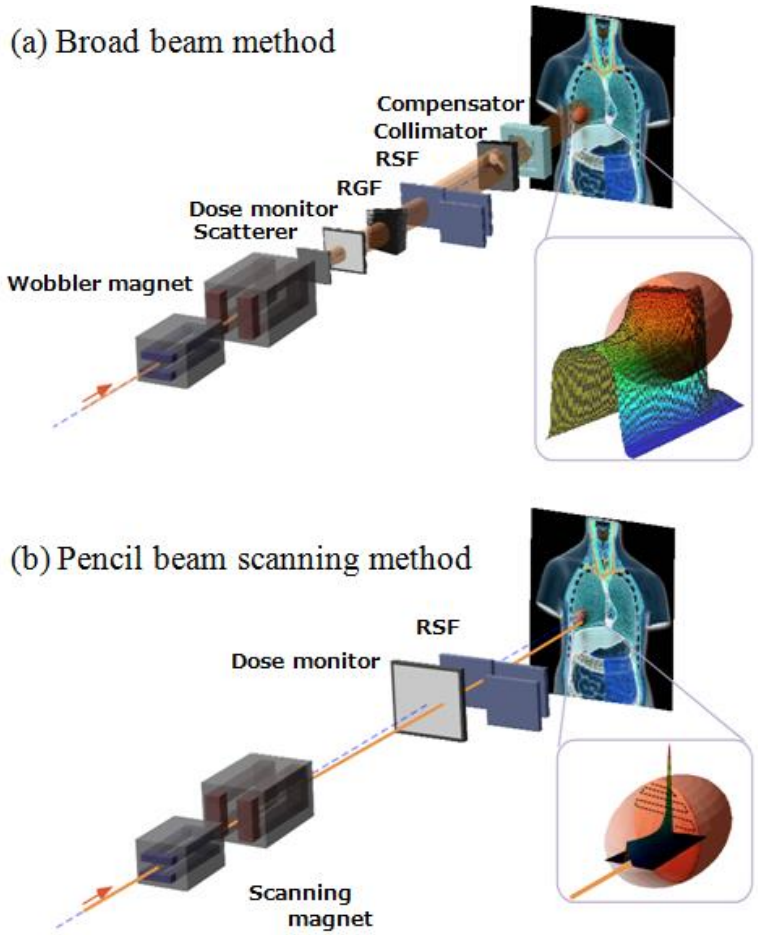

Fig. 2.2. Beam delivery system for carbon ion radiotherapy. (a) Concept ofbroad beam method. (b) Concept of pencil beam scanning method. RSF: Range shift filter, RGF: Ridge filter.

2.3.1. Broad beam method

(25) In the broad beam method, a narrow pencil beam, extracted from an accelerator, is broadened uniformly in the lateral and depth directions and part of the expanded uniform beam is clipped to conform to the high-dose region induced by the beam to the target tumour volume in a patient's body. The methods mainly used to widen the pencil beam uniformly in the lateral direction are double-scattering and wobbler-scattering. Single-scattering methods can be applied for small field size such as in radiosurgery.

(26) The double-scattering method (Fig. 2.1) makes a uniform irradiation field using two scatterers with different structures (Grusell et al., 1994; Gottschalk, 2008). The first scatterer, installed upstream in the irradiation system, is made of a uniform, heavy material (lead is commonly used) and the pencil beam is broadened by multiple Coulomb scattering. The distribution of the beam takes on a Gaussian-like shape with small tails. The second scatterer, placed downstream from the first one, is made of two materials; a high-Z component of decreasing thickness as a function of distance to the beam centre and a low-Z component of increasing thickness with distance to the beam centre.

(27) The wobbler-scatterer method (Fig. 2.3) generates a uniform irradiation field using a combination of a wobbler-magnet system and a scattering system (Torikoshi et al., 2007). The wobbler-magnet system is a pair of bending magnets, which are installed so that the direction of their magnetic fields is mutually orthogonal. By applying alternating currents to the two magnets, which are out of phase with each other by 90°, the pencil beam delivered from the accelerator is rotated in a circular pattern. The radius of the circle can be changed by varying the effective current supplied to the wobbler-magnet system. The annular beam is broadened by the scattering system placed downstream from the wobbler-magnet system.

(28) Uniform broadening of a beam, in the depth direction, corresponds to producing an SOBP. The SOBP is formed by superposing many different pristine Bragg peaks. In other words, the SOBP is the response to the energy modulation of a mono-energetic beam. There are two main ways of modulating the beam energy and superimposing Bragg peaks; one uses a ridge filter device (Larsson, 1961; Kostiuchenko et al., 2001) and the other uses a rotating range modulator (Koehler et al., 1975). The ridge filter device is composed of many uniform bar-ridges, manufactured with highly precise processing technology, which are set parallel to each other on one plane as shown in Fig. 2.4. Ridge filter devices, corresponding to different SOBP widths, are often prepared for both a high energy beam and a low energy beam. Since the cross-sectional shape of the bar-ridge determines the thickness, appropriate design of the bar-ridge allows delivery of a homogeneous weighted dose to the target region.

(29) A rotating range modulator is a wheel with a cyclic part of different water-equivalent thickness for different central angle regions. As a beam passes through the cyclic part, its energy is modulated by the thickness in the region where the beam passes. The depth-dose distribution formed using the rotating range modulator has a time structure corresponding to the rotation frequency of the modulator.

(30) After the broadening of a beam in the lateral and depth directions, the beam is shaped to the target tumour, projected in the beam's eye view. A customised patient collimator, the MLC or their combination is used for the two-dimensional shaping of a uniform beam. The customised patient collimator is a block that has a tumour projection-shaped aperture. The block is thicker than the maximum range of the beam and often made of brass, which is easy to cut with a wire-electrical discharge machine or a milling machine. Although the customised patient collimator needs to be manufactured for each irradiation direction; it reduces blurring of the lateral dose falloff because the patient collimator can be placed near the body surface of the patient.

(31) The MLC is a device that has many pairs of thin leaves (Fig. 2.5). These leaves are shifted to suitable positions to make the aperture fit the tumour projected shape. Use of a MLC device has the advantage of increased speed and reduced costs for treatment preparation because no individual patient collimators need to be manufactured. On the other hand, due to the mechanic limitations, the MLC often cannot be positioned close to the patient's surface as the block collimator. The larger gap between the end of the collimator and the patient surface spoils the sharp lateral dose falloff to some extent. Therefore, the MLC is not often used when precise field shaping is required.

(32) A range shifter device is applied for the sake of adjusting the residual range in a patient's body. The range shifter device is composed of several energy absorbers having different thicknesses, and the total thickness of the system can be

changed by selecting suitable absorbers. The beam range can be adjusted uniformly by using the range shifter device. Range shifter devices are not commonly used in the treatment head (except for fine tuning) as synchrotrons can deliver the desired energy and cyclotrons typically use energy degraders at the cyclotron exit to send the desired energy into the treatment room.

(33) A patient compensator is a block that has an engraved depression in the shape of the distal surface of the target volume. The block is often made of high-density polyethylene which is easy to engrave and is a low atomic number material to reduce scattering of the beam. Patient compensators, like patient collimators, also need to be manufactured for each irradiation direction.

(34) Regarding patient exposure to radiation, the beam efficiency is low for the broad beam method due to the loss of ion particles before reaching the patient. There is a loss of beam intensity at every device used to modulate and shape the beam, and those points can also generate undesired radiation, such as neutrons.

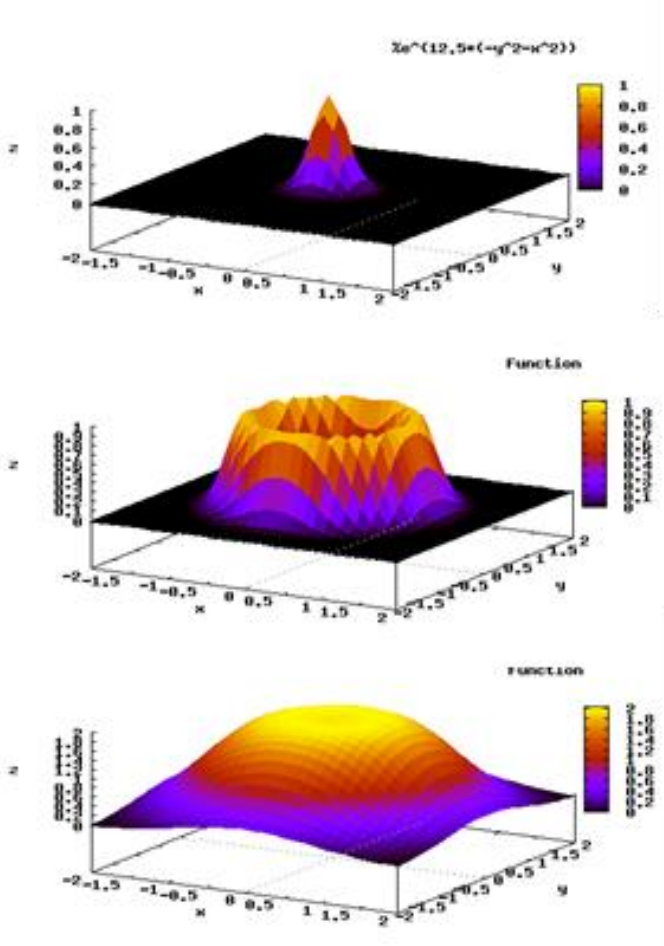

Fig. 2.3. Uniform broad beam generated by the wobbler-scattering method. Upper: A pencil beam delivered from an accelerator source. Middle: A beam rotated by wobbler magnets. Bottom: A beam broadened by a scattering system placed downstream from the wobbler magnet system.

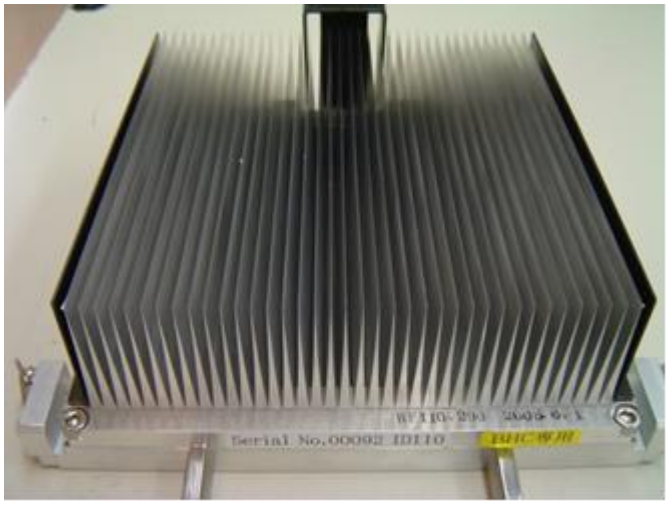

Fig. 2.4. Ridge filter. Ridge filter devices, corresponding to different SOBP widths, are often prepared for high energy and a low energy beams.

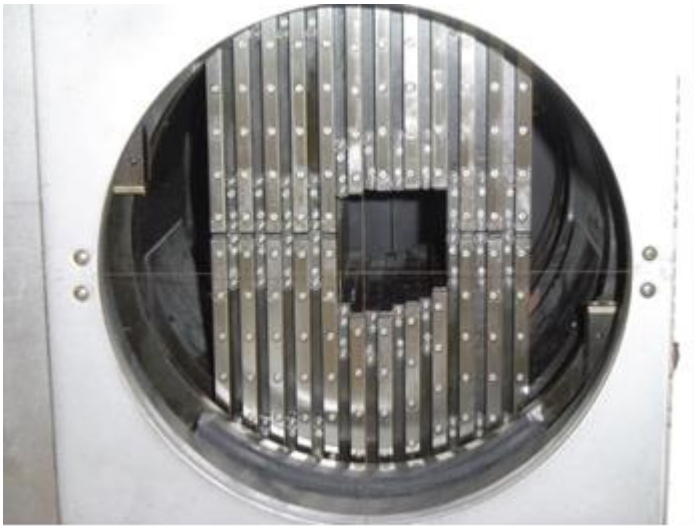

Fig. 2.5. Multi-leaf collimator (MLC).

2.3.2. Layer stacking method

(35) In the broad beam method, with a range modulator, a constant SOBP over the field area results in an undesirable dose to the normal tissue proximal to the target (Goitein, 1983; Kanai et al., 1993; Kanematsu et al., 2002). Therefore, in order to avoid unwanted doses, a layer stacking method was developed. The layer stacking method is a way of stacking multiple mini-SOBPs along the depth direction and changing apertures of the MLC as if the lineation of the cross-sectional surface of the target tumour volume is drawn. Regarding patient exposure to radiation, the efficiency of beam usage is also low for the layer stacking method.

2.3.3. Pencil beam scanning method

(36) Pencil beam scanning is a method to achieve a highly conformal field by three-dimensional scanning of a pencil beam, extracted from an accelerator, within the target tumour volume. A conceptual diagram of a pencil beam scanning method is shown in Fig. 2.2(b).

(37) Historically, the first proton beam scanning was achieved with a low energy beam (70 MeV), which was not used in patient treatments (Kanai et al., 1980). A new project for treating deep-seated tumours with a proton pencil beam scanning was started in 1992 at Paul Scherrer Institute (PSI) (Pedroni et al., 1995). almost in parallel to PSI, the Gesellschaft für Schwerionenforschung (GSI) in Germany developed a pencil beam scanning for carbon ions using a horizontal, fixed beam line for treating skull base tumours. The scanning system at GSI is based on a raster scanning technique, which uses a double magnetic scanning system and dynamically changes the beam energy with the synchrotron (Haberer et al., 1993).

(38) The pencil beam is scanned laterally usually using orthogonal scanning magnets so as to form a lateral irradiation field. The scanning speed along one direction is higher than that along the other orthogonal direction. This allows the use a mechanical shifting system along the slowly scanning axis, instead of a scanning magnet, for example as used on the Gantry I at PSI. It is then scanned longitudinally by either a range shifter device or a stepwise energy change by the accelerator. The pencil beam scanning method is characterised by a high beam efficiency of almost 100%, and therefore has benefits from lower production of neutrons.

2.3.4. Rotating gantry system

(39) The rotating gantry system allows a wide choice of beam orientation compared with a fixed port irradiation system. In clinical practice, in the fixed beam delivery systems, the beam is limited to either the horizontal or vertical direction, and thus the patient has to be fixed in a supine, prone or sitting position. The patient is often rolled into new positions by moving to get a better combination of beams. This often places a burden on the patient, complicates treatment planning, and leads to imprecision in positioning. It also limits the accurate beam delivery due to the possible movement of internal structures and organs by rolling the patient. The rotating gantry system, which allows 360° rotation around the patient, resolves many of these problems and is the standard for conventional X-ray tele-therapy systems. The rotating gantry for ion beam radiotherapy is much larger than for photons; typically 10 m in diameter in commercial proton radiotherapy systems.

2.3.5. Respiratory gating irradiation

(40) Organ motion during patient positioning and beam delivery degrades the precision in dose delivery. In particular, breathing causes movement of up to a few centimetres in the thoracic and abdominal regions, which may also influence the whole body when the patient is in the prone position. In order to solve the problem, breath hold and active breath control during the treatment have been proposed (Wong et al., 1999). Respiratory gating of radiation exposures also effectively mitigates such motion effects by synchronising the beam extraction with the respiration. Breathing motion can be detected with, for example, an infrared light spot and a position-sensitive charge coupled device camera, which gives a respiration waveform signal. The organs are normally more stable at the end of expiration, and gating for beam extraction is usually set to this phase of respiration. The respiration pattern and its reproducibility are patient dependent. Therefore, real-

time detection of the respiration waveform, fast and robust gating logic, and responsiveness of the beam extraction system are essential for a respiratory gating system.

2.3.6. Verification of dose distribution in body auto-activation

(41) High energy ion beams used in ion beam radiotherapy induce nuclear reactions in a patients' body (Tobias et. al., 1977). These reactions may produce β^+ decayed nuclei such as ^{15}O and ^{11}C. By detecting coincidentally the pair annihilation gamma rays from these nuclei, the dose distribution in the body can be verified using the following process. First, the distribution in the body of the β^+ decayed nuclei produced by incident ions in the body is calculated combining with treatment planning data and nuclear reaction data. Second, this distribution is compared with the measurement of PET (Enghardt et al., 1992; Parodi et al., 2008). Finally, the dose distribution is assessed with consideration of a washout effect (Mizuno et al., 2003). There are developing techniques of 3D dose verification by auto-activation as well as range verification (Nishio et al., 2005).

3. PHYSICAL ISSUES FOR RADIOLOGICAL PROTECTION

(42) Absorbed dose is used as the primary quantity for clinical dose prescription. It is known to be a good index for the biological or clinical effects of photon and electron beam irradiation. In addition to that, in the case of ion beams, their biological effects depend not only on the absorbed dose but also on the radiation quality, which can vary markedly in the irradiated volume. In this section, physical issues related to radiological protection in ion beam radiotherapy are described.

3.1. Traveling of ions in matter

3.1.1. Stopping power

(43) A high energy ion gradually loses its energy mainly via Coulomb interaction with nearby electrons when traveling in matter. The quantity, energy loss per unit path length, is often called the stopping power, dE/dx. The amount of energy given to the matter per unit path length is small as the duration of interaction is short while the particle remains at high speed. The stopping power increases drastically when the particle is slowed down and comes to the end of its range. This rapid increase in the stopping power toward the end of the range forms a peaky energy loss, known as the Bragg peak. The stopping powers of various ions have been compiled in ICRU Report 49 (ICRU, 1993a) and ICRU Report 73 (ICRU, 2005a).

3.1.2. Multiple scattering and straggling

(44) The Coulomb interaction between an incident ion and matter determines not only the stopping power but also multiple scattering. The extent of scattering in a single Coulomb interaction between the incident particle and an electron may be negligible; however, due to the vast number of interactions, the resultant deflection can be significant. These deflections are not identical for all incident particles of the same energy due to statistical fluctuations in the interactions. Such fluctuation causes a variation in energy and range to a cohort of particles. This statistical fluctuation is called energy straggling. Both multiple scattering and range straggling become less prominent as its mass increases. This is one of the reasons for the superior lateral penumbra dose localisation realised in ion beam radiotherapy, especially in carbon ion therapy.

3.2. Production of secondary radiation

3.2.1. Nuclear reaction model

(45) To reach a deep-seated tumour, in ion beam radiotherapy, the primary particle is accelerated to 150-500 MeV/n, which corresponds to about 60-80 % of the speed of light. When such a highly energetic particle collides with a nucleus in matter, a nuclear reaction can occur. In the reaction, both the incident particle (if heavier than a proton) and the target nucleus can break into fragment particles. The process can be described by the participant-spectator model, because in high-energy reactions, where the projectile velocity is much higher than that of nucleons in the

projectile known as the Fermi-velocity, it is assumed that only the nucleons within the overlapping region of the projectile and target nuclei are participating in the reaction and therefore called 'participants'. The spectator is emitted immediately after the collision (within about 10^{-22} seconds) through a direct process. It can originate from either the projectile nucleus or the target nucleus and retains its original velocity. In other words, the spectator from the projectile (projectile fragment) is emitted in the forward direction with relatively high energy. Then it moves together with the rest of the primary particles in a therapeutic beam. Since the mass of the projectile fragment is smaller than that of the primary particle, it has a larger ranges and can travel beyond the Bragg peak. This region, where the projectile fragments deposit energy beyond the Bragg peak, is called a fragment tail. It should be emphasized that this projectile fragmentation and the resultant formation of the fragment tail occurs only for incident ions heavier than protons.

3.2.2. Decay of unstable residual nucleus

(46) When the residual fragment nucleus is unstable, it will decay to a stable form according to its intrinsic physical half-life. Because the target fragments do not move very much, the matter containing the unstable fragment particles should be treated as a radioactive material. This production of unstable nuclei is known as activation. The activation is in general a nuisance as the nuclei can be a potential source of secondary exposure for the patient and workers. However, it is possible to use the activation reaction as auto-activation. The spatial distribution of auto-activation can be associated with the distribution of the incident beam, and the activation distribution can be measured by detecting a pair of annihilation gamma-rays emitted from a β^+-decay nucleus (Enghardt et al., 1992; Parodi et al., 2008).

3.2.3. Cross section

(47) The probability (P) of the nuclear reaction is expressed by a cross section σ. As a first approximation, the cross section of a fragment reaction is governed by the geometrical size of the projectile nucleus (Sihver et al., 1993). Cross section data have been compiled, for example, by Chadwick (1998).

3.3. Spatial distribution of radiation

(48) The spatial distribution of absorbed dose is the result of the physical interactions described above. For easy understanding, the spatial dose distribution of an ion beam is described in two different regions based on the dose level and radiation quality; i) the directly irradiated volume in the field, where the primary particles dominate the delivered dose, and ii) its surrounding volume out of the field, where secondary particles play a major role in dose delivery.

3.3.1. In-field volume

(49) The calculated depth-dose distributions of proton and carbon ion beams in water, as obtained by the Monte Carlo simulation code, the Particle and Heavy Ion Transport code System (PHITS) (Iwase et al., 2002; Niita et al., 2006), are shown in Fig. 3.1. The peak-to-plateau ratio decreases due to the effects of fragmentation and

straggling as the incident energy increases. The straggling also affects the broadening of the distal falloff.

(50) Approximately half of the total number of primary particles can reach the end of the range without experiencing fragment reactions (Matsufuji et al., 2005). The rest are broken into fragment particles. Among these, the fluence rates of hydrogen and helium tend to be comparable to those of primary carbon ions in the vicinity of the range end. In the case of proton beams, the projectile fragments are not involved in the beam; however, an increase in LET causes an enhanced biological effect at the very end of the range (Paganetti, 2003). This change in radiation quality should be considered for ion beam radiotherapy when estimating its biological or clinical effectiveness.

(51) The penumbra is often used to describe the sharpness of the beam spot after passing through a collimator (Kanematsu et al., 2006). The width of lateral falloff, in the penumbra from 80% of the maximum dose to 20% is expressed as P80-20. The penumbra is composed of scattered primary particles in both proton and carbon ion beams and of secondary charged particles in a carbon ion beam. In case of a proton beam, the distribution is treated as a single Gaussian function (Pedroni et al., 2005), as shown in Fg.3.2. A low-dose halo structure arises from a single or a few Coulomb scatterings. Inelastic scattering is practically negligible. For a carbon ion beam, the penumbra is approximated with three Gaussian distributions (Kusano et al., 2007). The above mentioned complex structure, especially like that associated with a carbon ion beam, causes a change in radiation quality in the irradiation field when the field size is small (Nose et al., 2009).

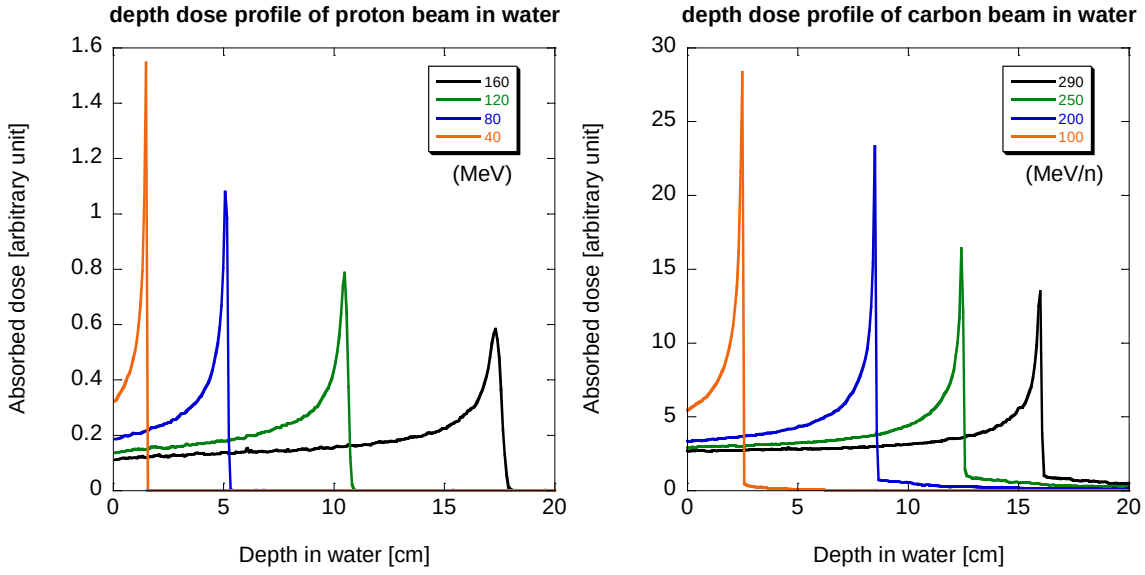

Fig. 3.1. Projected depth-dose distributions in water for protons with incident energies of 160, 120, 80 and 40 MeV (left) and for carbon ions with incident energies of 290, 250, 200 and 100 MeV/n (right) calculated using PHITS.

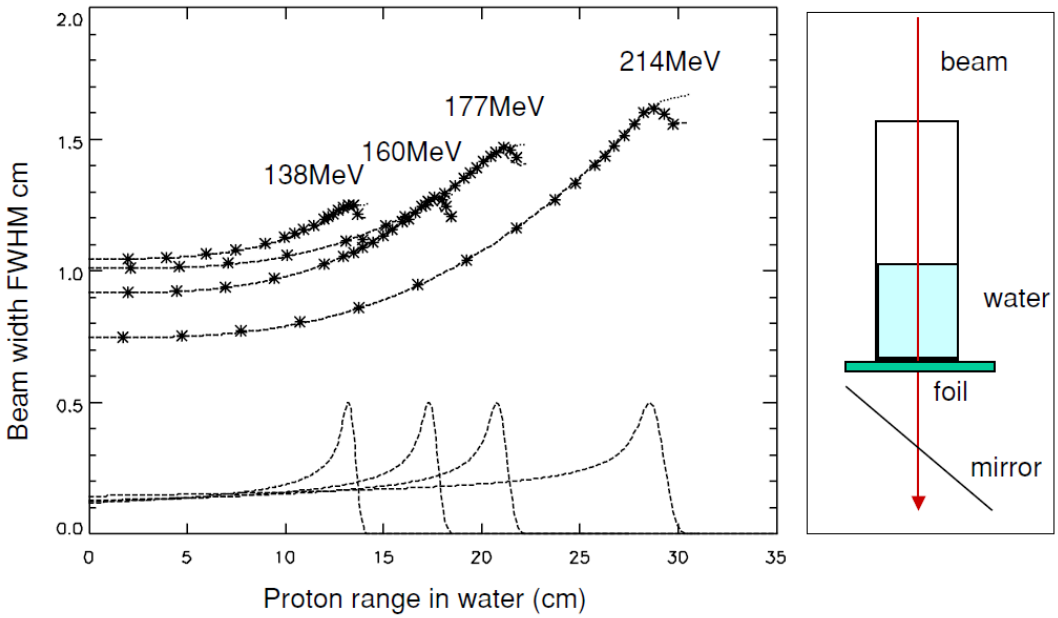

Fig. 3.2. Lateral beam broadening of proton beam as a function of its kinetic energy. Reprinted from Pedroni et al., 2005. (Permission needed)

3.3.2. The out-of-field volume: secondary radiation

(52) The out-of-field volume is characterised by secondary charged particles, as shown in the fragment tail and neutrons, which are released in nuclear reactions and distributed widely. Even in the in-field volume, particle fragments are involved in the therapeutic beam. However, most of the absorbed dose is delivered by primary particles. The effect of secondary particles becomes significant when no primary particles are present. In case of carbon ion radiotherapy, attention should be paid in treatment planning, if an OAR is present or not on the beam axis, beyond the end of the range. Thus the fragment tail is included in the beam kernel used in treatment planning for carbon ion radiotherapy.

(53) Except for the fragment tail, the effect of heavy secondary charged particles is not significant. Neutrons and charged particles generated by them are a main concern when considering the dose outside of the field. Due to their neutral charge, neutrons can scatter widely. This wide spreading means a sparse energy density, i.e., the effect of neutrons is, as a first approximation, considered to be negligible for the assessment of tumour control or acute radiation responses of normal tissues. The influence of neutrons concerns the development of late effect. The distribution of secondary neutrons is very different for proton and carbon ion beams. In carbon ion beams, neutrons can be emitted as both participants and spectators; this is not possible for proton beams since neutrons are not produced from the spectators. Since the spectators retain their original motion from before the reaction, neutrons, as projectile fragments, have high energy and are strongly forward directed.

(54) Neutrons from target fragments and the participants show a wide and isotropic distribution in the centre-of-gravity frame, and their energies are less than those of projectile fragments. This lack of projectile fragments as secondary neutrons in a proton beam, characterises the quasi-isotropic distribution of neutrons while the high energetic neutrons, in the forward direction, are added to the quasi-isotropic distribution in case of the carbon ion beam. It should be noted that the

distribution is greatly affected by the configuration of the beam line devices and the room design as neutrons are produced in such devices and scattered throughout the whole room (Silari, 2001; Tayama et al., 2006; Yonai et al., 2008; Mesoloras et al., 2006; Zacharatou Jarlskog et al., 2008).

(55) Production data of secondary particles, in the range of ion beam radiotherapy, have been compiled in detail by Nakamura and Heilbronn (2006). The yield of neutrons increases as the incident energy or target mass number increases. Beam line devices such as collimators or ridge filters, made of heavier materials, are the main neutron production sources.

4. RADIOBIOLOGICAL IMPLICATIONS

(56) The effect of ionising radiation is dependent on the absorbed dose, the dose rate, and the quality of radiation (ICRP, 2003b). In this section, the biological responses to radiation and health risks associated with radiation exposure are described. Specific issues associated with ion beam radiotherapy will be discussed in Chapter 5.

4.1. Interactions of radiation with DNA

(57) The critical target for the biological effects of ionising radiation in biological cells is the DNA molecule, although extranuclear damage also plays a role. Ionising radiation produces base change, single and double-strand breaks (dsb) in DNA by the direct deposition of energy or by an indirect reaction with radicals formed from the ionisation of water within a few nanometers of DNA. The approximate numbers of events in a mammalian cell, after exposure to low LET radiation versus high LET radiation for a dose of 1 Gy are given in Table 4.1. Both qualities of radiation produce 100,000 ionisations in the nucleus. The number of initial chromosome aberrations are also similar, however, the resultant number of lethal type chromosome aberrations differ markedly. This is because exposure to high LET radiation gives rise to more complex structured damage, which is less easily repaired or the repair is more error-prone (Goodhead et al., 1993; Sutherland et al., 2001). This type of damage contrasts with DNA lesions arising spontaneously via oxidative radicals, which are more randomly distributed in DNA and simple in their chemical structure. Error-prone DNA damage can lead to gene mutations and chromosome aberrations.

Table 4.1. Average yield of damage in a single mammalian cell for an absorbed dose of 1 Gy.

Event	Low LET	High LET
Track in nucleus	1,000	2
Ionisation in nucleus	100,000	100,000
Ionisation in DNA	1,500	1,500
Base damage	10,000	10,000
DNA ssb	850	450
RBE for DNA dsb	≈1	≈1
PCC break: Initial	6	12
PCC break: 8 hr	<1	4
Chromosome aberrations	0.3	2.5
Complex aberrations	10%	45%
Lethal lesions	0.5	2.6
Cells inactivated	30%	85%

LET: linear energy transfer; ssb: single-strand break; RBE: relative biological effectiveness, ssb: single-strand break, dsb: double-strand break, PCC: premature chromosome condensation. Reprinted with permission from Nikjoo H et al, 1998.

4.2. Health effects of ionising radiation

(58) The health effects of radiation exposure can be classified into deterministic effects (tissue reactions) and stochastic effects. Deterministic effects result from cell killing, cell loss or inflammation and are characterised by threshold doses. Stochastic effects are cancer induction and heritable effects. These result from genetic and epigenetic alterations and are assumed to have no threshold dose.

4.2.1. Deterministic effects (tissue reactions)

(59) The radiation effects on normal tissues are grouped into early reactions (days to weeks) and late reactions (months to years). The principal factors which influence the incidence and severity of normal tissue damages are total dose, dose per fraction, fractional dose rate, time interval between fractions, overall treatment time and dose-volume parameters. Clinical characteristics of early and late reactions and threshold dose are summarised in Table 4.2 (ICRP *Publication 103*, 2007b). It should be noted that recent epidemiological evidence suggests that there are some tissue reactions with very late manifestation, where threshold doses are lower than previously considered, particularly for the lens of eye and circulatory diseases (ICRP, 2012).

Early tissue reactions

(60) Early tissue reactions are expressed in rapidly proliferating tissues such as skin epithelium, gastrointestinal mucosa, gonads and the hematopoietic systems. These tissues have a hierarchical organisation with a proliferative compartment, with stem and progenitor cell populations, and the post-mitotic compartment of mature functional cells. The time course and types of injuries are dependent on turnover time of the specific cells and tissues. For example, the lifespan estimates range from a few days in granulocytes and the intestinal mucosa to more than 100 days for erythrocytes.

Late tissue reactions

(61) Late reactions are expressed in slowly proliferating tissues, such as lung, heart, kidney and central nervous systems, with the incidence of events still increasing with time, even more than 10 years after irradiation. Studies of atomic bomb survivors have shown an association between radiation and cardiovascular disease, stroke, digestive disorders and respiratory disease at very long times after exposure. There was little evidence of excess risk for doses below 0.5 Sv (UNSCEAR, 2008). Lung is a sensitive organ for late tissue reactions in terms of fibrosis, and fibrosis is a dose-limiting disease when a large volume of the chest is irradiated. The late reaction in skin is characterised by a thinning of dermal tissue, telangiectasia, and the possibility of late necrosis, as distinct from skin epidermal reactions, which are expressed as an early tissue reaction.

(62) Cataract is defined as detectable changes in the transparency of the lens of the eye. Small opacities can be detected after doses of 0.5-2.0 Gy. The dose for 1% incidence of cataract with visual impairment was considered to be around 1.5 Gy, but the value was revised to 0.5 Gy by ICRP (2012). Cataractogenesis is significantly spared by reducing dose-rate or by fractionation of the total dose for low LET photons (Belkacemi et al., 1996).

(63) The evidence on vascular disease has become available. An acute threshold dose of about 0.5 Gy was proposed for both cardiovascular and cerebrovascular diseases by ICRP (2012).

Volume effects

(64) The volume of tissue irradiated is a critical determinant of clinical 'tolerance'. There is a threshold volume of irradiation below which no functional damage of the whole organ is manifested, even after high radiation doses. The complication depends on the dose distribution and/or irradiated volume rather than the magnitude of dose in a small volume. Organs have been grouped into those with either a parallel organisation such as kidney and liver, or those with a serial organisation such as the intestine and spinal cord (Withers et al., 1988). However, others consider physiologically and anatomically related effects, including the vasculature, to be more important in the determination of the volume effect (Hopewell and Trott, 2004).

Table 4.2. Projected threshold estimates for acute absorbed doses, for a 1% incidence of morbidity and mortality, involving adult human organs and tissues after whole body gamma-ray exposure. Reproduced from ICRP *Publications 103* (ICRP, 2007b) and *118* (ICRP, 2012).

Effect	Organ/tissue	Time to develop effect	Absorbed dose (Gy)[e]
Morbidity (1% Incidence):			
Temporary sterility	Testes	3–9 weeks	~ 0.1[a,b]
Permanent sterility	Testes	3 weeks	~ 6[a,b]
Permanent sterility	Ovaries	< 1week	~ 3[a,b]
Depression of blood-forming process	Bone marrow	3–7 days	~ 0.5[a,b]
Main phase of skin reddening	Skin (large areas)	1–4 weeks	<3–6[a,b]
Skin burns	Skin (large areas)	2–3 weeks	5–10[a,b]
Temporary hair loss	Skin	2–3 weeks	~ 4[a,b]
Cataract (visual impairment)	Eye	> 20 years	~ 0.5[a,c]
Mortality:			
Bone marrow syndrome:			
– without medical care	Bone marrow	30–60 days	~ 1[b]
– with good medical care	Bone marrow	30–60 days	2–3[b,d]
Gastro-intestinal syndrome:			
– without medical care	Small intestine	6–9 days	~ 6[d]
– with good medical care	Small intestine	6–9 days	>6[b,c,d]
Pneumonitis	Lung	1–7 months	6[b,c,d]

[a] ICRP (1984, 2012).
[b] UNSCEAR (1988).
[c] Edwards and Lloyd (1996).
[d] Scott and Hahn (1989), Scott (1993).

[e] Most dose values are rounded to the nearest Gy; ranges indicate area dependence for skin and differing medical support for bone marrow.

4.2.2. Stochastic effects

(65) DNA damage to single cells can induce gene mutations or chromosome aberrations, which are critical for the induction of cancer and heritable diseases by radiation. For these diseases, the probability of occurrence depends on the radiation dose. A general model used for radiological protection is that the risks for stochastic effects increase linearly with no threshold, and this is referred to as the linear-non-threshold (LNT) model. Radiation-induced heritable risks have not been demonstrated in humans.

Cancers

(66) Cancer dose response relationships after acute low LET radiation exposure can be fitted at doses below 2 Gy by a linear or a linear-quadratic model for solid cancers and leukemia, respectively. At higher doses there might be a decrease or leveling off the risk with increasing dose because of competing effects of mutation and cell killing. The second cancers found after radiotherapy with fractionated doses, develop mainly after an accumulated dose larger than several tens of gray (Sachs and Brenner, 2005; Suit et al., 2007).

(67) Cancer risk due to radiation exposure is dependent on the tissues, gender and age-at-exposure. Risk models suggest relatively large risk parameters for breast, lung and colon (Preston et al., 2007).

(68) The inheritance of mutations of dominant tumour suppressor genes or DNA damage response genes may increase the probability of radiation-induced cancers. The risk of cancer development to the individuals with these genetic disorders will be high and additional risk is of concern at high doses during diagnosis and therapy using radiation. However, the presence of rare genetically susceptible sub-populations will not distort the risk estimation in typical human populations (ICRP *Publication* 79, 1998a).

(69) In radiation therapy, optimisation requires not only the delivery of the prescribed radiation dose to the target volume but also the protection of neighbouring normal tissues (ICRP, 2007d).

Heritable effects

(70) Although there continues to be no direct evidence in humans, there is evidence that radiation induces heritable effects in experimental animals. ICRP *Publication 103* provides the estimated hereditary risk up to the second generation of about 0.2% per Sv, which is much smaller than the estimated cancer risk of 5.5% per Sv.

4.3. Effects on embryos, fetuses and children

(71) The mammalian embryos and fetuses are highly radiosensitive during prenatal development (NCRP, 2013). Prenatal development is divided into three stages; pre-implantation (up to 10 days post-conception), organogenesis (3-7 weeks post-conception), and the fetal period. The risk of lethality to a developing organism is highest during the implantation stage. A dose around 100 mGy, produces

significant pre-implantation deaths in mice after irradiation during the zygotic stage (Pampfer and Streffer, 1988). With further fetal development, the radiosensitivity decreases. Malformations are mainly induced after irradiation in the organogenesis period. With exposure during the early development of the brain (8-15 weeks post-conception), severe mental retardation and a decrease in the intelligence quotient (IQ) may occur. The threshold doses are 300 mGy and 100 mGy, respectively (ICRP *Publication 90*, 2003a). *In utero* exposure was also shown to increase the risk of all types of childhood cancer in the largest case-control Oxford Study of Childhood Cancers (Bithell and Stewart, 1975). However, several cohort studies have found no clear evidence of an increase in radiation-induced childhood cancer (Boice and Miller, 1999; Schulze-Rath et al., 2008; Schonfeld et al., 2012). A recent report of atomic bomb survivors suggested that adult-onset cancer risk from *in utero* exposure is lower than that the cancer risk following exposure in early childhood (Preston et al., 2008).

(72) Children are more susceptible to radiation than adults in some types of tumours (UNSCEAR, 2013). Late deterministic effects after radiotherapy such as retardation of growth, hormonal deficiencies, organ dysfunction, and intellectual and cognitive functions are more severe in children than adults (UNSCEAR, 1993 Annex I, pp.903). Cataract prevalence increases with decreasing age-at-exposure (Nakashima et al., 2006). Young children are also susceptible to radiation induction of cancers. The excess risk of all solid cancers declines by 17% per decade of the age-at-exposure (ICRP *Publication 103*, pp. 197, 2007b). It should be noted that children have distinctly different organ susceptibility from adults, with a higher risk of both thyroid and skin cancers but lower risk of lung cancer (Preston et al., 2007).

4.4. Radiobiological factors

(73) Biological effects of ionising radiation are dependent on various factors including LET, track structure, energy, cell cycle stage at irradiation, oxygen concentration, dose-rate and the mode of dose fractionation.

4.4.1. LET and energy

(74) With increasing LET, the biological effect of radiation increases. The RBE of a particle relative to low LET radiation reaches a maximum value at around LET values of 100-200 keV/μm, depending on ion species. It falls for higher LET values due to ‘wasted’ dose or ‘overkill’. This tendency is considered due to overt-clustering of DNA lesions with some cells experiencing only cytoplasmic rather than nuclear damage, or the cell experiences no direct ionisation. In other cells, the amount of energy deposited by a single particle exceeds the amount required to kill the cell. Even for the same LET, the RBE is a function of the ion species. Thus, the RBE increases as a function of LET (up to a maximum) for a specific particle, while the RBE might even decrease with LET when comparing different particles. This fact demonstrates the limitations of the LET concept because the micro-structure of energy deposition event, or track structure, is only roughly approximated by the LET concept.

(75) For neutrons, the biological effects are strongly dependent on the neutron energy, being highest at ~ 0.4 MeV (Hall et al., 1975).

4.4.2. Cell cycle stage

(76) For low LET radiation, sensitivity varies, depending on the stage in the cell cycle. The most radiosensitive phase is G2/M. Cells are resistant in the stationary phase and late S phase. Generally, the dependence on cell cycle disappears when the cells are irradiated with high LET radiation, especially at low doses per fraction.

4.4.3. Oxygen

(77) The response of cells to low LET radiation is influenced by cellular concentration of oxygen. This reacts with the radicals formed by the hydrolysis, to produce more reactive oxygen species. Hypoxic cells are 2.5 to 3 times more radio-resistant than well oxygenated cells after exposure to low LET radiation. The OER is defined as the ratio of radiation doses to give the same level of biological effects in hypoxia to air. The OER decreases with increasing LET. The OER is close to unity for radiation with LET values greater than 200 keV/μm (Barendsen, 1968).

4.4.4. Dose-rate and fractionation

(78) With low LET radiation a reduction in the dose-rate or a multiple fractionation of the dose results in a reduction in the effects of a given dose of radiation. This is ascribed to the efficient repair of sublethal damage and cellular recovery. The therapeutic success of fractionation with low LET radiation for many tumours lies in the difference in radiosensitivity and repair capability between tumour cells and cells in healthy tissues. Because high LET radiation produces more complex damage, that is less easily repaired, the effects of dose fractionation and dose rate are smaller for high LET radiation.

4.5. RBE for ion beams and neutrons

(79) High LET radiation induces complex forms of DNA dsb, which are difficult to repair and are effective in cell killing as well as in mutation induction, transformation and cancer induction. The Commission introduced radiation weighting factor, w_R, for use in radiological protection to take into account the differences in the effects of different types of radiation (ICRP, 1991). In circumstances with radiotherapy using high LET radiations, the relevant values of RBE are important for the effective treatment of cancer. ICRP *Publication 92* reported an overview of RBE and w_R (ICRP, 2003b).

4.5.1. RBE values for ion beam radiation in deterministic effects

(80) RBE values are dependent on the dose deposition characteristics of the test radiation. For cell killing, at 10% cell survival using a colony forming assay, the RBE of helium and carbon particles increases up to a value of 3-4, being maximal at about 100keV/μm, and then falls for higher LET values (Ando and Kase, 2009). RBE values of less than 2 have been adopted for protons with energies of 50-2300 MeV, for endpoints such as clonogenic cell survival, the LD50/30 and intestinal crypt survival (ICRP, *Publication 92*, pp. 49, 2003b; Niemer-Tucker et al.,1999). The biological effect of protons, for the cataractogenic effect, is similar to that for photons, but the RBE for iron (190 keV/μm) and argon (88 keV/μm) rises to a value of 50-200 at low dose, for the same endpoint (Brenner, 1993).

4.5.2. RBE for ion beam radiations in stochastic effects

(81) RBE values are defined for a given endpoint and dose/level of effect. In contrast, radiation weighting factors (w_R) used in radiaological protection are defined as a conservative weighting factor for stochastic effects at low doses of radiation. Based on the linear-quadratic (LQ) formalism, as the dose response model, the RBE value reaches its maximum at an (imaginary) zero dose, then gradually decreases as the dose level increases. Thus w_R is related to the maximum RBE value. It should be emphasized that w_R values are designed for the practice of radiological protection, not for specific risk assessment (ICRP *Publication 92*, pp.30, 2003b).

(82) There is a good concordance between DNA dsb, especially complex clustered damage, and radiation-induced gene or chromosome mutations. In general, the dose-response relationship for mutation induction is linear-quadratic for low LET radiation, and tends towards a linear relationship for high LET radiation. The maximum RBE values are around 20-40, for particles with an LET in the range 50-70 keV/μm (Edwards, 1997; ICRP *Publication 92*, pp.61, 2003b).

(83) RBE values for the induction of *in vitro* neoplastic transformation in C3H10T1/2 cells increases up to a value of about 10 for an LET of 100-200 keV/μm (Yang et al., 1985, 1996). RBE values for 14, 30 and 172 keV/μm carbon ions, for transformation of HeLa X human skin fibroblast cell line CGL1, are 1.0, 2.5 and 12, respectively (Bettega et al., 2009).

(84) There are no data on the effects of ion beams that relate to stochastic effects in humans. Thus, risk estimates are derived from experiments on animals. The RBE value for 60 MeV protons, with an average LET of 1.5 keV/μm, compared with 300 kV X-rays, does not exceed 1.0 for both shortening of lifespan and tumour induction in mice (Clapp et al., 1974). A w_R value equal to 2.0 is recommended for protons (ICRP, 2007b). RBE for iron ions with an LET of 193 keV/μm and 253 keV/μm are 40 and 20, respectively, for the induction of Harderian tumours (Alpen, 1993). This indicates that a single w_R value for heavy ions is not appropriate. RBE values for ion beams are dependent upon the dose range used, being higher for lower doses (Fry et al., 1985; Imaoka et al., 2007). They are also tissue dependent, with a small value for leukemia (IARC, 2000, pp. 430). Although the Commission considers that the selection of a single value of w_R is an oversimplification, w_R = 20 is recommended for alpha-particles, fission fragments and heavy ions.

4.5.3. RBE for neutrons for stochastic effects

(85) The RBE of neutrons varies significantly with energy. The most effective neutron energy for pruducing chromosome aberrations in human lymphocytes is 0.4 MeV (Schmid et al., 2003). The RBE value, compared with ^{60}Co gamma-ray as reference radiation, is close to 100 (ICRP, 2003b). The RBE value for oncogenic transformation increases from 3.7 to 7.2 for 40keV to 350 keV of neutrons (Miller et al., 2000). The RBE values for mouse epithelial tumour induction are reported to be 20-30. The recommended w_R is represented as a continuous function with the maximum value of 20 at 1 MeV.

(86) Based on the RBE values for stochastic effects, the w_R proposed by the Commission for each type of radiation is given in Table 4.3. It should be noted that values of w_R are given for the radiation incident on the human body or, for internal radiation sources, emitted from the incorporated radionuclide, and are therefore independent of the organ or tissue considered.

Table 4.3. Recommended radiation weighting factors (w_R) (ICRP, 2007b).

Radiation type	Radiation weighting factor, w_R
Photons	1
Electrons and muons	1
Protons and charged pions	2
Alpha particles, fission fragments, heavy ions	20
Neutrons	A continuous function of neutron energy (2.5-20)

All values relate to a radiation incident involving the body or, for internal radiation sources, emitted from the incorporated radionuclide(s).
* Note the special issue of Auger electrons discussed in Section B.3.3 of Annex B in *Publication 103* (ICRP, 2007b).

4.5.4. RBE for the fetuses and children

(87) With regard to intra-uterine lethality, malformation and growth retardation in animal experiments, RBE values for high LET radiation have been proposed to be around 3 (ICRP, 2007b). No adequate human *in utero* and childhood exposure data are yet available to determine RBE values for ion beams for both deterministic and stochastic effects.

5. RADIATION EXPOSURES IN ION BEAM RADIOTHERAPY

5.1. Medical exposure of patients from therapeutic irradiation

5.1.1. In-field treatment volume

(88) The use of an ion beam greatly reduces the entrance dose due to its physical depth-dose characteristics, i.e., the Bragg peak, compared with the photon and electron beams used in conventional radiotherapy. In addition, a carbon ion beam has physical and biological characteristics that differ from proton beams: a lower scattering power, less fragment tail and a higher RBE value in the SOBP region. By using these characteristics, treatment planning in ion beam radiotherapy theoretically achieves a potentially curative radiation dose that has to be delivered to the target volume. Simultaneously the undesired exposure in normal tissues is reduced, if comapered to conventional radiotherapy.

(89) The in-field dose is considered in the treatment planning of each patient in view of side effects (deterministic effects), whereas the out-of-field dose is not usually considered. The method and process of treatment planning in proton radiotherapy have been described in ICRU Report 78 (2007). The treatment planning is essentially the same both in proton and carbon ion radiotherapy. There is a trade-off between dose escalation and the higher conformity required in the target volume for tumour local control and the dose or dose-volume constraints when considering the radiation toxicity in radiotherapy (Tsuji et al., 2005; Tsujii et al., 2008; Marucci et al., 2004; Kawashima et al., 2011). The dose distribution and dose volume histogram often play an important role in finding the best treatment plan based on clinical dose escalation studies (Kamada et al., 2002; Mizoe et al., 2004).

(90) The ratio of the Bragg peak absorbed dose versus the entrance absorbed dose is higher for carbon ions than for protons. However, as RBE is dose dependent (more significant for heavier ions), lower doses outside of the target, depending on their LET values, have to be scaled with a higher RBE value at biologically equivalent doses (ICRP, 2003b). Nevertheless, the price to be paid for such a possible advantage of lower peak/plateau ratio when using carbon ions is the creation of fragments causing residual dose just after the Bragg peak. This phenomenon is negligible for protons.

(91) Palm and Johansson (2007) compared conventional radiotherapy, IMRT, and proton radiotherapy with respect to the conformity index and dose distributions in the target volume, OARs, and non-target tissues, based on published treatment planning studies. They also studied published measurements and Monte Carlo simulations of the out-of-field dose distributions, and clearly demonstrated that a more favorable dose distribution could be obtained in the OARs and non-target tissue using proton radiotherapy compared with IMRT. IMRT and proton radiotherapy have a similar ability to improve the dose distribution in the target volume, which may increase the probability of tumour control, as well as the dose conformity compared with conventional radiotherapy. Both forms of treatment also reduced the maximum dose to OARs. Palm and Johansson (2007) also noted that the size of the penumbra has a large impact on dose conformity in the target and on the maximum dose to OAR volumes adjacent to the target volume. This means that

carbon ion radiotherapy can reduce the maximum dose to OARs because a carbon ion beam has a lower scattering power.

(92) An example, showing the comparison of the dose distributions with IMRT and carbon ion (broad beam method) radiotherapy treatment plans for a parotid gland cancer, is shown in Fig. 5.1. The target-volume (cyan line) is almost totally covered by the 95% iso-dose line (red line) in both plans. The dose convergence in the low dose region in the plan for carbon ion radiotherapy is superior to that for IMRT. These reductions in the undesired exposure can lead to reduced side effects in OAR. The undesired exposure dose near or in the irradiation field depends on the treatment planning of each patient, but still follows the conclusions given above, even using the broad beam method.

a) The plan for IMRT

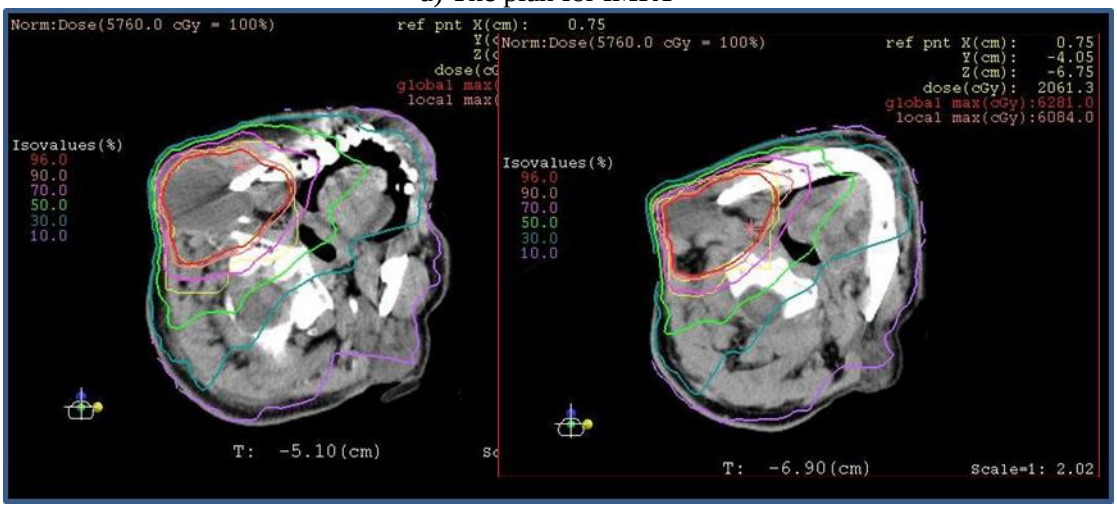

b) The plan for carbon ion radiotherapy

Fig. 5.1. Comparison of dose distributions in treatment plans for IMRT and carbon ion radiotherapy, using the broad beam method, for parotid gland cancer.

5.1.2. Out-of-field volume

(93) Ion beam radiotherapy should emerge as a useful irradiation treatment technique, deliver high doses in a very limited and well-defined volume, while sparing most of the rest of the body. However, the type of beam delivery, i.e., broad or scanning beam, might influence the dose, at a distance, outside the target volume (Hall, 2006).

Which types of radiation influences the dose in the out-of-field volume?

(94) The simulated partial contributions to the total absorbed dose, in a Lucite phantom, from protons, neutrons and photons in proton radiotherapy, for prostate cancer, are shown by Clasie et al. (2010). There is a large proton contribution to the total dose at a distance less than 10 cm from the field edge, due to primary protons, regardless of the irradiation method. Also, protons scattered by the final collimator make a 10-15% contribution to the total dose at a distance greater than 15 cm from the field edge in a beam produced by the broad beam method. The photon dose contribution increases with distance from the field edge, for example, to 60% at 60 cm from the field edge by the scanning method. However, after considering their higher biological effectiveness, at a distance greater than 10 cm from the field edge, the largest fraction of the total equivalent dose is due to neutrons.

(95) There are two components to the secondary neutrons produced in ion beam radiotherapy: (i) neutrons produced in the patient (internal neutrons); and (ii) neutrons produced in the beam line devices (external neutrons). Internal neutrons are an inevitable dose component with the use of both broad and scanning beam methods because they are produced by interactions of the charged particles that deliver the potentially curative dose to the target volume. External neutrons are produced in nuclear reactions with primary charged particles in beam line devices. The distribution of the proton and neutron flux for a prostate treatment using double-scattering proton radiotherapy, obtained using Monte Carlo simulation, are shown in Fig. 5.2 (Fontenot et al., 2008). All beam line devices, which the primary charged particles inevitably enter, become a source of external neutrons. The dose contribution from neutrons, produced in each device to the total dose to the patient, depends on the location, the material of the device, the configuration and the number of primary particles that enter the device. Such dependence is discussed in detail below.

(96) Several investigations, using Monte Carlo simulations, have been undertaken to evaluate the contribution of internal and external neutrons to the total dose for prostate and lung cancer treatments in proton radiotherapy using the broad beam method (Jiang et al., 2005; Fontenot et al., 2008; Zacharatou Jarlskog et al., 2008; Taddei et al., 2009). Internal neutrons were shown to contribute significantly to the dose near the target irradiation volume, while external neutrons became the main contributor to organ doses further away from that volume.

(97) Fontenot et al. (2008) calculated equivalent doses in each organ using Monte Carlo N-Particle eXtended (MCNPX) simulations (Pelowitz, 2008), assuming the beam characteristics of the passive scattering nozzle used in M.D. Anderson Proton Therapy Center. For a simulated prostate treatment, external neutrons accounted for more than 98% of the neutron equivalent dose for organs, such as the oesophagus and thyroid, distant from the treatment volume. On the other hand, approximately 40% of the neutron equivalent dose was attributed to internal neutrons for organs near the treatment volume such as the bladder, rectum and gonads. The dose distribution from neutrons depends on the body size (Zacharatou Jarlskog et al., 2008; Athar and Paganetti, 2009).

(98) Yonai et al. (2009) calculated the proportional contribution of neutrons, produced in each beam line device and a water phantom, to the ambient dose equivalent on the treatment couch in carbon ion radiotherapy at the Heavy Ion Medical Accelerator in Chiba (HIMAC) using the PHITS code (Iwase et al., 2002; Niita et al., 2006). The main source was external neutrons (those produced in components other than water), which was the same as in proton radiotherapy. The contribution of internal neutrons, to the total neutron ambient dose equivalent, was only 10% at 25 cm from the beam axis. The contribution decreased with distance from the beam axis.

(99) These results clarified that neutron exposure in ion beam radiotherapy, with the scanning method, was lower than that with the broad beam method. This is because the number of external neutrons produced associated with the scanning method, is smaller compared to that with the broad beam method.

(100) In carbon ion radiotherapy, the fragmented charged particles produced by the incident carbon beam are also a contributor to the dose at a position close to the irradiation volume. Their characteristics are discussed in Chapter 3. In the current TPS, dose in the fragment tail region is considered. On the other hand, the lateral distribution of the lighter fragmental particles, such as protons, is not simulated accurately because of the higher scattering power, including a lateral 'kick' at the point of production of fragments (Kanai et al., 2004; Matsufuji et al., 2005; Kusano et al., 2007). Although the dose is considerably lower than that from the primary particles, it is necessary, for the dose assessment in the out-of-field volume, to include laterally-distributed fragmental charged particles in carbon ion radiotherapy.

What influences the production of secondary neutrons?

i) Beam line devices

(101) The fluence, energy spectrum and angular distribution of secondary neutrons from nuclear reactions with ion beams depend on the energy and the species of the incident particles and the target nuclei, as described in Section 3. In addition, the secondary neutrons are moderated or shielded by the beam line devices. Therefore, the neutron dose at the patient position depends on the material, the location and the configuration (thickness and shape, etc.) of each beam line component and their relationship, i.e., the design of the beam delivery system.

(102) The neutrons produced in collimators are the predominant component of the external neutron dose in irradiation using the broad beam method. This is because the collimators are located close to the patient, and many primary particles stop at this location in the beam line (Brenner et al., 2009; Yonai et al., 2009; Hecksel et al., 2010).

(103) Installation of a pre-collimator has a considerable impact on reducing the secondary neutron dose (Zheng et al., 2007; Brenner et al., 2009; Yonai et al., 2009). The pre-collimator allows a flexible arrangement in the beam delivery system, compared with the final collimator. This is because the pre-collimator has little effect on the treatment beam, such as the beam penumbra. If it is far from the patient and can be increased in thickness, then the production of secondary neutrons can be moderated or shielded. Brenner et al. (2009) and Yonai et al. (2009) also showed that using collimators made of a material with a greater shielding effect, such as nickel, effectively reduced the secondary neutron dose.

(104) Other components which influence the secondary neutron production are range-shifting and range-modulating devices. Using MCNPX simulations, Polf et al. (2005) calculated the fraction of dose equivalent due to neutrons produced by a

Lucite range modulation wheel (RMW), a final brass collimator and a Lucite phantom, 50 cm downstream from the iso-center, along the beam axis with an increasing RMW step thicknesses (thicknesses of the Lucite slab assuming the RMW) assuming the characteristics of a beam line in the Harvard Cyclotron Laboratory. This study indicated that neutrons produced in range-shifting and range-modulating devices contribute to the dose of the patient more when the range shifter is thicker and/or the SOBP width is larger. More consideration, as to the influence of these devices, is needed in proton radiotherapy compared with carbon ion radiotherapy, because, due to the higher scattering power, the beam delivery system in proton radiotherapy is shorter than that in carbon ion radiotherapy. Shielding methods to reduce the neutron dose to patients have been proposed by Taddei et al. (2008) and Yonai et al. (2009).

ii) Beam parameters

(105) The influences of beam parameters have been investigated by several groups (Mesoloras et al., 2006 ; Zheng et al., 2007; Zacharatou Jarlskog et al., 2008; Polf et al., 2005; Yonai et al., 2008; Shin et al., 2009; Athar and Paganetti, 2009; Hecksel et al., 2010). The following parameters are considered to have the major influence on the neutron dose to patients in ion beam radiotherapy using the broad beam method.

- Beam energy
  The total number of neutrons definitely increases with increasing energy, because their path becomes longer and therefore the likelihood for reactions increases. As a result, the neutron absorbed dose per therapeutic dose increases with the energy of the primary beam.
- SOBP width
  As the modulator is thicker, the number of external neutrons increases because primary particles have more nuclear reactions and lose more energy in the range modulator. When the width of the SOBP is increased, more primary particles are needed to deliver a prescribed dose to a target volume. Thus the total neutron dose from internal neutrons per target dose increases with the SOBP width.
- Snout or beam nozzle, position (distance between the final collimator and the treatment isocentre)
  The neutron dose decreases as the snout position is located farther away from the patient because the neutron source is farther away from the patient.
- Beam size (which is defined as the size of a laterally-uniform field produced by the double-scattering or wobbler-scatterer methods).
  The neutron dose component in the target dose increases, as the beam size increases, when the aperture size is fixed. This phenomenon is observed regardless of the technique used to make a laterally uniform field: *i.e.* the double-scattering or wobbler-scatterer method. This is largely because more primary particles are needed to deliver a prescribed dose to a target volume, when the beam size is larger.
- Aperture size (which is determined by aperture size of collimators. This is almost equivalent to the beam size irradiated to the patient when excluding the beam divergence)
  The number of external neutrons decreases and the number of internal neutrons increases as the aperture size is increased, when the beam size is fixed. This is because the number of primary particles entering the final

collimator decreases and the number of primary particles entering the patient increases. Consequently, the total neutron dose would change depending on the fraction of the contribution of internal and external neutron doses.

(106) The beam parameters are determined by the treatment planning and the snout position is determined geometrically. Usually the snout is as close to the patient as possible to minimise the penumbra size. Therefore, using the broad beam method, the only way to reduce the external neutron dose is to minimise the beam size, i.e., to maximise the beam efficiency. Yonai et al. (2008) showed that this approach effectively reduces the neutron dose. However, in practice it is laborious to minimise the field size for each patient, because it is necessary to manage a large number of sets of beam parameters and to install a lot of scatterers, when using a double-scattering method. A practical approach is required; for example, the use of several beam sizes such as small, medium and large.

(107) The parameters in the scanning method that have the main effect on the neutron dose to patients are beam energy and the number of primary particles, because the number of external neutrons with the scanning method is much smaller compared to the number produced with the broad beam method.

How much is the dose in the out-of-field volume?

(108) Measurements and calculations of the out-of-field doses for proton radiotherapy have been reported (Xu, et al., 2008). The dose equivalent by neutrons, as a function of distance to the field edge for proton radiotherapy, is shown in Fig. 5.3. Three studies, Yan et al. (2002) (measurements with Bonner sphere), Polf et al. (2005) (Monte Carlo simulation with MCNPX) and Zheng et al. (2007) (Monte Carlo simulation with MCNPX), have assessed the in-air neutron dose equivalent for proton radiotherapy using the broad beam method. Schneider et al. (2002) measured the in-air neutron dose equivalent with a rem-meter for a scanning proton radiotherapy beam, except for one measured point close to the field edge where the neutron dose equivalent was measured using CR-39 in a water phantom. The other three studies only investigated the in-phantom dose. Ambient neutron dose equivalents measured in air tend to show higher values compared with the neutron dose equivalent in a phantom, as shown in Fig. 5.4. However, in-air data are helpful to understand differences between different facilities and different irradiation techniques. Although there are differences in the beam parameters and the experimental and calculation geometry used to establish the results, it is confirmed that the neutron dose in ion beam radiotherapy with the scanning method is significantly less than that with the broad beam method because the number of external neutrons is small or insignificant.

(109) Yonai et al. (2008) measured the neutron ambient dose equivalent at the patient position in four proton radiotherapy facilities in Japan with approximately the same parameter settings beam-shaping devices with exactly the same experimental setup, in order to investigate the facility dependence of the neutron dose (Fig. 5.5). This study showed that the variation by the facility-dependency was within a factor of three, regardless of the method to make the uniform irradiation field, namely the double-scattering or wobbler-scatterer methods. A facility-dependency was derived for two components: i) differences in the beam line devices and ii) differences in the operational beam parameters used in routine treatment, especially the field size, as noted above. It was also found, for the broad beam method, that the neutron dose in carbon ion radiotherapy is less than that in proton radiotherapy, when the beam parameters are the same.

(110) Gunzert-Marx et al. (2008) at GSI measured the energy spectra, angular distributions and yields of secondary charged particles and fast neutrons produced by 200 MeV/n ^{12}C ions, stopping in water. The absorbed dose outside treatment volume due to neutrons was estimated to be less than 1 % of the treatment dose. The level of the neutron doses in proton radiotherapy is similar to that in carbon ion radiotherapy, even though the neutron yield is much higher for carbon ions. This is explained by the fact that a much higher number of protons are needed to produce the same target volume dose as for carbon ions.

(111) Organ-specific information on the absorbed dose and biological effectiveness, in the patient, is essential for assessing risks, because secondary neutrons are the main component of the out-of-field dose, and the undesired dose is not uniformly distributed in the human body. However, at present there are only a few studies related to this issue when compared with those on in-air dose assessment. Measurements were generally made using a microdosimetric technique to obtain the lineal energy distributions (Wroe et al., 2007; 2009, Yonai et al., 2010), which are related to the biological effectiveness. Calculations were carried out using a computational anthropomorphic phantom and Monte Carlo codes such as Geant4 (Agostinelli et al., 2003), FLUKA (Fasso et al., 2005), MCNPX (Pelowitz, 2008), PHITS (Iwase et al., 2002; Niita et al., 2006), or SHIELD-HIT (Gudowska et al., 2004).

(112) Wroe et al. (2007, 2009) have measured the dose-averaged quality factor (Q_D) and dose equivalent (H) in proton fields obtained by using the broad beam method at the Loma Linda University Medical Center for various clinical treatments, using a silicon-on-insulator (SOI) microdosimeter and either an anthropomorphic phantom or a block phantom made of Lucite or polystyrene. With the broad beam method, Yonai et al. (2010) have also measured Q_D and H in the proton field at the National Cancer Center Hospital East (NCCHE) and those in the carbon ion field. For this a tissue-equivalent proportional counter (TEPC) and a water phantom were used. For the 235 MeV proton beam, the measured H per treatment absorbed dose and Q_D obtained by Wroe et al. (2007, 2009) and Yonai et al. (2010) are compared in Fig. 5.4. It should be noted that not only neutrons but also other types of radiation contribute to these dose equivalents and quality factors. H is lower as the location moves farther from the beam axis and on the upstream side of the phantom. H measured by Yonai et al. (2010) was two to three times higher than those by Wroe et al. (2007; 2009). This should be attributed to facility dependence as discussed above. Q_D is higher at lower water-equivalent depth (WED), because the contribution of secondary neutrons produced in the beam line devices with a high quality factor is higher. As the position is closer to the field edge (within ~20 cm from the field edge), Q_D is decreased by 2 mainly due to the scattered incident protons. From these results, the following conclusions for 235 MeV proton beam were drawn: i) at a position within ~20 cm from the field edge, Q_D is 2-5; ii) at a position close to the beam line devices, Q_D is 7-8, and iii) at other positions, Q_D is 5-6. It is expected that these values depend slightly on beam energy as shown below.

(113) Measured H, per treatment absorbed dose, and Q_D for the 400 MeV/n carbon ion beam at HIMAC, is shown in Fig. 5.6 (Yonai et al., 2010). H is lower as the location moves farther away from the beam axis and on the upstream side of the phantom. Q_D is lower as the location moves closer to the beam axis, but does not depend on an off-axis distance. The fragmental charged particles, especially protons, which are generated in the patient, strongly influence H and Q_D at the locations close to the field edge. Q_D is 2-4 within ~50 cm from the field edge, and at other locations,

Q_D is relatively constant between 4 and 5. In both proton and carbon ion beams, H is higher and Q_D is constant or slightly lower, as the incident beam energy is higher (Wroe et al., 2009; Yonai et al., 2010).

(114) Several studies have used computational anthropomorphic phantoms and Monte Carlo simulations to calculate organ doses for proton radiotherapy. Jiang et al. (2005) used the Geant4 code to simulate an adult male, VIP-Man, using two proton radiotherapy treatment plans, for lung and paranasal sinus cancers. To calculate equivalent dose to each organ, the absorbed dose in each voxel was accumulated and the neutron fluencies and energies at the surface of each organ were stored to be used for calculating the average neutron radiation weighting factor based on the *Publication 60* (ICRP, 1991).

(115) Mesoloras et al. (2006) used a bubble detector and an anthropomorphic phantom to experimentally evaluate the neutron dose equivalent to a representative point for the fetus of a mother receiving proton radiotherapy using the broad beam method. Their results are included in Fig. 5.3. In practice, a bubble detector can only measure the absorbed dose, not the biologically effective dose. They used the average neutron quality factor derived by Jiang et al. (2005) based on the Monte Carlo calculations.

(116) Zacharatou Jarlskog and Paganetti (2008) used the Geant4 code to assess and compare organ doses for paediatric and adult patients. It was shown that paediatric patients would receive higher organ equivalent doses than adults from neutrons generated in the treatment head, because younger patients have smaller body sizes. The equivalent doses, averaged over all fields, as a function of phantom age (i.e., patient's age) for 15 organs are shown in Fig. 5.7. The doses vary more significantly with patient's age for organs further away from the target volume.

(117) Monte Carlo simulations are a necessary tool to assess the organ-specific doses and the change in the dose with beam parameters. However, since experimental data are scarce as noted above, experimental verification of Monte Carlo simulations is limited. Additional experimental data are required for accurate dose estimation.

(118) Since the secondary neutron dose is facility dependent, it is desirable that each facility measures the secondary neutron dose to the patient. For this purpose, measurement of the ambient dose equivalent, with a rem-meter, is convenient; its values may indicate the maximal secondary dose in phantoms as shown in Fig. 5.4.

(119) Careful considerations on dead time and signal pile-up in the measurement are required, especially for a pulsed beam. Since the neutron dose depends on the beam parameters and measurement setup, the standardisation of these measurements is needed. In addition, a critical level is needed for proton and carbon ion radiotherapy similar to dose reference levels for diagnostic procedures. Further discussions are needed to establish the regulation and the critical level.

Is out-of-field dose in proton and carbon ion radiotherapy higher than that in external photon radiotherapy modalities?

(120) Many studies have been carried out to investigate out-of-field exposure of patients receiving external photon beam therapy such as conventional radiotherapy, three-dimensional conformal radiotherapy (3D-CRT), IMRT, tomotherapy and SRT as compared with proton and carbon ion radiotherapy. Several review papers have also summarised the dosimetric data (Stovall et al., 1995; Palm and Johansson, 2007; Xu et al., 2008).

(121) When considering out-of-field exposure in external beam photon therapy, the stray photons scattered by the collimator and patient as well as leakage from the treatment unit heads are more important than secondary neutrons at relatively low primary photon energies. Above 10 MeV secondary neutrons produced in photonuclear reactions inrease with increasing primary photon energy. Scattered photons dominate near the irradiation field, whereas leakage photons are more isotropic. The neutron dose contribution is relatively independent of distance from the field edge; however, it depends on depth and beam energy. Out-of-field doses in external photon beam radiotherapy also depends strongly on the treatment plan such as field size and the total monitor units (MU) and on the accelerator type, due to collimator angle and design including shielding devices (Van der Giessen, 1996; Kry et al., 2005a). Recently, exposure during IMRT was investigated by many groups together with 3D-CRT, because IMRT (and tomotherapy) requires more MUs to deliver the same prescribed dose to a tumour (Followill et al., 1997; d'Errico et al., 2001; Vanhavere et al., 2004; Kry et al., 2005a,b, 2007; Howell et al., 2005, 2006).

(122) Athar et al. (2010) compared proton and 6-MV IMRT treatments for a variety of treatment plans and patient age groups. They concluded that in-field, there is a distinct advantage for proton beams due to the lower integral dose. Out-of-field but within 20 cm distance there was an advantage for IMRT while farther away the neutron equivalent dose from proton radiotherapy was clearly lower than the scattered photon dose in IMRT.

(123) Yonai et al. (2010) compared the out-of-field dose in proton and carbon ion radiotherapy using the broad beam method with that in IMRT as obtained by Kry et al. (2007). Assuming that the treatment dose was 66 Gy(RBE)[2] for a 400 MeV/n carbon ion beam and 74 Gy(RBE) for a 235 MeV proton beam, which are the typical conditions for treatment of prostate cancer, the total dose equivalents at 13 cm from the beam axis and 20 cm depth in a water phantom is up to 190 mSv for both beams. Also, the dose equivalent at 25 cm from the beam axis and 5 cm depth in a water phantom is 57 mSv for the carbon ion beam and 192 mSv for the proton beam when assuming two opposed beams. These values are comparable to or less than those of lung, oesophagus and thyroid in 3D-CRT and IMRT for prostate cancer.

[2] Gy(RBE): RBE weighted absorbed dose (ICRU, 2007).

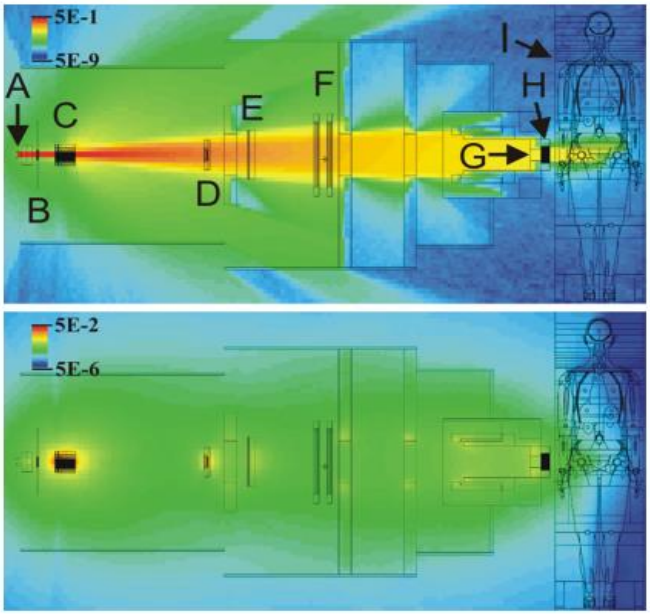

Fig. 5.2. Distributions of the proton (top) and neutron (bottom) flux for a prostate treatment using double-scattering proton radiotherapy, obtained using Monte Carlo simulation. A proton pencil beam (A) enters through a vacuum window and traverses a profile monitor (B). The rotating range modulator wheel (C) and second scatterer (D) spread the beam longitudinally and laterally. Also modeled are the range shifter (E), main and sub-dose monitors (F) and the snout, which contain the patient-specific aperture (G) and range compensator (H). Units of the legends are particles per cm^2 per incident proton. Reprinted from Fontenot et al., 2008. (Permission needed)

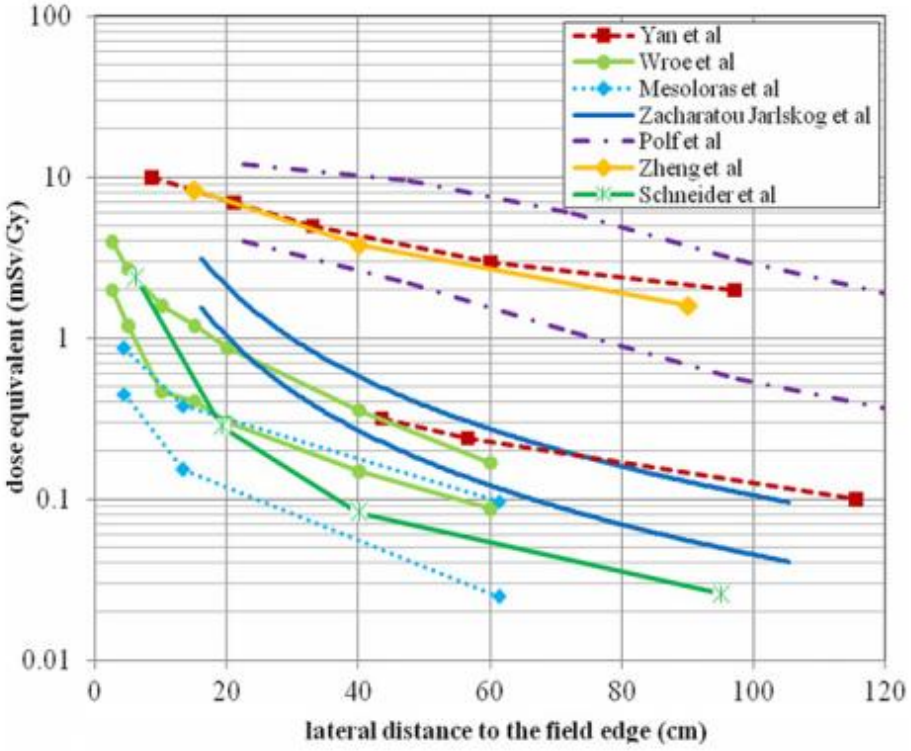

Fig. 5.3. Neutron dose equivalent as a function of distance to the field edge reported by three different proton experiments (Yan et al., 2002, Wroe et al., 2007, Mesoloras et al., 2006) and two sets of Monte Carlo simulations using passive scattering techniques (Polf and

Newhauser 2005, Zheng et al., 2007). Monte Carlo simulations by Zacharatou Jarlskog et al. (2008) show neutron equivalent doses. Also included are data from proton beam scanning (Schneider et al., 2002). Because of the significant dependence of neutron doses on beam parameters in proton therapy, two curves are shown from each publication to represent the best- and worst-case scenarios. Reproduced from Xu et al., 2008. (Permission needed)

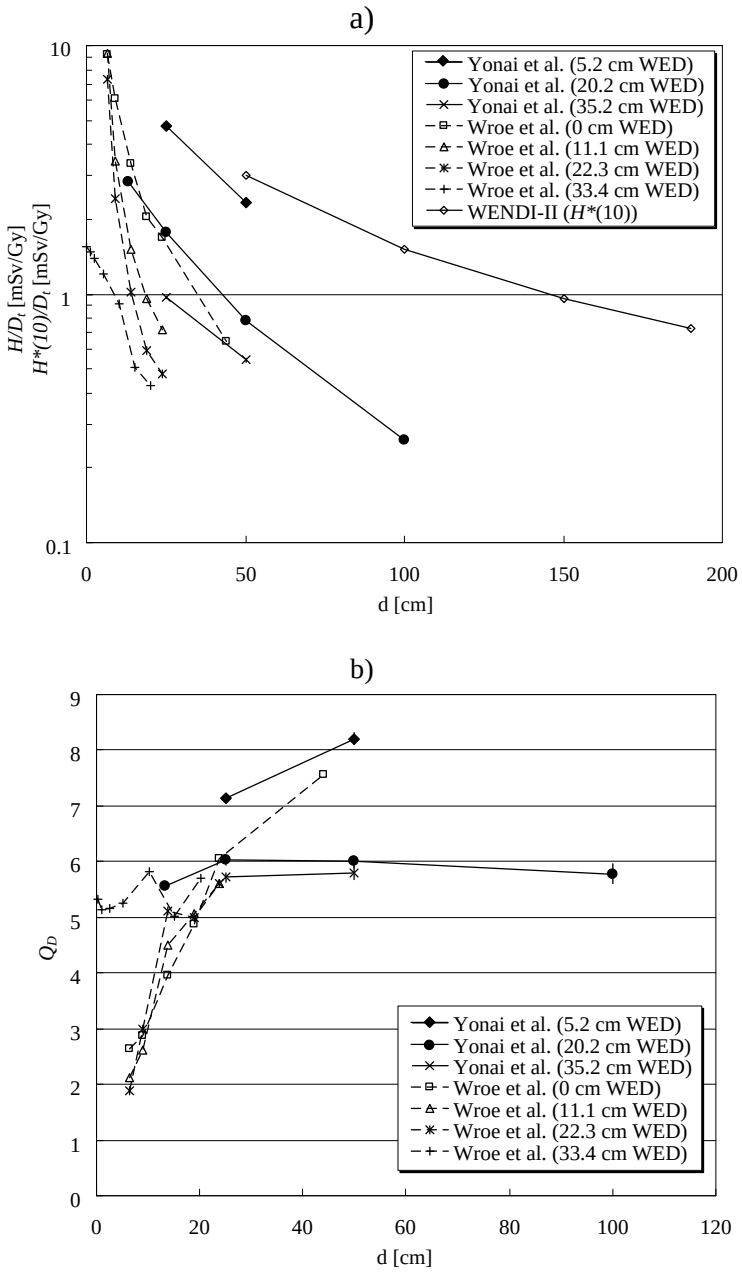

Fig. 5.4. Comparison of measured *H values* per treatment absorbed dose at the centre of the range-modulated region, H/D_t, and Q_D by Wroe et al. (2007, 2009) and Yonai et al. (2010) for the 235 MeV proton beam. Here, the Q(y)-y relationship from the ICRU Report 40 (1986) was used in both studies. WED means the water-equivalent depth of the measured position. a) Dose equivalent per treatment absorbed dose at the centre of the range-modulated region, H. Measured neutron ambient dose equivalents, $H^*(10)/D_t$ obtained with the rem-meter WENDI-II are also shown (Yonai et al., 2008). b) Dose-averaged quality factor, Q_D. The error bar represents the standard deviation. (Permission needed)

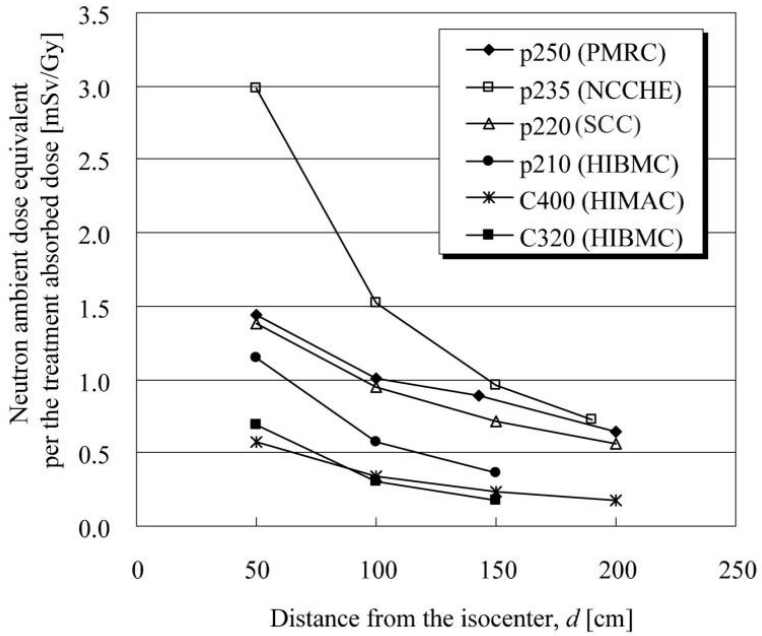

Fig. 5.5. Measured ambient dose equivalent in the proton and carbon radiotherapies with broad beam mtehod. The legends show the beam species, the energy and facility. “p” and “C” indicate the beam species of proton and carbon ions, respectively. The numerical value following “p” or “C” indicates the beam energy in MeV/n. Modified from Yonai et al., 2008. (Permission needed)

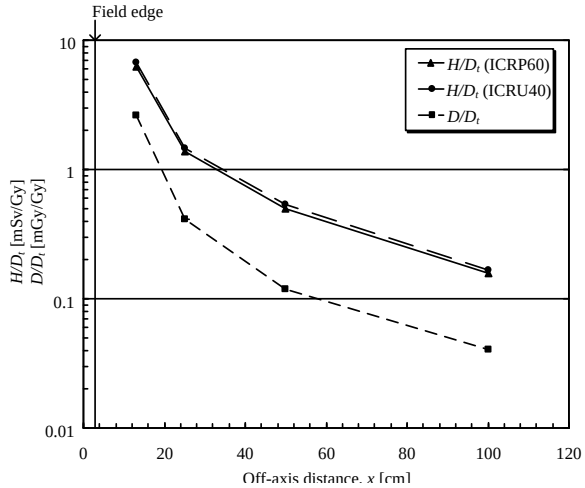

a) D/D_t and H/D_t on the line d=20 cm.

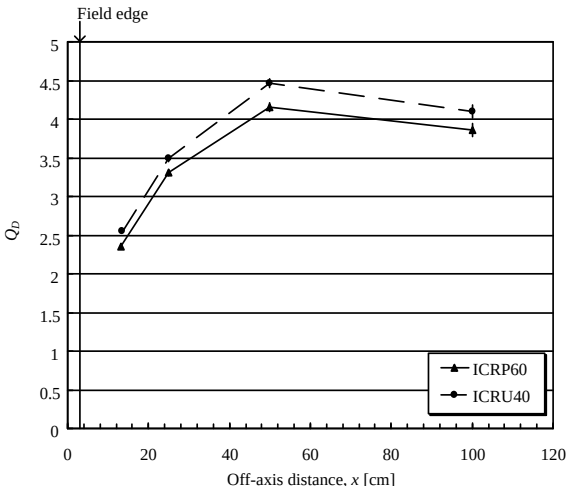

c) D/D_t and H/D_t on the line x=25 or 50 cm.

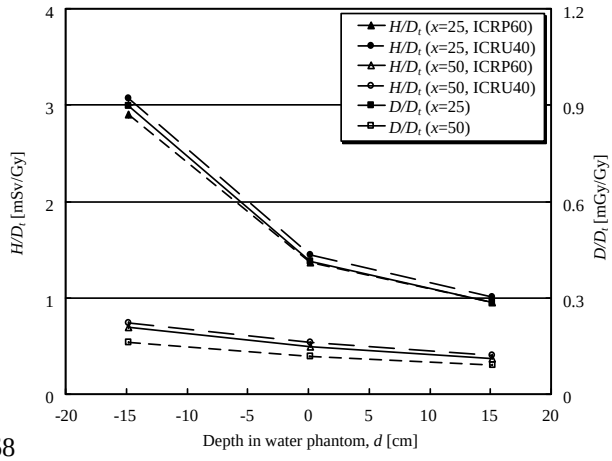

b) Q_D on the line d=20 cm.

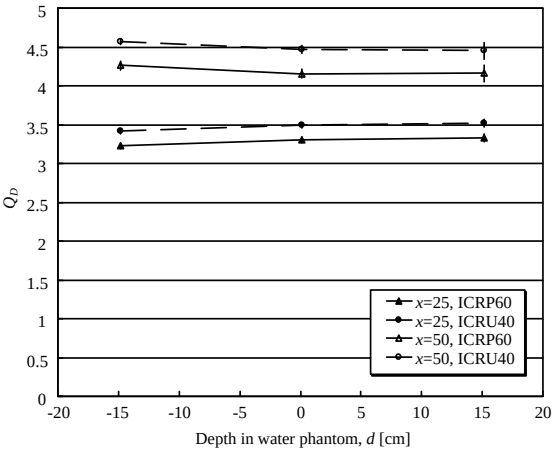

d) Q_D on the line x=25 or 50 cm

Fig. 5.6. Measured absorbed dose per treatment absorbed dose at the centre of the range-modulated region, D/D_t, dose equivalent per treatment absorbed dose at the centre of the range-modulated region, H/D_t, and dose-averaged quality factor, Q_D, for the 400-MeV/n carbon beam. a) D/D_t and H/D_t on the line d=20 cm. b) Q_D on the line d=20 cm. c) D/D_t and H/D_t on the line x=25 or 50 cm. d) Q_D on the line x=25 or 50 cm. The error bar represents the statistical error. Reprinted from Yonai et al, 2010. (Permission needed)

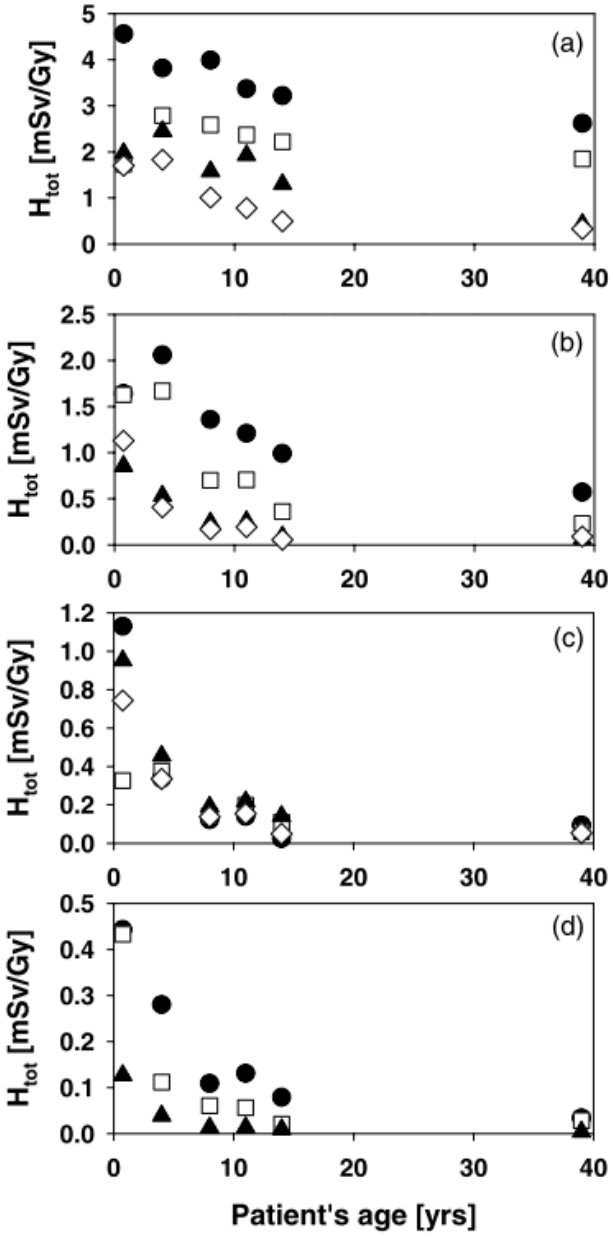

Fig. 5.7. Equivalent dose as a function of phantom age averaged over all fields. (a) Lenses (closed circles), thyroid (open squares), thymus (closed triangles) and lungs (open diamonds). (b) Oesophagus (closed circles), heart (open squares), liver (closed triangles) and stomach (open diamonds). (c) Spleen (closed circles), gall bladder (open squares), adrenals (closed triangles) and pancreas (open diamonds). (d) Kidneys (closed circles), small intestine (open squares) and bladder (closed triangles). Reprinted from Zacharatou Jarlskog and Paganetti, 2008. (Permission needed)

5.1.3. Risk assessment of stochastic effects, especially second cancers

(124) The expanding use of radiotherapy, coupled with improvement in long-term patient survival, constant vigilance is needed to monitor and evaluate the possible risks of second cancer after radiotherapy (NCRP, 2011). The second cancer risk to a patient depends on both the volume of the high dose region in the irradiation field

and the low dose region outside the field. Proton and carbon ion radiotherapy achieves the best dose distribution for the target volume as mentioned above, and obviously, results in not only reducing side effects in OARs but also minimising second cancer risk within or near the irradiation field. Second cancer risk in the low dose region, that is whole-body exposure, remains a controversial issue. As shown in Section 5.1.2, this exposure is considerably lower than that close to the treatment target volume, but it may not be negligible for risk assessment, especially for younger patients.

(125) Fontenot et al. (2009) assessed the second cancer risk from proton radiotherapy with the broad beam method and 6-MV IMRT, taking into account contributions from primary and secondary radiations for prostate cancer. Doses from the primary and secondary radiations were determined from the treatment planning and Monte Carlo simulation, respectively. The risk was estimated by using risk models from the BEIR VII Report (2006). They concluded that proton radiotherapy can reduce the incidence of second cancer in prostate cancer patients compared with IMRT, even if the dose from secondary neutrons is included. However, the primary beam is the dominant contributor to the second cancer risk for both modalities, and the impact of the neutrons produced in proton radiotherapy is of secondary importance. Though the methods to calculate the risk are different in Schneider et al. (2007) and Fontenot et al. (2009), the relative risk estimates for proton radiotherapy with the scanning method agree remarkably well.

(126) Newhauser et al. (2009) assessed the absolute lifetime risk of second cancer after receiving craniospinal proton radiotherapy by using Monte Carlo simulations, and combined their work with the previous risk assessment from only the primary beam by Mirabell et al. (2002). They showed that the risk of second cancer from IMRT and conventional photon treatments were 7 and 12 times higher than the risk from proton treatment with the scanning method, respectively, and 6 and 11 times higher than from that with the broad beam method, respectively. It was also noted that the risk of proton radiotherapy was dominated by primary proton radiation, not secondary neutrons, which is the same conclusion reached by Fontenot et al. (2009). These studies concluded that the undesired dose in the out-of-field volume is negligible for the second cancer risk in proton radiotherapy.

(127) Zacharatou Jarlskog and Paganetti (2008) estimated the risk caused by neutrons outside the treatment volume and the dependence on the patient's age based on the BEIR risk models. Their findings are the followings:

- The main contributors (>80%) to the neutron-induced risk were neutrons generated in the treatment head.
- A change in treatment target volume causes a variation of the risk by up to a factor of 2. Young patients are subject to greater risks than adult patients because of the geometric differences and age dependence of the risk models.
- Although the organ-specific risks seem to be rather small, the total risk for all organs is not negligible. This holds true in particular for very young patients.

(128) Athar and Paganetti (2009) have used computational whole-body (gender-specific and age dependent) voxel phantoms. They analyzed second cancer incidence risks for various organs as a function of patient age and field size based on two risk models. For example, in an 8-year-old female patient treated with a spinal proton radiotherapy field, breasts, lungs and rectum had the highest radiation-induced lifetime cancer incidence risks. These were estimated to be 0.71%, 1.05% and 0.60%, respectively. Risks for male and female patients decrease as their age at treatment time increases.

(129) Schneider et al. (2008) also investigated the risks for an adult treated for prostate cancer and a 14-month-old child with a rhabdomyosarcoma of the prostate using the organ equivalent dose (OED) concept (Schneider et al., 2005). Proton radiotherapy with the broad beam method was added by assuming that the neutron dose was higher than that with the scanning method by a factor of 5. They showed that second cancer risk in the adult after IMRT or passive proton radiotherapy is not increased by more than 15% compared with conventional radiotherapy. In the child, the risk remains practically constant or is even reduced for proton therapy. Also, the followings were concluded.

- The cumulative risk in the child can be as large as 10 to 15 times higher than that in the adult.
- The ratio of the volume which receives dose lower than 2 Gy relative to the volume which receives dose more than 2 Gy varies in the adult patient between 10 and 20 and in the child only between 7 and 9. Therefore, the impact of scatter and leakage radiation is more pronounced for the adult patient.
- IMRT and proton radiotherapy (regardless of the irradiation method) will lower the risk for the child when compared with 3D-CRT.

(130) These results indicate that the reduction of undesired dose in the out-of-field volume through the use of scanning beam method or an additional shielding technique can lower the risk. Each facility should control (manage) the out-of-field dose and make an effort to reduce it.

(131) Unfortunately, no publications on the risk assessment in carbon ion radiotherapy are available at present. However, undesired dose in normal tissue is at least comparable to that in proton radiotherapy, and consequently, the risk should be similar. Additional questions on a higher RBE for the induction of cancers are still to be solved (ICRP, 2003b). Informration and data are needed for this point, particularly by treatment centres already using carbon ions in clinical practice. Also, epidemiological studies for the second cancer risk are required for the treatment centres.

(132) The risk assessment includes a large uncertainties of dose assessments. Additionally, there are uncertainties on biological effects, the dose-response relationship in the low dose region, and effects of dose rate and fractionation, etc. as mentioned in Section 4. Monte Carlo simulations also must be further verified experimentally; therefore more experimental information is desired because the available literature is still limited compared with that on photon radiotherapy. In addition, it should be remembered that doses by primary and secondary radiations depend on treatment planning and facility.

(133) At this time it is difficult to draw a general conclusion concerning the second cancer risk after ion beam radiotherapy. However, there is no evidence that the second cancer risk after ion beam radiotherapy is higher than the risk after external photon radiotherapy.

5.2. Medical exposure of patients from imaging procedures

(134) Imaging procedures involved in ion beam radiotherapy include X-ray CT for treatment planning, radiographic and fluoroscopic procedures for treatment rehearsal and patient setup verification at the beginning of each dose fraction, and fluoroscopy and respiratory-correlated CT such as time resolved CT (4DCT) for

organ motion tracking during ion beam delivery. Although these imaging procedures provide significant information for ion beam radiotherapy, they also give additional radiation doses to the patient. There have been concerns about the total imaging doses in recent years (Murphy et al., 2007). Doses delivered by each imaging procedure have been published widely through the literature. This section provides data to allow medical staff to estimate the total radiation doses[3] delivered to patients from imaging procedures during ion beam radiotherapy and in the follow-up after treatment.

5.2.1. Review of dose delivered to patients from imaging procedures

Conventional CT

(135) CT remains the primary method used for radiotherapy treatment planning, as well as being one of the types of diagnostic imaging. CT procedures deliver relatively high doses, compared with other radiography techniques and it is therefore important to recognise the dose from CT imaging.

(136) The principal dosimetric quantities used in CT are the CT dose index (CTDI) and dose length product (DLP). CTDI is defined as the integral along a line parallel to the axis of rotation of the dose profile for a single rotation, divided by the nominal X-ray beam width (ICRP *Publication 87*, 2001). CTDI is assessed as the absorbed dose in air using a pencil ionisation chamber with an active length of 100 mm. Reference dosimetry for CT is based on such measurements made within a standard CT dosimetry phantom, which comprises homogeneous cylinders of polymethyl methacrylate (PMMA) with diameters of 16 cm (head) and 32 cm (body). Dose values in these phantoms are expressed as weighted CT dose index (CTDIw) of five reference points in the phantom. As nearly all scanners on the market today are multi-detector CT (MDCT) systems with spiral scan mode, the standard dose paramater today is CTDIw divided by the pitch expressed as CTDIvol [mGy]. DLP represents the overall energy delivered by a given scan protocol, and the DLP can be integrated over the scan length. Reference doses in CTDI and DLP from a number of studies are given in *Publications 87* and *102* (ICRP, 2001, 2007a).

(137) Doses to patients are optimally characterised by absorbed doses to each tissue or organ (organ dose) of the body, although this approach is rather difficult for routine use. One common method for estimating organ doses is based on measurements using small dosimeters, such as thermoluminescence dosimeters (TLDs) and radiophotoluminescence glass dosimeters (RGDs), set in various organ positions within an anthropomorphic phantom representing the patient. Another method is dose calculation using conversion factors derived from Monte Carlo simulation of photon interactions within a computational anthropomorphic phantom. Examples of mean organ doses to adults based on measurements or calculations for various CT examinations, using single-slice CT (SSCT) and multi-slice CT (MSCT), are shown in Table 5.1 (Shrimpton et al., 1991; Nishizawa et al., 1991; Fujii et al.,

[3]Quantities expressed as absorbed dose in air, such as Entrance Surface Dose, ESD and Dose Area Product (DAP) have been commonly used in clinical practice. However, the quantity that is actually measured with current dosimetry equipment is air kerma. ICRU Report 74 (ICRU, 2005b) and IAEA code of practice (IAEA, 2007) recommend the use of the field-related quantities, incident air kerma ($K_{a,i}$), entrance surface air kerma (K_e), air kerma-area product (P_{KA}) and computed tomography air kerma index (C_K). Thus, the medical community should also be familiar with these quantities. Nevertheless, in this document, quantities expressed in dose to air are given as they appear in the literature.

2007; Nishizawa et al., 2008a, b; Mori et al., 2009; Huang et al., 2009). Doses delivered to a patient in a given examination will be highly dependent on the characteristics of the CT scanner, the size of the patient, the anatomical region under investigation and the technical factors used in each examination. Therefore, the doses will vary between institutions and even between different equipment and techniques within an institution. For children, organ doses in CT examinations have been evaluated using a paediatric physical or computational phantom. These dose data have been published in several reports (Zankl et al., 1995; Fujii et al., 2007; Lee et al., 2007; Nishizawa et al., 2008a,b). Zacharatou Jarlskog et al. (2008) reported on the out-of-field doses due to neutron radiation in proton radiotherapy, using the broad beam method, for brain lesions and compared the doses to the radiation expected from a chest CT scan (Table 5.2). The equivalent doses for thyroid, lung and stomach from proton radiotherapy are of the same order of magnitude as the dose from multiple CT scans.

(138) Fast dynamic CT (often referred to as 4DCT) allows a temporal sequence of 3D images during the breathing cycle. Prior to or during treatment, 4DCT is used to accurately determine the target volume of tumours, by minimising image degradation caused by respiratory motion. One method for data acquisition is to perform a continuous helical scan and sort the sonogram data according to physiological signals or time stamps. Another method is to perform 4DCT in the cine mode where the scanner operates without couch movement and acquires one respiration cycle of CT data at each cough position, before moving to the next position. Keall et al. (2004) have shown that air kerma, free-in-air, in thoracic 4DCT in continuous helical scan mode with a pitch factor of 0.125 will be in the range of 250-400 mGy. Mori et al. (2009) have reported organ doses in 4DCT cine mode (Table 5.1).

Radiography and fluoroscopy

(139) Radiography is used for the treatment rehearsal and in the daily verification of patient setup, at the start of every fraction. Fluoroscopy, with image intensifiers (I.I.) and flat panel detectors (FPD), is also used for the treatment rehearsal. These procedures mostly involve taking orthogonal radiographs from anterior-posterior (AP) and lateral (LAT) viewpoints.

(140) The dosimetric quantities in radiography and fluoroscopy are expressed in terms of air kerma free-in-air, entrance surface dose (ESD) and dose-air product (DAP). ESD is defined as the absorbed dose to air at the centre of the beam, including backscattered radiation. DAP is defined as the absorbed dose to air averaged over the area of the X-ray beam in a direction perpendicular to the beam axis, multiplied by the area of the beam in the plane. Hart et al. (2007) have reported reference doses in ESD and DAP for common radiographic and fluoroscopic X-ray imaging procedures.

(141) Jones et al. (1985) have shown the mean organ doses per unit ESD using Monte Carlo techniques for individual X-ray beam projections in various X-ray examinations. Organ doses in medical X-ray examinations can be estimated using Monte Carlo programme (PCXMC) developed by STUK, the Radiation and Nuclear Safety Authority of Finland (Tapiovaara et al., 2008). Organ doses will vary widely depending on the projection of the X-ray beam, X-ray equipment and the physical factors used. Organ doses for a given type of examination have large variations among institutions as much as two or three orders of magnitude. Hart et al. (2007) have reported that ESDs in a chest radiograph for children should be much smaller

than for adults since lower doses for children would be sufficient to produce a satisfactory image.

(142) Fluoroscopy commonly takes periods ranging from 30 sec to 1 min for a treatment simulation. Fluoroscopy is also required for respiratory motion management techniques including beam gating and dynamic tracking. Typical fluoroscopic units with I.I. will automatically adjust fluoroscopic technical parameters such as the tube potential and tube current to obtain acceptable images. Thus, the dose levels will vary widely between examinations because the automatic settings will differ from site to site and according to the patient's weight. Murphy et al. (2007) have reported that the typical ESD to a patient would be approximately 20 mGy/min for pre-treatment fluoroscopic procedures.

Cone beam CT (CBCT)

(143) CBCT is used for treatment planning and verification of the target volume, although it is subject to cupping artefacts and inaccuracies in the Hounsfield number.

(144) There have been studies on dose levels from CBCT for different scan sites. Islam et al. (2006) reported doses evaluated using 30-cm- and 16-cm-diameter cylindrical water phantoms. For a tube voltage of 120 kVp, 330 projections at 2 mAs per projection and a source/detector distance of 154 cm, the typical doses to the phantom at the centre of and on the surface of the body phantom were 16 mGy and 23 mGy, respectively. For the head phantom, the centre and surface doses were 30 and 29 mGy, respectively. Some authors have reported organ doses evaluated with an adult anthropomorphic phantom (Endo et al., 1999; Kan et al., 2008: Sawyer et al., 2009). The typical technical parameters and organ doses in CBCT are summarised in Table 5.3. Tables 5.1 and 5.3 showed that organ doses in CBCT examinations can be two or three times higher than in X-ray CT. Thus, CBCT will deliver a substantial amount of dose to the critical organ near the target volume. Kan et al. (2008) have indicated that there was no significant difference in the matching accuracy of planning between using standard and lower mode CBCT images and hence, it is possible to reduce the radiation doses by using only X-ray CT.

Nuclear medicine procedures

(145) Nuclear medicine procedures such as planar imaging using a gamma camera, single photon emmission CT (SPECT), PET and/or PET-CT scan are performed as one type of diagnostic imaging method before the ion beam radiotherapy and for follow-up after treatment. Internal dose estimations in the patients after nuclear medicine procedures are required for radiological protection and one method for estimating organ dose for a reference patient from the administration of various radiopharmaceuticals is to use organ dose coefficients given in *Publications 53, 80* and *106* (ICRP, 1987, 1998b, 2008). These dose coefficients are estimated based on biokinetic models and estimates of the bio-kinetic data for individual radiopharmaceuticals and are given for adults and children of 1, 5, 10, and 15 years of age. The mean absorbed doses to tissues and organs are given as mGy per unit activity administered (MBq) and can be estimated by multiplying the dose coefficients for individual radiopharmaceuticals by the activity of the administered radiopharmaceuticals.

Table 5.1. Mean organ doses in various CT examinations.

Examination	Head		Chest				
CT scanner	SSCT [1]	SSCT [2]	SSCT [1]	SSCT [2]	MSCT [4]	MSCT [5]	4DCT [7]
Tissue or organ	Organ doses (mGy)						
Thyroid	1.85	0.55	2.25	1.86	23.4	13.0	66.4
Lung	0.09	0.08	22.4	19.6	19.2	20.9	61.4
Oesophagus	-	-	-	-	17.6	18.8	54.5
Breast	0.03	0.11	21.4	15.9	16.0	13.0	46.2
Liver	0.01	0.02	5.64	8.96	14.7	13.9	29.6
Stomach	<0.01	0.02	4.06	9.19	15.3	14.3	25.5
Colon	<0.01	<0.01	0.07	0.15	2.89	1.5	3.8
Ovaries	<0.01	<0.01	0.08	0.11	0.13	0.1	0.1
Bladder	<0.01	<0.01	0.02	0.09	0.16	0.1	0.2
Testes	<0.01	<0.01	<0.01	0.05	0.12	0.1	0.3
Red bone marrow	2.67	1.45	5.94	5.69	5.94	8.2	17.4
Skin	2.62	-	4.42	-	18.0	2.5	11.2

2032

Examination	Abdomen			Pelvis		Abdomen and pelvis		Whole body CT
CT scanner	SSCT [1]	SSCT [2]	MSCT [3]	SSCT [1]	SSCT [2]	MSCT [4]	MSCT [5]	MSCT [6]
Tissue or organ	Organ doses (mGy)							
Thyroid	0.05	0.17	0.44	<0.01	0.03	-	0.4	10.4
Lung	2.70	1.68	8.19	0.05	0.13	-	6.3	6.8
Oesophagus	-	-	2.29	-	-	-	7.6	6.5
Breast	0.72	0.78	5.87	0.03	0.11	-	8.1	7.6
Liver	20.4	27.8	19.5	0.68	0.49	19.0	14.4	8.3
Stomach	22.2	26.9	21.0	1.06	0.47	20.3	17.9	7.5
Colon	6.60	1.00	16.5	15.1	19.2	19.6	17.9	8.1
Ovaries	8.00	0.61	1.43	22.7	15.1	15.7	20.5	8.8
Bladder	5.07	0.42	1.24	23.2	10.6	19.4	18.3	6.3
Testes	0.70	0.10	0.17	1.72	1.04	11.1	6.9	8.4
Red bone marrow	5.58	2.16	5.76	5.62	5.60	9.29	8.7	6.0
Skin	4.76	-	3.21	3.72	-	5.04	3.7	7.0

2033

2034 [1] Shrimpton et al., 1991. [2] Nishizawa et al., 1991. [3] Nishizawa et al., 2008b.
2035 [4] Nishizawa et al., 2008a. [5] Fujii et al., 2007. [6] Huang et al., 2009.
2036 [7] Mori et al., 2009.

2037

2038

2039 Table 5.2. Equivalent doses for thyroid, lung, and stomach due to neutron radiation
2040 calculated in passive scattered proton radiotherapy considering a 70 Gy treatment for brain
2041 lesions (modified from Zacharatou Jarlskog et al., 2008).

	9 month old	4 year old	11 year old	14 year old
	Equivalent dose (mSv)			
H to thyroid from proton therapy	80.8	130.3	110.7	103.4
H to thyroid from chest CT scan	8.0	9.0	5.2	6.9
Therapy/CT scan (thyroid)	10.1	14.4	21.2	14.9
H to lung from proton therapy	79.1	85.5	36.5	23.1
H to lung from chest CT scan	15.0	13.9	12.0	12.6

Therapy/CT scan (lung)	5.3	6.2	3.0	1.8
H to stomach from proton therapy	52.8	19.0	9.0	2.5
H to stomach from chest CT scan	11.0	4.9	5.9	5.0
Therapy/CT scan (stomach)	4.8	3.9	1.5	0.5

The therapeutic dose was modified with a scaling factor of 1.5 to account for fractionation (BEIR-VII, 2006). The values are compared with radiation to be expected from a chest CT scan as a function of patient's age (Lee et al., 2007).

Table 5.3. Mean organ doses in various CBCT examinations.

Examination	Head			Chest		Pelvis	
Reference	Endo (1999)	Sawyer (2009)	Kan (2008)	Endo (1999)	Kan (2008)	Sawyer (2009)	Kan (2008)
Tube voltage (kV)	120	125	125	120	125	125	125
mAs/projection	2.0	2.0	2.0	2.0	2.0	1.2	2.0
The number of projections	360	1125	650-700	360	650-700	1350	650-700
Tissue or organ	Organ doses (mGy)						
Thyroid	135.3	7.8	110.8	27.7	7.9	0.2	0.4
Lung	4.0	1.1	5.7	67.1	53.4	0.9	0.8
Oesophagus	7.3	1.5	38.1	68.5	35.9	0.8	0.8
Breast	3.0	1.3	2.1	47.2	46.9	0.6	1.2
Liver	1.1	0.1	0.7	34.4	38.7	2.9	6.3
Stomach	1.0	0.2	0.7	26.8	43.7	2.1	5.9
Colon	-	0.1	0.5	-	3.5	19.9	54.3
Ovaries	0.1	0.1	0.2	0.7	0.6	40.6	37.5
Bladder	-	0.1	0.2	-	0.7	36.4	52.9
Testes	0.1	0.1	-	0.8	-	31.3	-
Red bone marrow	13.5	6.9	8.0	21.9	30.4	8.9	20.3
Skin	-	6.9	9.2	-	27.7	11.6	25.9

5.2.2. The total imaging doses for ion beam radiotherapy

(146) This section describes the total imaging dose delivered to patients from various imaging procedures in ion beam radiotherapy. The following shows an example of the dose from each imaging procedure in carbon ion radiotherapy at HIMAC.

(147) For an adult patient with prostate cancer the organ doses from imaging procedures required for carbon ion radiotherapy are considered as follows. Doses to the colon are important because of its high radiosensitivity. Typical imaging procedures and colon doses in each procedure involved in carbon ion radiotherapy for prostate cancer at HIMAC are summarised in Fig. 5.8. At the procedure 1 of the diagnostic examination before treatment, when a patient undergoes a diagnostic pelvic CT scan, colon doses from Table 5.1 can be estimated to be approximately 15-20 mGy. At the procedure 2 of the treatment planning, when the patient undergoes a single X-ray CT procedure, colon doses can be approximately 15-20 mGy. At the procedure 3 of the treatment rehearsal, the patient undergoes

orthogonal X-ray radiographic procedures, colon doses in an orthogonal radiograph were estimated using Monte Carlo programme (PCXMC) to be approximately 0.4-0.5 mGy. When the patient undergoes radiographic procedures, the total colon doses can be estimated to be 3-4 mGy. At the procedure 4, the patient undergoes the radiographic procedures for the daily patient setup verification at the start of each fraction. Given a fraction number of 16 fractions/4 weeks in a treatment for prostate cancer and 4 orthogonal radiographs per fraction, then colon doses in a total of 64 orthogonal radiographs can be estimated to be approximately 25-35 mGy. Finally, at the procedure 5 of the follow-up after the treatment when the patient undergoes a diagnostic pelvic CT scan, the colon doses can be approximately 15-20 mGy. Thus, the typical total colon doses delivered from various imaging procedures during the ion beam radiotherapy and after the treatment would reach approximately 100 mGy. This value can vary proportionally to the treatment fractions and frequency of X-ray imaging which are adopted at an ion beam radiotherapy facility.

5.2.3. Exposure of comforters and carers

(148) High energy ion beams, such as protons or carbon ions, induce nuclear reactions in a patient's body, resulting in the activation of nuclei. This requires the assessment of radiation exposures to the person who stays close to the patient after the ion beam radiotherapy, such as working staff, comforters and carers, and family members.

(149) Tsujii et al. (2009) have reported the results of irradiation experiment with ion beam with soft tissue substitute materials. For evaluation of the exposure of patient's family members, the following scenario was assumed: the patient leaves the treatment room 2 min after the end of the irradiation and a member of his/her family attends him/her for 2 hr. The ion beam radiotherapy for a patient would be carried out for 20 to 30 fractions of irradiation at most. In the case of carbon ion treatment of 30 fractions, the exposure of the family member was calculated to be 23.5 μGy for HIMAC and 20.8 μGy for the Hyogo Ion Beam Medical Center (HIBMC). The exposure was calculated to be around 130 μGy in the case of proton treatment of 30 fractions at HIBMC. The doses from activation in proton radiotherapy were higher than those in carbon ion radiotherapy partly because proton radiotherapy required more particle fluence delivered to the patient than carbon ion radiotherapy. Most radioactive nuclides produced by ion beam radiotherapy have very short physical half-lives. Even if the time when the family member attends the patient is prolonged more than 2 hr, the additional increase in exposure is negligible. Therefore, Tsujii et al. (2009) concluded that the exposure of a patient's family member is substantially lower than the public dose limit of 1 mSv/year.

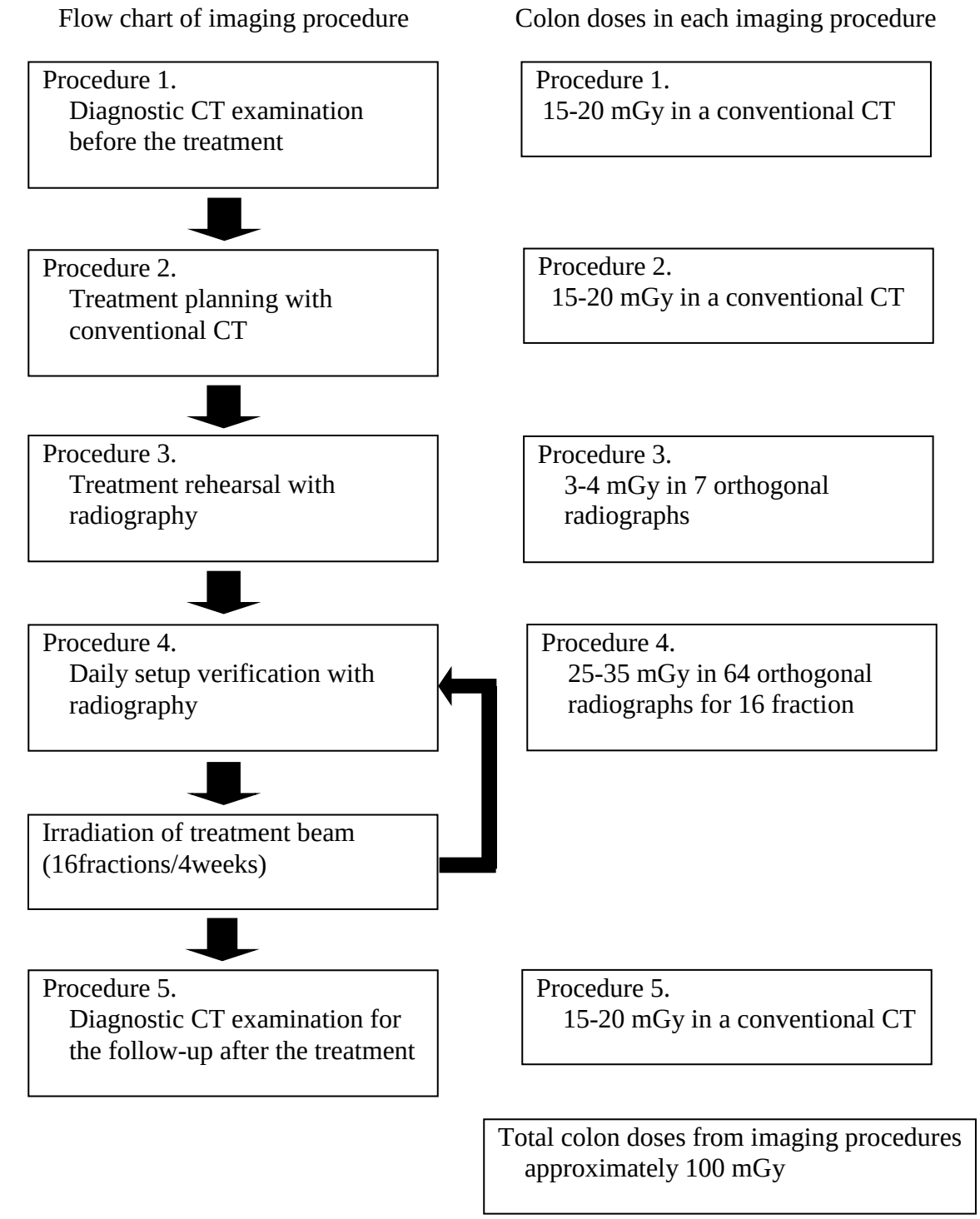

Fig. 5.8. An example of imaging procedures and colon doses in each procedure associated with carbon ion radiotherapy for prostate cancer at HIMAC.

5.3. Occupational exposure

(150) During the ion beam radiotherapy, interactions occur with atomic nuclei in the air of the treatment room, the patient's body and beam line devices, and then the beams activate the materials depending on the ion species, energy and irradiation

area. The sources for the occupational exposures to radiation workers in the facilities are not the therapeutic beams themselves but the activated materials related to radiotherapy. The activity is highest just after irradiation of the patient since the physical half-lives of the induced radioactivity are relatively short, and the radioactivity steadily decreases according to the half-lives of the radionuclides.

(151) In ion beam radiotherapy facilities, there are many medical radiation workers including physicians, radiological technologists[4], medical physicists, nurses, and operators. According to their roles in radiotherapy, some of them will enter the treatment room for preparation tasks before irradiation, take the patient into the treatment room, set the patient position and irradiation equipment, and take the patient outside the room after irradiation. After irradiation, a patient compensator and a patient collimator are moved into the depository. In addition to the medical staff, personnel of the manufacturers and suppliers related to radiotherapy have the opportunity to be inside the facility for maintenance of the beam delivery system and equipment when radiotherapy is not being carried out, and they also would possibly be exposed by residual radionuclides.

(152) The occupational exposures to workers in radiotherapy facilities depend on the induced radioactivity levels in the beam delivery system and equipment, and the position of and time spent by the medical staff and maintenance personnel in the treatment room regarding their contact with, or distance to, the activated materials. The shielding abilities of the irradiation system and rooms are also important factors affecting radiological protection for the workers. Among medical radiation workers, radiological technologists receive the highest level of occupational exposures from the induced radioactivity because of their roles in the radiotherapy. Based on actual measurements and calculations of induced radioactivity in the specific radiotherapy, the doses to these medical workers can be estimated for assurring adequate radiological protection. In fact, many studies have reported dose estimations by both measurements and calculations in radiotherapy, and significant information has been acquired.

(153) For radiotherapy with linear accelerators, Almen et al. (1991) measured the absorbed doses to the trunk and to the hands of 24 radiological technologists working with accelerators for radiotherapy by using TLDs, and estimated that the annual absorbed dose was 2 mGy, primarily caused by radiation penetrating the walls of the treatment room; induced activity in the accelerator contributed one-third to the doses. The absorbed dose to the trunk varied from 1.0 to 2.8 mGy, and the range for the hands was between 0.7 and 3.3 mGy per year. As the induced activities in metals in the accelerator, immediately after a treatment ^{28}Al (physical half-life = 2.3 min) and ^{62}Cu (9.7 min), and later ^{187}W (24 hr) and ^{57}Ni (36 hr) dominated. Fischer et al. (2008) reported comparisons of activation products and induced dose rates at the isocentre of four high-energy medical linear accelerators. They analysed the gamma spectra, and calculated dose rates. There were 21 radionuclides having physical half-lives between 2.3 min and 5.3 yr. Among these induced radionuclides, ^{28}Al, ^{62}Cu, ^{56}Mn, ^{64}Cu, ^{187}W, ^{57}Ni, ^{196}Au, ^{54}Mn, ^{60}Co and ^{124}Sb were considered important for calculating the induced dose rate at the isocenter. The estimated annual doses to radiological technologists were between 0.62 and 2.53 mSv/yr. Perrin et al. (2003) derived a model to calculate induced dose rate around an 18 MV ELEKTA

[4] In this section, the term “radiological technologist” is used. However, “radiation therapist” and “therapeutic radiographer” have been used in the literature depending on the professional categorisation followed in a country.

linear accelerator. The modelled induced dose rates agreed with measured dose. The maximum annual whole body dose was estimated to be 2.5 mSv for 60,000 MU per week.

(154) For proton radiotherapy, to investigate neutron shielding consideration for a proton radiotherapy facility of the University of Pennsylvania, Avery et al. (2008) calculated the spectra of neutrons produced by 100, 175 and 250 MeV proton beams using the Geant4 Monte Carlo simulation code, and estimated dose equivalent rates at various points in the facility based on the calculated spectra data. The annual dose equivalents at various points around the shielding were between 0.02 and 1.19 mSv, and the results showed that the shielding would be adequate for both the public and radiation workers. Newhauser et al. (2005) developed a neutron radiation area monitoring system for proton radiotherapy facilities consisting of measurement equipment, a computer and software. The system can record and display neutron dose equivalent. Exposures to the maintenance staff from residual radionuclides after synchrotron shutdown at the Loma Linda University Proton Treatment Facility were estimated based on the dose measurement around the accelerator and review of the personnel dosimetry records by Moyers et al. (2009). At 300 mm from the surface of the accelerator, all average exposure rates were below 1.7×10^{-2} mSv/hr. The average annual dose equivalents for seven maintenance personnel bodies were 2.0×10^{-2} to 2.1×10^{-1} mSv in 2006.

(155) For carbon ion radiotherapy, by the experiments with 230 and 100 MeV/n argon, carbon, neon, helium, phosphorus ions, Yashima et al. (2002, 2003, 2004a, b) obtained the radioactive spallation products in a thick copper target at the HIMAC facility (in practice, 400 MeV/n ions are also used for radiotherapy). They found agreement with other experimental data and the energy dependence of the reaction yields. They also calculated the spatial distribution of residual radioactivities in copper by the PHITS code, and found the PHITS provided calculated results in good agreement with the measurements.

(156) As evidence to consider proper radiological protection in ion beam radiotherapy, Tsujii et al. (2009) collected information from representative facilities in the world for ion beam radiotherapy concerning the practical radiological protection at each facility. These therapy facilities are controlled by the same government regulations as for ordinary accelerator facilities. Activation levels of the beam line devices and of patients were actually measured in two carbon ion radiotherapy and four proton radiotherapy facilities in Japan. The practical maximum doses to radiological technologists were assessed based on the measurement data of the induced radioactivity. The dose equivalents to the radiological technologist were estimated in the sequential process of detaching a patient immobilisation device, patient collimator and patient compensator (putting it on a side table) and storing the patient collimator and the patient compensator (moving it to a depository), with the assumption that the radiological technologist repeats the process sequence 20 times a day and 260 days a year, as seen in Table 5.4. Tsujii et al. (2009) estimated that, for example, annual effective doses in 290 MeV/n and 400 MeV/n carbon ion radiotherapy at HIMAC were 1.06 mSv and 0.67 mSv, respectively, and that the annual skin equivalent doses were 9.7 and 4.1 mSv, respectively, as seen in Table 5.5. At the HIBMC for carbon ion radiotherapy, the annual effective doses were estimated to be 0.53 mSv and the annual skin equivalent doses were 5.4 mSv under the same conditions and assumptions as those at HIMAC. At three proton radiotherapy facilities, the annual effective doses were estimated to be 2.3-5.5 mSv and the annual skin equivalent doses were 31-73 mSv, as seen in

Table 5.6. The activation doses in proton radiotherapy were higher than those in carbon ion radiotherapy because the fluences of protons to the patients were generally higher than those of carbon ions.

(157) Table 5.7 summarises estimated annual doses for medical workers. The Commission recommended the dose limits of occupational and public exposures in *Publication 60* (ICRP, 1991). For occupational exposures, the dose limit in 5 years is 100 mSv (mean dose 20 mSv/y), and the maximum dose limit in a year is 50 mSv. On the other hand, the dose limit for the public is 1 mSv in a year. The Commission published new recommendations in *Publication 103* (ICRP, 2007b). Tsujii et al. (2009) concluded from comparing estimated doses of radiological technologists mentioned above with these dose limits of occupational exposure, the current regulations for photon radiotherapy are also applicable to ion beam radiotherapy. The same radiological protection methods of general linear accelerator radiotherapy can be applied for the protection of occupational exposures based on the data. For occupational exposure in planned exposure situations, the Commission recommended in 2011 that an equivalent dose limit for the lens of the eye of 20 mSv in a year, averaged over defined periods of 5 years, with no single year exceeding 50 mSv (ICRP, 2012). In general, the doses of the skin could be the maximum among organ doses in X-ray examinations. In addition, the distance between the X-ray entrance surface of the patient and the lens of the eye of the practitioner could not be so close to the patient, and hence the doses of the lens would not exceed the new dose limit recommended by the Commission when ordinary radiological protection is performed for the radiation workers.

Table 5.4. Activities, required times and distances from the radiation source for a radiation technologist working in a carbon ion radiotherapy facility.

Activity*	Time from beam stop to activity start	Time needed for the work	Source to evaluation point distance					
			Effective dose			Skin dose		
			MLC	Collimator	Compensator	MLC	Collimator	Compensator
A	25 s	30 s	50 cm	30 cm	30 cm	50 cm	30 cm	30 cm
B	55 s	10 s	50 cm	30 cm	30 cm	1.5 cm	0 cm	0 cm
C	1 min 05 s	10 s	50 cm	30 cm	30 cm	1.5 cm	30 cm	0 cm
D	1 min 15 s	15 s	-**	-**	30 cm	-**	-**	0 cm
E	1 min 30 s	10 s	-**	30 cm	-**	-**	0 cm	-**

The evaluation of the effective dose uses the dose rate by gamma rays and the evaluation of the equivalent dose to the skin uses the total dose rate by β and gamma rays (Tsujii et al., 2009).

*Activity: A, detaching the patient fastening device; B, detaching the patient collimator (putting it on a side table); C, detaching the amends filter (putting it on a side table); D, storing the amends filter (moving it to a depository); and E, storing the patient collimator (moving it to a depository).

** Because of the long distance, the dose contribution is ignored.

Table 5.5. Evaluation of effective dose and equivalent dose of skin for a radiation technologist working in a carbon ion radiotherapy facility (Tsujii et al., 2009).

Activity	Effective dose (μSv)			Equivalent dose of skin (μSv)		
	HIMAC*	HIMAC**	HIBMC	HIMAC*	HIMAC**	HIBMC
A	0.108	0.085	0.054	0.119	0.125	0.099
B	0.034	0.018	0.017	0.759	0.252	0.417
C	0.034	0.017	0.017	0.331	0.226	0.136
D	0.005	0.007	0.006	0.299	0.192	0.111
E	0.023	—	0.007	0.358	—	0.277
Total dose (μSv)	0.203	0.128	0.101	1.866	0.795	1.040
Annual dose (mSv)	1.057	0.665	0.530	9.701	4.132	5.410
Total dose for 3 months (mSv)	0.264	0.166	0.133	—	—	—

HIMAC: Heavy-Ion Medical Accelerator in Chiba
HIBMC: Hyogo Ion Beam Medical Center
*290MeV/n carbon ion irradiation of about 150 mm underwater range.
**400 MeV/n carbon ion irradiation of about 250 mm underwater range.

Table 5.6. Evaluation of effective dose and equivalent dose of skin for a radiation technologist working in a proton ion radiotherapy facility (Tsujii et al., 2009).

Activity	Effective dose (μSv)			Equivalent dose of skin (μSv)		
	HIBMC	PMRC	SCC	HIBMC	PMRC	SCC
A	0.294	0.205	0.496	0.538	0.431	1.138
B	0.096	0.066	0.157	2.918	2.309	5.002
C	0.095	0.065	0.153	0.940	1.042	2.284
D	0.049	0.016	0.078	1.071	0.928	3.030
E	0.051	0.085	0.180	1.982	1.289	2.673
Total dose (μSv)	0.585	0.438	1.064	7.449	5.999	14.127
Annual dose (mSv)	3.040	2.276	5.531	38.742	31.196	73.459
Total dose for 3 months (mSv)	0.760	0.569	1.383	—	—	—

*Activity: A, detaching the patient fastening device; B, detaching the patient collimator (putting it on a side table); C, detaching the amends filter (putting it on a side table); D, storing the amends filter (moving it to a depository); and E, storing the patient collimator (moving it to a depository).
HIBMC: Hyogo Ion Beam Medical Center
PMRC: Proton Medical Research Center at Tsukuba University
SCC: Shizuoka Cancer Center

Table 5.7. Summary of estimated annual doses for medical workers (Tsujii et al., 2009)

Type of radiotherapy	Author	Annual effective dose (mSv)	Annual skin equivalent dose (mSv)	Annual equivalent dose to the body (mSv)
X-ray	Fischer et al. Perrin et al.	- -	- -	0.6-2.5 2.5

Proton	Moyers et al. Tsujii et al.	- 2.3-5.5	- 31.2-73.5	0.02-0.21 -
Carbon ion	Tsujii et al.	0.5-1.1	4.1-9.7	-

5.4. Public exposure

(158) The sources of public exposures in radiotherapy are different from those of occupational exposures. The major radioactive sources are not the radioactivity produced in the therapy-related devices but those in the patient. By coming into contact with patients in undergoing radiotherapy, the public can be exposed. The sources of exposure can also include the radioactivity in the exhausted air and the waste water from treatment facilities to the environment. However, the activation levels of the sources on public exposures are lower than on occupational exposures because of the physical half-lives of radioactivity and the way of exposure.

(159) Tsujii et al. (2009) calculated the air activations by protons, fast neutrons and thermal neutrons in NCCHE from consideration of the sources of occupational and public exposures including the effects on the environment, radioactive concentrations of the treatment room air and the exhaust from facilities, and the waste water. The levels of the activations were lower than the Japanese regulatory levels which are based on ICRP recommendations. As the transfer from the patient to the wastewater through urine, the concentration levels were estimated using the data of Monte Carlo simulations, and the influence to the environment was found to be negligible. These data suggest that the doses are significantly lower than the public dose limit because of limited contact with the induced radioactivity, and that methods of radiological protection from the public exposures in photon radiotherapy facilities are adequate in ion beam radiotherapy facilities.

6. RADIATION SAFETY MANAGEMENT FOR ION BEAM RADIOTHERAPY FACILITIES

6.1. Radiation safety management for the facilities

(160) In countries where ion beam radiotherapy has already been practiced, a national regulatory framework is in place for radiation sources including medical linear accelerators, and radiation-safety standards for experimental high-energy particle accelerator facilities are applied. At an international level, recommendations to national authorities on approaches for defining the scope of radiological protection control measures are given in *Publication 104* (ICRP, 2007c). Requirements on national authorities and users of radiation sources are given in the International Safety Standards for Protection against Ionizing Radiation and for the Safety of Radiation Sources (IAEA, 1996). These safety standards include not only requirements for the optimisation of radiological protection but also those for prevention of accidental exposure for emergency, such as switch off, interlocks and warning signals. Advice on how international safety requirements can be met in radiotherapy is given in the IAEA report (2006). Lessons from accidental exposures in radiotherapy are provided in *Publications 86* and *112* (ICRP, 2000, 2009) and IAEA report (2000). However, in addition to general issues for safety and security that need to be addressed, specific issues associated with high-energy ion beamss, such as exposures due to activation of the irradiation equipment, should also be addressed by management of the facilities. This chapter provides advice on specific radiation safety management that is required to ensure optimisation in these facilities and compliance with the dose limits for occupational and public exposures. Measures to prevent accidental exposure are given in Chapter 7.

6.2. Management of exposure due to activation of devices

(161) Specific issues for relevant safety management in ion beam radiotherapy facility are associated with exposures from activated equipment and patients that are directly irradiated by high-energy ion beams. The devices of concern are those directly exposed to the treatment beams, especially if they are placed near patients or manually handled by radiological technologists: these include patient immobilisation devices, collimators, patient compensator, ridge filter, range shifters and dosimetric instruments. The levels of dose received from handing these devices are shown in Tables 5.6 and 5.7. Those levels are well below the relevant dose limits.

6.3. Management of radioactivity due to activated nuclides

6.3.1. Air activity concentration in the treatment room

(162) The occupational exposure from air activated during beam acceleration and transport should be evaluated. Activity concentration in air of a treatment room has been estimated (Tsujii et al., 2009). Radioactivity A_{1i} (Bq) of a nuclide induced by ion beams can be calculated by the following equation:

$$A_{1i} = \lambda_i \sigma_i L N = \lambda_i \sigma_i L \frac{V_{tr} \times D \times 10^{-3}}{E \times 1.6 \times 10^{-13}}$$

where λ_i (sec^{-1}) is the decay constant of the nuclide i, σ_i is air cross section (cm^{-1}), N is the number of incident particles, L (cm) is the track length in air which therapeutic ion beams pass through, D (Gy) is absorbed dose in water over volume V_{tr} (cm^3), and E (MeV) is total energy of the incident particles.

(163) Radionuclides, which are possibly produced by air activation with their attributes, are listed in Table 6.1. (Tsujii et al., 2009).

(164) In the ion beam radiotherapy facility, air activation by secondary neutrons should be considered as well as that by the main beam. Radioactivity A_{2i} (Bq) of a nuclide induced by secondary fast neutrons can be calculated by the following equation:

$$A_{2i} = \lambda_i \sigma_i N R_n L_N$$

where R_n is the number of neutrons which have energy higher than 20 MeV and L_N is the effective flight path of fast neutrons in the treatment room.

(165) Radioactivity A_{3i} (Bq) of a nuclide i induced by secondary thermal neutrons can be calculated by the following equation:

$$A_{3i} = \lambda_i \sigma_i \Phi V$$

where λ_i (s^{-1}) is the decay constant of the nuclide i, Φ ($cm^{-2}sec^{-1}$) is thermal neutron flux in the treatment room, σ_i (cm^{-1}) is air cross section for nuclide i, and V (cm^3) is the volume of the treatment room. The main nuclides ^{41}Ar are induced by the ^{40}Ar (n,γ) reaction and the cross section is 660 mb for thermal neutrons.

(166) Activity concentration of nuclide i in air of the treatment room C_R (Bq cm^{-3}) averaged over time T (sec) can be calculated by

$$C_{Ri} = \frac{A_{1i} + A_{2i} + A_{3i}}{VT(\lambda_i + v/V)}\left[1 - e^{-(\lambda i + v/V)T}\right]$$

where the ventilation rate of the room is v (cm^3 sec^{-1}).

(167) Annual effective dose of workers due to internal exposure (E_{in}) during work in the treatment room can be evaluated by

$$E_{in} = \sum_i (e_{inh\,i} \cdot C_{Ri} \cdot B \times 10^6 \times O \times 2000)$$

where $e_{inh\,i}$ is the dose coefficient for inhalation of nuclide i , B (m^3 h^{-1}) is breathing rate, and O is occupancy factor in the treatment room. Significant proportions of ^{3}H, ^{11}C, ^{13}N, and ^{15}O produced in air of the treatment room would be in the form of gases. The behaviour of the gases should be taken into account to estimate the dose, especially the value of $e_{inh\,i}$ according to *Publication 68* (ICRP, 1994).

6.3.2. Discharge of air from the radiotherapy facilities

(168) In addition to estimating the radioactive concentration in air activated in the treatment room, shown in section 6.3.1, the concentration of air discharge also should be estimated in the design stage of the facility to confirm compliance with the authorized discharge limit given by a regulatory body to evaluate dose to the public living in the surrounding area. The concentration also should be monitored by an appropriate measurement system in the operational stage, only when the radioactive concentration in air is estimated to be beyond the maximum concentration level given by the regulatory agency.

(169) Activity concentration of nuclide of exhaust from the facility (C_X) averaged over time *T(s)* can be calculated by

$$C_{xi} = \frac{vA_i}{v_T T(\lambda_i + v/V)}\left[1 - e^{-(\lambda i + v/V)T}\right]$$

where the ventilation rate of whole facility is v_T ($cm^3\ s^{-1}$).

6.3.3. Management of solid waste

(170) When the devices or the component parts, which were activated with the radiotherapy beam, are replaced, the consideration to avoid unnecessary exposure is required. If they are put into temporary storage, this storage may be in or out of a controlled area depending on the radioactivity concentration.

(171) If a clearance system has been introduced or will be introduced, the activated materials should be treated as a candidate for clearance to reuse or recycle in the case that the activity concentration is lower than the clearance level criteria. Clearance level is established by national regulatory authorities by reference to levels proposed in the IAEA safety guide (IAEA, 2004).

6.3.4. Release of patients and management of their excreta

(172) The time required for the release of the patient, who has received ion beam radiotherapy and the necessity of management of the excreta, should be considered in relation to the exposure of any member of the patient's household. As shown in Section 5.2.3, the dose to the comforters and carers was found to be well below 5 mSv/episode, which is within the dose constraint provided in *Publication 103* (ICRP, 2007b). The dose is also much lower than 1 mSv/year, the dose limit for the general public provided in *Publication 103* (ICRP, 2007b).

6.4. Monitoring system for management of radiological protection

(173) A monitoring system should be established in facilities to ensure radiological protection in public exposure, occupational exposure and the medical exposure of patients. The system should include supplying an appropriate monitoring device for the evaluation of these exposures including both external and internal exposures. External dose of gamma-rays and neutrons should be monitored by area monitors or survey monitors. Activity concentrations of the nuclides can be monitored with appropriate gas monitor and dust monitor equipment in the treatment room. If the concentration is not monitored, it should be assessed by calculation.

6.5. Quality assurance in management of radiological protection of the facilities

(174) A quality assurance (QA) programme for management of radiological protection should be established. The programme should covers the following items: i) maintenance of records of relevant procedures and results; ii) measurements of the physical parameters of the irradiation instrument, the apparatus for shielding, the devices for beam forming and measuring instruments; iii) verification of the appropriate calibration and conditions of dosimetry and monitoring instruments; and iv) continuous quality improvement.

Table 6.1. Nuclides which are possibly produced by air activation (Tsujii et al., 2009).

Nuclide	Half-life	Production reaction	Cross section (mb) (Sullivan, 1992)	Air cross section (cm^{-1})
^{3}H	12.3 y	$^{16}O(x,sp)^{3}H$ $^{14}N(x,sp)^{3}H$	30 30	1.4×10^{-6}
^{7}Be	53.3 d	$^{16}O(x,sp)^{7}Be$ $^{14}N(x,sp)^{7}Be$	5 10	4.4×10^{-7}
^{11}C	0.340 h	$^{16}O(x,sp)^{11}C$ $^{14}N(x,sp)^{11}C$	5 10	4.4×10^{-7}
^{13}N	9.956 m	$^{16}O(x,sp)^{13}N$ $^{14}N(x,sp)^{13}N$	9 10	4.9×10^{-7}
^{15}O	2.037 m	$^{16}O(x,sp)^{15}O$	40	4.2×10^{-7}

7. PREVENTING ACCIDENTAL EXPOSURES OF PATIENTS FROM ION BEAM RADIOTHERAPY

(175) New technologies in radiotherapy brought highly conformal dose distribution, i.e., dose escalation in the target volume without increasing the radiation dose to neighbouring healthy tissues. On the other hand, even subtle errors during the treatment process would easily bring severe consequences. In order to avoid such accidental exposures, there is a need for prospective, structured and systematic approaches to the identification of system weakness and the anticipation of failure modes (ICRP, 2009).

7.1. Accidental exposures to patients undergoing radiotherapy

(176) Typical accidental exposures where the radiation administered is not given as intended can be classified as follows:

i) a patient receives the treatment planned for a different patient;

ii) the patient is correct, but the wrong part of the body (e.g., wrong site or wrong side) is irradiated;

iii) the patient and the part of the body are correct, but an unplanned volume is irradiated; and

iv) the patient, site and volume are correct, but the wrong dose is given.

The first two types of events may also happen in general medical practices other than radiotherapy and be discussed in terms of general patient safety. On the other hand, the latter two can be attributed more specifically to radiotherapy process, which is briefly described in this chapter.

(177) Disseminating the knowledge and lessons learned from accidental exposures is crucial in preventing reoccurrence. This is particularly important in radiotherapy: the only application of radiation in which very high radiation doses are deliberately given to patients to achieve cure or palliation of disease (ICRP, 2009).

(178) Ion beam radiotherapy can be categorised as external-beam radiotherapy. As shown in Section 2.1.5, the procedure consists of patient immobilisation, planning CT, treatment planning, patient positioning and beam delivery, in the same way as the external-beam radiotherapy. Lessons from accidental exposures in conventional external-beam radiotherapy are applicable to prevent those from ion beam radiotherapy. Retrospective compilations of lessons learned from the review and analysis of accidental exposures in radiotherapy have been published (IAEA, 2000; ICRP, 2000, 2009; WHO, 2008). These are useful to check whether a given ion beam radiotherapy department has sufficient provisions in place to avoid accidental exposures similar to those reported. As an example, major accidental exposures caused by errors in the calibration and commissioning of radiotherapy equipment have led to putting preventive measures in place, such as an independent redundant determination of the absorbed dose to detect possible beam calibration errors.

7.2. Potential accidental exposures in ion beam radiotherapy

(179) As described in Chapter 2, one of the features of ion beams for radiotherapy is dose localisation characterised by the Bragg Peak, sharp distal falloff and lateral

penumbra. It enables one to focus dose distribution on the target volume (e.g., malignant tumour) adjacent to OAR where dose should be as low as possible. There are potential advantages to patients from ion beam radiotherapy, but substantial concerns persist as uncertainties in beam parameters and target position are more critical in ion beam radiotherapy. The TPS customised to ion beam radiotherapy can design precise collimators and range compensators to spare OAR. The TPS also generates various beam parameters for an accelerator, and possibly large datasets for scanning magnets and fluence distribution in case of scan irradiation. It should be noticed that these functions of the TPS are specific to ion beam radiotherapy and not necessarily directly related to lessons in conventional external-beam radiotherapy. Thus, in addition to events that can occur in any radiotherapy practices, it is necessary to identify initiating events that are specific to the systems and procedures employed at the ion beam radiotherapy department. Since lessons from published events with these systems and procedures are not yet available, retrospective approaches are not sufficient in ion beam radiotherapy, and prospective approaches to identify potential risks should be carefully considered for comprehensive quality assurance (QA) programme. Table 7.1 shows an example of risk assessment specific to ion beam radiotherapy, with possible initiating events associated to each task of the radiotherapy process, together with the potential consequences of each initiating event and its preventive measures.

Table 7.1. A simplified example of safety assessment for ion beam radiotherapy

The list of events is not exhaustive, but is rather a sample to show how the assessment can be performed. The listed events are specific to ion beam radiotherapy, and therefore, other events of general nature that are also applicable to photon or electron beam radiotherapy are not listed here.

No.	Initiating event	Possible consequence	Preventive measures
Task or step: Commissioning of TPS			
1	Input of wrong datasets for CT-value vs Water Equivalent Length (WEL)	Irradiation of unplanned volume with short or excess in beam range. If OAR is covered with the volume, the consequence might be severe.	Independent or redundant verification of CT-WEL data. Comparison of dose calculation with measurement for a phantom.
Task or step: Patient Immobilisation			
2	Wrong thickness and materials of immobilisation devices	Irradiation of unplanned volume with short or excess in beam range. If OAR is covered with the volume, the consequence might be severe.	Check of thickness and materials at acceptance
Task or step: Treatment Planning			
3	Wrong selection of CT-WEL datasets for planning CT	Irradiation of unplanned volume with short or excess in beam range. If OAR is covered with the volume, the consequence might be severe.	Independent or redundant verification of CT-WEL data. Comparison of dose calculation with measurement for a phantom.
4	Oversight and/or wrong processing of metallic artefact	As above	Independent or redundant verification of CT Image and processing
Task or step: Data Transfer from TPS			
5	Wrong beam energy (and/or width of SOBP) transferred from TPS to numerical controlled machine	Irradiation of unplanned volume. If OAR is covered with the volume, the consequence might be severe.	Independent or redundant verification of range-energy data. Comparison of plan with measurement for dose distribution.
6	Wrong collimator shape data transferred from TPS to beam controller	As above	Check of light field and/or X-ray image of beam's eye view. Comparison of design plan with measurement for the shape of collimator.

7	Wrong MU value transferred from TPS to beam controller	Unplanned dose delivery. Over dose might result in severe complication. Underdose might result in poor local control.	Dosimetry before patient treatment. Check of MU value in previous fractionation.
Task or step: Manufacturing Collimator and Range Compensator Specific to Patient			
8	Inappropriate cutting	Irradiation of unplanned volume. If OAR is covered with the volume, the consequence might be severe	Comparison of design plan with measurement for the shape of collimator and range compensator.
Task or step: Dose Xalibration			
9	Inappropriate dose calibration	Unplanned dose delivery. Overdose might result in severe complication. Underdose might result in poor local control.	Independent or redundant check of measurement, calibration coefficient and correction factors before treatment.
Task or step: Irradiation			
10	Misunderstanding of prescribed dose by confusion about units, physical dose and biological (clinical) dose.	Unplanned dose delivery. Over dose might result in severe complication. Underdose might result in poor local control.	Independent check of unit of prescribed dose. Enhancement of communication and training among staff.
11	Wrong snout position	Irradiation of unplanned volume. If OAR is covered with the volume, the consequence might be severe.	Independent check of snout position. Enhancement of communication and training among staff.
12	Using couch different from treatment planning	Irradiation of unplanned volume with short or excess in beam range when beam penetrating the couch.	Independent identification of couch specific to the irradiation. Online monitor of respiration, gate and beam signals during irradiation.
13	Irradiation out of phase in respiration	Irradiation of unplanned volume. If OAR is covered with the volume, the consequence might be severe.	Check of respiration phase generator before irradiation. Online monitor of respiration, gate and beam signals during irradiation.
14	Unplanned insertion of equipment on the beam line.	Irradiation of unplanned volume with short in beam range	Check of position of beam-line equipment before irradiation

7.3. Quality assurance programme and audit

(180) A comprehensive quality assurance (QA) programme can lead to the detection of systematic errors and decrease the frequency and severity of random errors (ICRP, 2000). Although no comprehensive QA programme standard specific to ion beam radiotherapy has been published, some professional bodies are preparing documents regarding QA for ion beam radiotherapy: a QA guideline (JSMP, 2005) is being updated, an international safety standard is under development (IEC, 2012) and also International Commission on Radiation Units and Measurements (ICRU) are preparing a code of practice for ion beam radiotherapy (ICRU, 2007). These are expected to be useful to establish a comprehensive QA programme at an ion beam radiotherapy department.

(181) Independent external audits are a necessary part of a comprehensive QA programme in radiotherapy (IAEA, 2007). The ultimate purpose of a QA audit is to assess the current situation and to improve the quality of the radiotherapy process at the reviewed institution or programme. A comprehensive audit of a radiotherapy programme reviews and evaluates the quality of all the elements involved in radiation therapy, including staff, equipment and procedures, patient protection and safety, and overall performance of the radiotherapy department, as well as its interaction with external service providers. Possible gaps in technology, human resources and procedures will be identified so that the institutions affected will be able to document areas for improvement. Although such a comprehensive audit has not yet been established for ion beam radiotherapy, some activities of audit are being

carried out. In the United States, any proton radiotherapy facility participating National Cancer Institute (NCI)-supported clinical trial is required to accept an on-site dosimetry audit coordinated by the Radiological Physics Center (RPC), based on the Guidelines for the Use of Proton Radiation Therapy in NCI-Sponsored Cooperative Group Clinical Trials (RPC, 2012, Moyers et al., 2014). In Japan, dosimetry intercomparisons were also carried out by the National Institute of Radiological Sciences (NIRS) (Fukumura et al., 1998, 2008) and multi-institutional group discussed the guideline of comprehensive QA programme and carried out dosimetry intercomparison for ion beam radiotherapy (Ozawa et al., 2013). Every ion beam radiotherapy centre is recommended to participate regularly in an external audit programme to verify the calibration of treatment units, ideally with the periodicity of one year, but not less frequently than every five years. It has been reported that the size and number of discrepancies in beam calibration in centres that have participated regularly in external audits are much smaller than those in centres that have not participated in such programme (ICRP *Publication 86*, 2000).

(182) Since ion beam radiotherapy requires large accelerator and more complex systems than conventional radiotherapy, time dedication, training, and competence of staff need to be re-assessed. Once these issues have been addressed properly, a smooth, step-by-step, and safe transition over several years is necessary to maintain safety. It should be noticed that failure to do so may not only be a waste of resources but may also increase the likelihood of accidental exposures of patients.

8. CONCLUSIONS AND RECOMMENDATIONS

- Ion beams, such as protons or carbon ions, in radiotherapy provide excellent dose distribution to the targeted tumour tissue due primarily to their finite range, allowing significant reduction of the undesired exposure to normal tissues outside the target tumour.
- The first step for ion beam radiotherapy, similar to any medical procedure, is justification. The proper selection of the patient should be based on knowledge of radiation oncology, the specific tumour to be treated and available clinical results to provide the optimal benefit to the patient.
- Careful treatment planning is required for optimisation to maximise the efficiency of treatment and to minimise the dose to normal tissues: it depends on the specific treatment method and the specific targeted tumour. Theoretically, as compared with conventional radiotherapy, ion beam radiotherapy delivers radiation dose to the target volume in a more efficient manner, while reducing the undesired exposure to normal tissues. Nonetheless, the treatment planning must be sufficiently precise to avoid damaging critical organs or tissues within or near the target volume.
- An ion beam delivery system consists of an accelerator, a high energy beam transporter and an irradiation system. When ion beams pass through or hit these beam line structures, secondary neutrons and photons can be produced, as well as particle fragments and photons from the activated materials.
- Doses in the out-of-field volumes arise from the secondary neutrons and photons, particle fragments, and photons from activated materials. These doses should be considered from the standpoint of radiological protection.
- Imaging procedures are essential for the delineation of the target tumour, and appropriate treatment planning and daily adjustment of the beam delivery to the target. It is recognised that use of imaging procedures delivers additional radiation dose to the patient.
- Appropriate management is required for the therapy equipment and also for the air in the treatment room which is activated. Management should always be in conformity with criteria of the regulatory agencies. The current regulations for occupational exposures in photon radiotherapy are also applicable to ion beam radiotherapy with protons or carbon ions.
- After the treatment with ion beam radiotherapy, the patient is a radioactive source. However, radiation exposure to family members or public is small, and no specific care is required.
- Ion beam radiotherapy requires a much complicated treatment system than conventional radiotherapy, and extensive training of the staff and adequate quality assurance programme are recommended to avoid possible accidental exposure to the patient.

APPENDIX A. DOSIMETRY AND MODEL

A.1. Dosimetry techniques

(A 1) Absorbed dose is regarded as the primal factor to be controlled in radiotherapy. It is defined as the amount of energy ΔE absorbed in a material in a unit mass m.

$$D = \frac{\Delta E}{m} \quad \text{[J/kg, Gy]}$$

According to ICRU Report 85 (2011), the absorbed dose, D, is the quotient of $\mathrm{d}\bar{\varepsilon}$ by dm, where $\mathrm{d}\bar{\varepsilon}$ is the mean energy imparted by ionising radiation to matter of mass dm, thus

$$D = \frac{\mathrm{d}\bar{e}}{\mathrm{d}m}$$

The unit is J kg^{-1}and the special name for the unit of absorbed dose is gray (Gy).

(A 2) As the body of a patient is approximated as water in various local densities in radiotherapy, it is necessary to obtain the absorbed dose to water at the point of interest.

A.1.1. Ionisation chamber

(A 3) The most common experimental method currently in use in the field of radiotherapy to obtain the absorbed dose in water is to measure the amount of charge produced in certain amount of air in an ionisation chamber. Under the charged particle equilibrium condition where the charge produced outside of the region of interest (ROI) by radiation originated inside of the ROI is balanced with the one produced inside of the ROI by radiation originated outside of the ROI, absorbed dose in air D_{air} is linked to the amount of charge dQ in a unit mass dm via W-value.

$$\frac{\mathrm{d}Q}{\mathrm{d}m} = \frac{D_{air}}{(\bar{w}/e)}$$

W-value is the average energy expected to be consumed for the production of one ion pair.

(A 4) As the absorbed dose measured by an ionisation chamber is that in air not in water, it is necessary to convert the value from air to water. The conversion is valid only when the Bragg-Gray criteria of cavity theory are met. The cavity theory requires that the cavity (ionisation chamber) is small enough and causes no turbulence in fluence inside and outside of the cavity. Then, the absorbed dose in air and water,

$$D_{air} = \left(\frac{dE}{dx} \cdot \frac{1}{\rho} \right) \cdot \Phi_{air}$$

$$D_{water} = \left(\frac{dE}{dx} \cdot \frac{1}{\rho} \right)_{water} \cdot \Phi_{water}$$

are united as

$$D_{water} = \left(\frac{dE}{dx} \times \frac{1}{r}\right)_{air}^{water} \times D_{air}$$

(A 5) Under the $\Phi_{water} = \Phi_{air}$ approximation given by the cavity theory, the ratio of absorbed dose in water and air is equal to the ratio of mass stopping power in both media.

(A 6) Recombination of produced ion pairs is also an important factor to be considered in ionisation chamber dosimetry. There are two recombination modes: initial recombination and general recombination. In initial recombination, ion pairs produced along one radiation track are encountered and neutralised before reaching the anode or cathode. This recombination is possible when the density of the initial ion pair is high enough in contrast to the gradient of the electric field, therefore, this recombination is considered to be significant in a high LET beam. General recombination happens between ions originating from different tracks, and can happen even with a low LET beam if irradiated at a high dose rate.

A.1.2. Calorimetry

(A 7) Although ionisation chamber dosimetry is most widely used in radiotherapy due to its easy-handling, achievable accuracy and relatively high reproducibility, the estimation of absorbed dose in water is complex as described above and causes some uncertainty in the absolute dosimetry due to the uncertainty of parameters used in the procedure.

(A 8) Calorimetry would be the most direct approach in obtaining the absorbed dose, as almost all of the energy brought by radiation is finally turned into heat. The increase in temperature of the material ΔT is united as the absorbed dose D with thermal capacity h.

$$\Delta T = \frac{E(1-\delta)}{hm} = \frac{D(1-\delta)}{h}$$

Here, the parameter δ is called the heat defect and represents the ratio of imparted energy that is not spent as increasing heat as other processes such as chemical transformation, convection and so on.

(A 9) The difficulty with calorimetry is that an increase in temperature caused by radiation at the therapeutic range (1 Gy) is quite small. In the case of aluminum, the absorption of 1 Gy corresponds to about 1.1 mK rise in temperature. If 1% precision is necessary in dose assessment, the change of 10 μK must be measured. A thermistor incorporated in a Wheatstone bridge is often used for this purpose; however, special and delicate care is indispensable to achieve the necessary precision. Currently graphite is preferred as the medium for ion beam radiotherapy (Sakama et al., 2009).

A.1.3. TLD

(A 10) Among various and available accumulative (passive) dosimeters, the TLD is most commonly used in the field of radiotherapy. Once irradiated, the crystal in the TLD is excited and some of its electrons are trapped before falling to the ground state. Those trapped at a shallower potential are easily excited by room temperature and fall to the ground; however, those trapped at a deeper potential are stable for years under normal conditions. The portion can be extracted as a visible light by

heating up to 400 ~ 500ºC. The emitted light is monitored by a photomultiplier tube. As the amount of emitted light corresponds to the dose absorbed in the TLD, it is possible to estimate the absorbed dose at the point where the TLD is located.

(A 11) When using TLD, special care should be paid to its energy (LET) dependence. The response of the TLD drastically falls as LET increases. Supra-linearity is also a unique response of TLD. If radiation of 10 Gy or more is irradiated to the TLD, the emitted light exceeds the expected linear approximation.

A.1.4. Optically stimulated luminescence (OSL)

(A 12) OSL is based on a principle similar to that of thermoluminescence dosimetry. Instead of heat, light (from a laser) is used to release the trapped energy in the form of luminescence. The integrated dose measured during irradiation can be evaluated using OSL directly afterwards. The optical fiber optically stimulated thermoluminescent dosimeter consists of a small chip of carbon doped aluminum oxide (Al_2O_3:C) coupled with a long optical fibre, a laser, a beam splitter and a collimator, a photomultiplier tube (PMT), electronics and software. To produce OSL, the chip is excited with laser light through an optical fibre, and the resulting luminescence (blue light) is carried back in the same fiber, reflected through 90º by the beam splitter and measured in a PMT. The optical fibre dosimeter exhibits high sensitivity over the wide range of dose rates and doses used in radiotherapy. The OSL response is generally linear and independent of energy as well as the dose rate, although the angular response requires correction (Podgorsak, 2005).

A.1.5. RGD

(A 13) Silver ions in the RGD form a centre of luminescence which is stable at room temperature for more than a year. Once stimulated by the incidence of light such as N_2 gas laser and solid-state ultraviolet laser, the luminescent light is emitted. The amount of light observed by a photomultiplier shows a good relation to the absorbed dose of the detector. The response of the RGD for charged ion beams shows the stronger LET dependence than that of TLDs; however, it is advantageous in its ease of handling.

A.1.6. Code of practice

(A 14) Currently a code of practice for the estimation of absorbed dose of an ion beam is available for the use of ionisation chambers. IAEA has released it as TRS398 (Andreo et al., 2000). It provides guidance on the appropriate method to obtain the absorbed dose to water by using an ionisation chamber for photons, electrons and ion beams. Following the protocol, the absorbed dose at the point of interest D_C is determined by the following equation

$$D_C = M \cdot N_{D,W} \cdot k_Q$$

Here, M, $N_{D,w}$ and k_Q represent the measurement by the reference chamber, a calibration constant for absorbed dose to water, and a conversion coefficient of radiation quality, respectively. $N_{D,w}$ and k_Q are determined by calibrating the chamber with gamma-rays from a standard ^{60}Co source.

A.2. Application of Monte Carlo simulation codes

(A 15) Monte Carlo simulations in the field of ion beam radiotherapy have undergone remarkable improvements in the precision and computing time in recent years. SHIELD-HIT (Gudowska et al., 2004), FLUKA (Fasso et al., 2005), Geant4 (Allison et al., 2006) and PHITS (Iwase et al., 2002; Niita et al., 2006) have all been commonly applied to solve problems in ion beam radiotherapy. However, care should still be paid to the precision of the outcome.

A.3. Biological response model

(A 16) The biological and clinical effectiveness of ion beams are primarily governed by the absorbed dose; however, radiation quality also modulates the outcome.

A.3.1. Parameter of radiation quality

(A 17) The most commonly used quantity for specifying radiation quality is LET (ICRU, 1970). LET is a measure of the energy transferred to a material of thickness 'dx' as an ionising particle travels through it,

$$LET_{\Delta} = \frac{dE_{\Delta}}{dx}$$

'dE_{Δ}' refers to the energy loss due to electronic collisions, minus the kinetic energies of all secondary electrons with energy larger than 'Δ'. When 'Δ' approaches infinity, the LET_{Δ} becomes identical to the linear electronic stopping power.

(A 18) Absorbed dose is given as the product of stopping power and fluence as below.

$$D = \frac{dE}{dx} \cdot \frac{1}{\rho} \cdot \Phi$$

(A 19) In addition, microdosimetry is also within the scope of this section. The concept of microdosimetry and the difference between a microdosimetric quantity such as lineal energy or specific energy and the corresponding conventional quantity such as LET or absorbed dose is described. Particle dependence of these quantities is also shown, and biological models for ion beams based on the (macroscopic) LET or microdosimetric quantities are also introduced.

(A 20) If an incident beam is not monoenergetic, the averaged energy value can be calculated.

$$LET_T = \frac{\sum \left(LET_i \times \Phi_i \right)}{\sum \Phi_i} \cdot A$$

$$LET_D = \frac{\sum \left(LET_i \times LET_i \times \Phi_i \right)}{\sum \left(LET \times \Phi_i \right)} \cdot A$$

(A 21) LET_T is called the track-averaged LET and a simple mean of the LET spectra. LET_D is the LET-weighted average of the LET_T. LET_D is known to be a good index for biological effectiveness of ion beams used for radiotherapy.

(A 22) Though the LET is found useful in describing the biological effect of ion beams, some limitations should also be pointed out. The most important one is related to the definition of LET: LET only considers energy loss toward the particle direction, i.e., it is not defined for a volume. This is considered to be too

macroscopic when a cell nucleus, which is about 10 μm in diameter, is allocated as the main target. When the target size (cell nucleus) is so small, statistical fluctuation becomes large and the macroscopic and averaged values of absorbed dose and LET tend to have less meaning. Microdosimetry can be used to account for the problem of LET or absorbed dose (ICRU, 1983). Instead of absorbed dose or LET, it introduces specific energy or lineal energy.

A.3.2. Biological models

(A 23) Many biological models have been proposed, depending on aims. In this section, models which have been applied for ion beam radiotherapy for the prospective estimation of clinical effect at the step of treatment planning have been explained briefly.

LQ formalism

(A 24) The LQ formalism, or often practically called LQ model is the most popular model used in radiotherapy. It describes biological effects as a function of absorbed dose. For example, the probability of cell survival, '*S*', is indicated by:

$$S = \exp\left(-\alpha \cdot D - \beta \cdot D^2\right)$$

The constants α and β can be taken as to represent the radiosensitivity of a specific biological target, as a ratio α/β. The LET dependence is often absorbed in α and β, i.e., α and β depend not only on a biological endpoint but also on radiation quality, LET.

(A 25) The LQ model is usually considered to be valid for doses in the range of 1 to 10 Gy (for example, Brenner, 2008).

Local effect model (LEM)

(A 26) The LEM was developed in associated with the carbon ion radiotherapy project at GSI, Germany (Scholz et al., 1997; Elsässer and Scholz, 2007; Elsässer et al., 2008). Instead of macroscopic absorbed dose, it uses the track structure. The target cell is divided into a vast number of tiny voxels, and a modified LQ model is applied for every voxel to estimate the number of local lesions produced in the voxel. The total number of lesions is derived by summing up the local lesions and the fate of the cell is determined depending on the number of lesions. Here, α and β parameters used in the LEM are taken from X-ray irradiation information, i.e., the LEM assumed that the biological response to various radiations is in principle identical to that of X-rays and that microscopic differences in track structure modify the observed response.

(A 27) One of the advantages of the LEM over other models, like the microdosimetric kinetic model (MKM, see below), is that it fully exploits the details of track structure in nm-dimensions, whereas the micro-dosimetric approach is based on average energy depositions in μm-dimensions.

MKM

(A 28) The MKM (Hawkins, 1996) is very similar to LEM: it also divides the cell into a vast number of tiny voxels. The difference is that, instead of the statistically smoothed dose distribution used in the LEM, the MKM introduces the microdosimetric quantity. One of the advantages of the MKM over the LEM is that the microdosimetric quantity can be derived by using an experimental technique. It allows for example, for use in QA, assessing the biological effectiveness at any

point of interest in a complex therapeutic irradiation field. It has been confirmed that the two models in principle predict similar effects for cell killing after ion beam radiation (Kase et al., 2008).

REFERENCES

Agostinelli, S., Allison, J., Amako, K., et al., 2003. GEANT4—a simulation toolkit. Nucl. Instrum. Methods Phys. Res. A506, 250–303.

Allen, A.M., Pawlicki, T., Dong, C, et al., 2012. An evidence based review of proton beam therapy: The report of ASTRO's emerging technology committee. Radiother. Oncol. 103, 8–11.

Allison, J., Amako, K., Apostolakis, J., et al., 2006. Geant4 developments and applications. IEEE Trans. Nucl. Sci. 53, 270–278.

Almen, A., Ahlgren, L., Mattsson, S., 1991. Absorbed dose to technicians due to induced activity in linear accelerators for radiation therapy. Phys. Med. Biol. 36, 815–822.

Alpen, E.L., Powers-Risius, P., Curtis, S.B., et al., 1993. Tumorigenic potential of high-Z, high-LET charged-particle radiations. Radiat. Res. 136, 382–391.

Ando, K., Kase, Y., 2009. Biological characteristics of carbon-ion therapy. Int. J. Radiat. Biol. 85, 715–728.

Andreo, P., Burns, D.T., Hohlfeld, K., et al., 2000. Absorbed dose determination in external beam radiotherapy: An international Code of Practice for dosimetry based on standards of absorbed dose to water IAEA Technical Report Series No 398 IAEA, Vienna

Athar, B.S., Paganetti, H., 2009. Neutron equivalent doses and associated lifetime cancer incidence risks for head & neck and spinal proton therapy. Phys. Med. Biol. 54 (16), 4907–4926.

Athar, B.S., Bednarz, B., Seco, J., et al., 2010. Comparison of out-of-field photon doses in 6-MV IMRT and neutron doses in proton therapy for adult and pediatric patients. Phys. Med. Biol. 55, 2879–2892.

Avery, S., Ainsley, C., Maughan, R., et al., 2008. Analytical shielding calculations for a proton therapy facility. Radiat. Prot. Dosim. 131, 167–179.

Barendsen, G.W., 1968. Respone of cultured cells, tumors and normal tissues to radiations of different liner energy transfer. Curr. Topics Radiat. Res. Q4, 293–356.

BEIR-VII, 2006. Health Risks from Exposure to Low Levels of Ionizing Radiation, Phase 2, The National Academies Press, Washington DC.

Belkacémi, Y., Ozsahin, M., Pène, F., et al., 1996. Cataractogenesis after total body irradiation. Int. J. Radiat. Oncol. Biol. Phys. 35, 53–60.

Bettega, D., Calzolari, P., Hessel, P., et al., 2009. Neoplastic transformation induced by carbon ions. Int. J. Radiat. Oncol. Biol. Phys. 73, 861–868.

Bithell, J.F. and Stewart, A.M., 1975, Pre-natal irradiation and childhood malignancy: A review of British data from the Oxford survey. Br. J. Cancer 31, 271-287.

Boice, J.D.Jr., Miller, R.W., 1999. Childhood and adult cancer after intrauterine exposure to ionizing radiation. Teratology 59, 227–33.

Brenner, D.J., 2008. The linear-quadratic model is an appropriate methodology for determining isoeffective doses at large doses per fraction. Semin. Radiat. Oncol. 18, 234–239.

Brenner, D.J., Medvedovsky, C., Huang, Y., et al., 1993. Accelerated heavy particles and the lens VIII. Comparison between the effects of iron ions (190 keV/μm) and argon ions (88 keV/μm). Radiat. Res. 133, 198–203.

Brenner, D.J., Elliston, C.D., Hall E.J., et al., 2009. Reduction of the secondary neutron dose in passively scattered proton radiotherapy, using an optimized pre-collimator/collimator. Phys. Med. Biol., 54: 6065–6078.

Castro, J.R., Chen, G.T.Y., Blakely, E.A., 1985. Current consideration in charged-particle radiotherapy. Radiat. Res. 104, S263–S271.

Chadwick, M.B., 1998. Neutron, Proton, and Photonuclear Cross Sections for Radiation Therapy and Radiation Protection Conference: International Meeting on Computational

Methods in Track Structure Simulation in Physical and Biological Sciences, Theory and Applications, Oxford (GB).
Chauvel, P., 1995. Treatment planning with heavy ions. Radiation & Environmental Biophysics 34, 49–53.
Clapp, N.K., Darden, Jr., E.B., Jerigan, M.C., 1974. Relative effects of whole-body sublethal doses of 60-MeV protons and 300 kVp X rays on disease incidence in 1 RF mice. Radiat. Res. 57, 158–186.
Clasie, B., Wroe, A., Kooy H., et al., 2010. Assessment of out-of-field absorbed dose and equivalent dose in proton fields. Med. Phys. 37, 311–321.
d'Errico, F., Luszik-Bhadra, M., Nath, R., et al., 2001. Depth dose-equivalent and effective energies of neutrons generated by 6-18 MV X-ray beams for radiotherapy. Health Phys. 80, 4–11.
Edwards, A.A., 1997. The use of chromosomal aberrations in human lymphocytes for biological dosimetry. Radiat. Res. 148, S39–S44.
Edwards, A.A. Lloyd, D.C., 1996. Risk from deterministic effects of ionising radiation. Doc. NRPB Vol. 7 No.3.
Elsässer, T., Scholz, M., 2007. Cluster effects within the local effect model. Radiat. Res. 167, 319–329.
Elsässer, T., Krämer, M., Scholz, M., 2008. Accuracy of the local effect model for the prediction of biologic effects of carbon ion beams in vitro and in vivo. Int. J. Radiat. Oncol. Biol. Phys. 71, 866–872.
Endo, M., Nishizawa, K., Iwai, K., et al., 1999. Image characteristics and effective dose estimation of a cone beam CT using a video-fluoroscopic system. IEEE Trans. Nucl. Sci. 46, 686–690.
Enghardt, W., Fromm, W.D., Geissel, H., et al., 1992. The spatial distribution of positron-emitting nuclei generated by relativistic light ion beams in organic matter. Phys. Med. Biol. 37, 2127–2131.
Fasso, A., Ferrari, A., Ranft, J., et al., 2005. FLUKA: a multi-particle transport code. CERN-2005-10.
Fischer, H.W., Tabot, B., Poppe, B., 2008. Comparison of activation products and induced dose rates in different high-energy medical linear accelerators. Health Phys, 94, 272–278.
Followill, D., Geis, P., Boyer, A., 1997. Estimates of whole-body dose equivalent produced by beam intensity modulated conformal therapy. Int. J. Radiat. Oncol. Biol. Phys., 38, 667–672.
Fontenot, J.D., Lee, A.K., Newhauser, W.D., 2009. Risk of secondary malignant neoplasm from proton therapy and intensity-modulated X-ray therapy for early-stage prostate cancer. Int. J. Radiat. Oncology Biol. Phys. 74, 616–622.
Fontenot, J.D., Taddei, P.J., Zheng, Y., et al., 2008. Equivalent dose effective dose from stray radiation during passively scattered proton radiotherapy for prostate cancer. Phys. Med. Biol. 53, 1677–1688.
Fujii,, K., Aoyama, T., Koyama, S., et al., 2007. Comparative evaluation of organ and effective doses for paediatric patients with those for adults in chest and abdominal CT examinations. Br. J. Radiol. 80, 657–667.
Futami, Y., Kanai, T., Fujita, M., et al., 1999. Broad-beam three-dimensional irradiation system for heavy-ion radiotherapy at HIMAC. Nucl. Instrum. Method Phys. Res. A430, 143–153.
Fry, R.J., Powers-Risius, P., Alpen, E.L., et al., 1985. High-LET radiation carcinogenesis. Radiat. Res. 8, S188–S195.
Goitein, M. 1983. Beam scanning for heavy charged particle radiotherapy' Med. Phys. 10, 831–840.
Goiten, M., 2008. Radiation Oncology: A Physicist's Eye View, Springer.
Goodhead, D.T., Thacker, J., Cox, R., 1993. Weiss Lecture. Effects of radiations of different qualities on cells: molecular mechanisms of damage and repair. Int. J. Radiat. Biol. 63, 543–556.

Gottschalk, B., 2008. Passive Beam Scattering. In: Delaney, T.F., Kooy, H.M. (Eds.), Proton and Charged Particle Radiotherapy. Lippincott, Williams and Wilkins, Chapter 5A.

Grusell, E., Montelius, A., Brahme, A., et al., 1994. A general solution to charged particle beam flattening using an optimized dual scattering foil technique, with application to proton therapy beams. Phys. Med. Biol. 39, 2201–2216.

Gudowska, I., Sobolevsky, N., Andreo, P., et al., 2004. Ion beam transport in tissue-like media using the Monte Carlo code SHIELD-HIT. Phys. Med. Biol. 49, 1933-1958.

Gunzert-Marx, K., Iwase, H., Schardt, D., et al., 2008. Secondary beam fragments produced by 200 MeV u^{-1} ^{12}C ions in water and their dose contributions in carbon ion radiotherapy. New J. Phys. 10, 075003.

Haberer, T, Becher W., Schardt D., et al., 1993. Magnetic scanning system for heavy ion therapy. Nucl. Instrum. Methods Phys. Res. A330, 296–305.

Hall, E.J., Novak, J.K., Kellerer, A.M., et al., 1975. RBE as a function of neutron energy. I. Experimental observations. Radiat. Res. 64, 245–255.

Hall, E.J., 2006. Intensity-modulated radiation therapy, protons, and the risk of second cancers. Int. J. Radiation Oncology Biol. Phys. 65, 1–7.

Hart, D., Hillier, M.C., Wall, B.F., et al., 2007. Doses to patients from radiographic and fluoroscopic X-ray imaging procedures in the UK – 2005 Review. HPA-RPD-029, Chilton, UK.

Hawkins, R.B., 1996. A microdosimetric-kinetic model of cell death from exposure to ionizing radiation of any LET with experimental and clinical applications. Int. J. Radiat. Biol. 69, 739–755.

Hecksel, D., Anferov, V., Fitzek, M., et al., 2010. Influence of beam efficiency through the patient-specific collimator on secondary neutron dose equivalent in double scattering and uniform scanning modes of proton therapy. Med. Phys. 37, 2910–2917.

Hopewell, J.W., Trott, K.R., 2004. Volume effects in radiobiology as applied to radiotherapy. Radiother. Oncol. 56, 283–288.

Hosokawa, Y., Minowa, K., Sawamura, T., et al., 1995. Trial of overlapping of CT and MRI image for radiation therapy planning with shell. Dent. Radiol. 35, 53–57.

Howell, R.M., Ferenci, M.S., Hertel, N.E., et al., 2005. Investigation of secondary neutron dose for 18 MV dynamic MLC IMRT delivery, Med. Phys. 32, 786–793.

Howell, R.M., Hertel, N.E., Wang, Z., et al., 2006. Calculation of effective dose from measurement of secondary neutron spectra and scattered photon dose from dynamic MLC IMRT for 6 MV, 15 MV, and 18 MV beam energies. Med. Phys. 33, 360–368.

Huang, B., Law, M.W. Khong, P.L., 2009. Whole-body PET/CT scanning: estimation of radiation dose and cancer risk. Radiology 251, 166–174.

IAEA, 1996. International Basic Safety Standards for Protection against Ionizing Radiation and for the Safety of Radiation Sources, Safety Series 115.

IAEA, 2000. Lessons learned from accidental exposures in radiotherapy. Vienna: International Atomic Energy Agency, 2000. Safety reports series, ISSN 1020-6450; no 17, STI/PUB/1084, ISBN 92-0-100200-9.

IAEA, 2004. Application of the Concept of Exclusion, Exemption and Clearance, Safety Guide, IAEA Safety Standards Series No. RS-G-1.7.

IAEA, 2006. Applying Radiation Safety Standards in Radiotherapy, Safety Reports Series 38.

IAEA, 2007. Comprehensive audits of radiotherapy practices: a tool for quality improvement: Quality Assurance Team for Radiation Oncology (QUATRO), Vienna: International Atomic Energy Agency, 2007. STI/PUB/1297, ISBN 92–0–103707–4 http://www-pub.iaea.org/MTCD/publications/PDF/Pub1297_web.pdf

IARC, 2000. Monographs on the evaluation of carcinogenic risks to humans. vol.75, Ionizing radiation, Part 1: X- and gamma-radiation, and neutrons.

ICRP, 1984. Non-stochastic effects of irradiation. ICRP Publication 41, Ann. ICRP 14(3).

ICRP, 1987. Radiation Dose to Patients from Radiopharmaceuticals. ICRP Publication 53. Ann. ICRP 18(1-4).

ICRP, 1991. Recommendations of the International Commission on Radiological Protection. ICRP Publication 60, Ann. ICRP 21(1-3).
ICRP, 1994. Dose Coefficients for Intakes of Radionuclides by Workers. ICRP Publication 68. Ann. ICRP 24(4).
ICRP, 1998a. Genetic Susceptibility to Cancer, ICRP Publication 79, Ann. ICRP 28(1-2).
ICRP, 1998b. Radiation Dose to Patients from Radiopharmaceuticals Addendum 2 to ICRP Publication 53. ICRP Publication 80. Ann. ICRP 28(3).
ICRP, 2000. Prevention of accidental exposure to patients undergoing radiation therapy. ICRP Publication 86, Ann. ICRP 30(3).
ICRP, 2001. Managing patient dose in computed tomography. ICRP Publication 87. Ann. ICRP 30(4).
ICRP, 2003a. Biological Effects after Prenatal Irradiation (Embryo and Fetus), ICRP Publication 90, Ann. ICRP 33(1-2).
ICRP, 2003b. Relative Biological Effectiveness (RBE), Quality Factor (Q), and Radiation Weighting Factor (w_R). ICRP Publication 92, Ann. ICRP 33(4).
ICRP, 2007a. Managing Patient Dose in Multi-Detector Computed Tomography (MDCT). ICRP Publication 102. Ann. ICRP 37(1).
ICRP, 2007b. The 2007 Recommendations of the International Commission on Radiological Protection. ICRP Publication 103. Ann. ICRP 37(2-4).
ICRP, 2007c, Scope of Radiological Protection Control Measures. ICRP Publication 104, Ann. ICRP 37(5).
ICRP, 2007d. Radiological Protection in Medicine. ICRP Publication105, Ann. ICRP 37(6).
ICRP, 2008. Radiation Dose to Patients from Radiopharmaceuticals - Addendum 3 to ICRP Publication 53. ICRP Publication 106. Ann. ICRP 38(1-2).
ICRP, 2009. Preventing accidental exposures from new external beam radiation therapy technologies, ICRP Publication 112, Ann. ICRP 39(4).
ICRP, 2012. ICRP Statement on Tissue Reactions/Early and Late Effects of Radiation in Normal Tissues and Organs – Threshold Doses for Tissue Reactions in a Radiation Protection Context. ICRP Publication 118, Ann. ICRP 41(1/2).
ICRU, 1970. Linear Energy Transfer. ICRU Report 16.
ICRU, 1983. Microdosimetry. ICRU Report 36.
ICRU, 1986. The Quality Factor in Radiation Protection. ICRU Report 40.
ICRU, 1993a. Stopping Power and Ranges for Protons and Alpha Particles. ICRU Report 49.
ICRU, 1993b. Prescribing, recording, and reporting photon beam therapy. ICRU Report 50.
ICRU, 1999. Prescribing, recording, and reporting photon beam therapy (supplement to ICRU Report 50). ICRU Report 62.
ICRU, 2005a. Stopping of Ions Heavier Than Helium. ICRU Report 73.
ICRU, 2005b. Patient Dosimetry for X Rays used in Medical Imaging. ICRU Report 74.
ICRU, 2007. Prescribing, Recording and Reporting Proton-Beam Therapy. ICRU Report 78.
ICRU, 2011. Fundamental Quantities and Units for Ionizing Radiation (Revised). ICRU Report 85.
IEC, 2012. Particular requirements for the basic safety and essential performance of medical light ion beam equipment. International Electrotechnical Commission, 60601-2-64/Ed1/CD.
Imaoka, T., Nishimura, M., Kakinuma, S., et al., 2007. High relative biological effectiveness of carbon ion radiation on induction of rat mammary carcinoma and its lack of H-*ras* and *Tp53* mutations. Int. J. Radiat. Oncol. Biol. Phys. 69, 194–203.
Islam, M.K., Purdie, T.G., Norrlinger, B.D., et al., 2006. Patient dose from kilovoltage cone beam computed tomography imaging in radiation therapy. Med. Phys. 33, 1573–1582.
Iwase, H., Niita, K., Nakamura, T., 2002. Development of general-purpose particle and heavy ion transport Monte Carlo code. J. Nucl. Sci. Technol. 39, 1142–1151.
Jiang, H., Wang, B., Xu, X.G., et al., 2005. Simulation of organ-specific patient effective dose due to secondary neutrons in proton radiation treatment. Phys. Med. Biol. 50, 4337–435.

Jones, D.G., Wall, B.F., 1985. Organ doses from medical X-ray examinations calculated using Monte Carlo techniques. NRPB *Report R186*. Chilton, UK.

JSMP, 2005. Guidelines of Physical and Technological Quality Assurance for Particle Beam Therapy, Japan Society of Medical Physics.

Kamada, T., Tsujii, H., Tsuji, H., et al., 2002. Efficacy and safety of carbon ion radiotherapy in bone and soft tissue sarcomas. J. Clin. Oncol. 20, 4466–4471.

Kan, M.W., Leung, L.H., Wong, W., et al., 2008. Radiation dose from cone beam computed tomography for image-guided radiation therapy. Int. J. Radiat. Oncol. Biol. Phys. 70, 272–279.

Kanai, T., Endo, M., Minohara, S., et al., 1983. Biophysical characteristics of HIMAC clinical irradiation system for heavy-ion radiation therapy. Int. J. Radiat. Oncol. Biol. Phys. 44, 201–210.

Kanai, T., Kawachi, K., Kumamoto, Y., et al., 1980. Spot scanning for proton therapy, Med. Phys. 7, 355–369.

Kanai, T., Kawachi, K., Matsuzawa, H., et al., 1993. Broad beam three-dimensional irradiation for proton radiotherapy. Med. Phys. 10, 344–346.

Kanai, T., Fukumura, A., Kusano, Y., et al., 2004. Cross-calibration of ionization chambers in proton and carbon beams. Phys. Med. Biol. 49, 771–781.

Kanematsu, N., Endo, M., Futami, Y., et al., 2002. Treatment planning for the layer-stacking irradiation system for three-dimensional conformal heavy-ion radiotherapy. Med. Phys. 29, 2823–2829.

Kanematsu, N., Akagi, T., Yonai, S., et al., 2006. Extended collimator model for pencil-beam dose calculation in proton radiotherapy. Phys. Med. Biol. 51, 4807–4817.

Kase, Y., Kanai, T., Matsufuji, N., et al., 2008. Biophysical calculation of cell survival probabilities using amorphous track structure models for heavy-ion irradiation. Phys. Med. Biol. 53, 37–59.

Kawashima, M., Kohno, R., Nakachi, K., et al., 2011. Dose-Volume Histogram Analysis of the Safety of Proton Beam Therapy for Unresectable Hepatocellular Carcinoma. Int. J. Radiat. Oncol. Biol. Phys. 79, 1479–1486.

Keall, P.J., Starkschall, G., Shukla, H., et al., 2004. Acquiring 4D thoracic CT scans using a multislice helical method. Phys. Med. Biol. 49, 2053–2067.

Kry, S.F., Salehpour, M., Followill, D.S., 2005a. Out-of-field photon and neutron dose equivalents from step-and-shoot intensity-modulated radiation therapy. Int. J. Radiat. Oncol. Biol. Phys. 62, 1204–1216.

Koehler, A.M., Schneider, R.J., Sisterson, J.M., 1975. Range modulators for protons and heavy ions. Nucl. Instrum. Methods 131, 437–440.

Kostjuchenko, V., Nichiporov, D., Luckjashin, V., 2001. A compact ridge filter for spread out Bragg peak production in pulsed proton clinical beams. Med. Phys. 28, 1427–1430.

Kry, S.F, Salehpour, M., Followill, D.S., et al., 2005b. The calculated risk of fatal secondary malignancies from intensity-modulated radiation therapy. Int. J. Radiat. Oncol. Biol. Phys. 62, 1195–1203.

Kry, S.F., Followill, D.S., White, R.A., et al., 2007. Uncertainty of calculated risk estimates for secondary malignancies after radiotherapy. Int. J. Radiat. Oncol. Biol. Phys. 68, 1265–1271.

Kusano, Y., Kanai, T., Kase, Y., et al., 2007. Dose contributions from large-angle scattered particles in therapeutic carbon beams. Med. Phys. 34, 193-198.

Larsson, B., 1961. Pre-therapeutic physical experiments with high energy protons. Br. J. Radiol. 34, 143–151.

Lee, C., Lee, C., Staton, R.J., et al., 2007. Organ and effective doses in pediatric patients undergoing helical multislice computed tomography examination. Med. Phys. 34, 1858–1873.

Lievens, Y. and Pijls-Johannesma, M., 2013. Health economic controversy and cost-effectiveness of proton therapy. Sem. Radiat. Oncol. 23, 134–141.

Lundkvist, J., Ekman, M., Ericsson, S.C., et al., 2005. Proton therapy of cancer: potential clinical advantages and cost-effectiveness. Acta Oncol. 44, 850–861.

Marucci, L., Niemierko, A., Liebsch, N.J., et al., 2004. Spinal cord tolerance to high-dose fractionated 3D conformal proton-photon irradiation as evaluated by equivalent uniform dose and dose volume histogram analysis. Int. J. Radiation Oncology Biol. Phys. 59, 551–555.

Matsufuji, N., Komori, M., Akiu, K., et al., 2005. Spatial fragment distribution from a therapeutic pencil-like carbon beam in water. Phys. Med. Biol. 50, 3393–3403.

Mesoloras, G., Sandison, G.A., Stewart, R.D., et al., 2006. Neutron scattered dose equivalent to a fetus from proton radiotherapy of the mother. Med. Phys, 33, 2479–2490.

Miller, R.C., Marino, S.A., Napoli, J., et al., 2000. Oncogenic transformation in C3H10T1/2 cells by low-energy neutrons. Int. J. Radiat. Biol. 76, 327–333.

Miralbell, R., Lomax,A., Cella, L., et al., 2002. Potential reduction of the incidence of radiation-induced second cancers by using proton beams in the treatment of pediatric tumors. Int. J. Radiat. Oncol. Biol. Phys. 54, 824–829.

Mizoe, J., Tsujii, H., Kamada, T., et al., 2004. Dose escalation study of carbon ion radiotherapy for locally advanced head and neck cancer. Int. J. Radiat. Oncol. Biol. Phys. 60, 358–364.

Mizuno, H., Tomitani, T., Kanazawa, M., et al., 2003. Washout measurement of radioisotope implanted by radioactive beams in the rabbit. Phys. Med. Biol. 48, 2269–2281.

Mori, S., Ko, S., Ishii, T., et al., 2009. Effective doses in four-dimensional computed tomography for lung radiotherapy planning. Med. Dosim. 34, 87–90.

Moyers, M.F., Lesyna, D.A., 2009. Exposure from residual radiation after synchrotron shutdown. Radiation Measurements 44, 176–181.

Moyers, M F., Ibbott, G.S., Grant, R.L.,et al., 2014. Independent dose per monitor unit review of eight U.S.A. proton treatment facilities. Med. Phys. 01/2014; 41(1):012103

Murphy, M.J., Balter, J., Balter, S., et al., 2007. The management of imaging dose during image-guided radiotherapy: Report of the AAPM Task Group 75. Med. Phys. 34, 4041–4063.

Nakamura, T., Heilbronn, L., 2006. Handbook on secondary particle production and transport by high-energy heavy ions, World Scientific Publ. Co., New Jersey.

Nakashima, E., Neriishi, K., Minamoto, A., 2006. A reanalysis of atomic-bomb cataract data, 2000-2002: a threshold analysis. Health Phys. 90, 154–160.

NCRP, 2011. Second Primary Cancers and Cardiovascular Disease After Radiation Therapy. NCRP Report No. 170.

NCRP, 2013. Preconception and Prenatal Radiation Exposure: Health Effects and Prospective Guidance. NCRP Report No. 174.

Newhauser, W.D., Fontenot, J.D., Mahajan, A., et al., 2009. The risk of developing a second cancer after receiving craniospinal proton irradiation. Phys. Med. Biol. 54, 2277–2291.

Newhauser, W.D., Ding, X., Giragosian, D., et al., 2005. Neutron radiation area monitoring system for proton therapy facileties. Radiat. Prot. Dosim. 115, 149–153.

Niita, K., Sato, T., Iwase, H., et al., 2006. PHITS – a particle and heavy ion transport code system. Rad. Meas. 41, 1080–1090.

Nikjoo, H., Uehara, S., Wilson, W.E., et al., 1998. Track structure in radiation biology: theory and application. Int. J. Radiat. Biol. 73, 355–364.

Niemer-Tucker, M.M., Sterk, C.C., de Wolff-Rouendaal, D., et al., 1999. Late ophthalmological complications after total body irradiation in non-human primates. Int. J. Radiat. Biol. 75, 465–472.

Nishio, T., Sato, T., Kitamura, H., Murakami K., et al., 2005, Distributions of beta-pus decayed nuclei generated in the CH2 and H2O targets by the target nuclear fragment reaction using therapeutic MONO SOBP proton beam, Med. Phys. 32, 1070-1082.

Nishizawa, K., Maruyama, T., Takayama, M., et al., 1991. Determinations of organ doses and effective dose equivalents from computed tomographic examination. Br. J. Radiol. 64, 20–28.

Nishizawa, K., Mori, S., Ohno, M., et al., 2008a. Patient dose estimation for multi-detector-row CT examinations. Radiat. Prot. Dosim. 128, 98–105.

Nishizawa, K., Mori, S., Ohno, M., et al., 2008b. Patient dose estimation on multi detector-row CT from abdomen for adult and abdomen-pelvis for child examinations. Jpn. J. Med. Phys. 27, 153–162.

Nose, H., Kase, Y., Matsufuji, N., et al., 2009. Field size effect of radiation quality in carbon therapy using passive method. Med. Phys. 36, 870–875.

Osaka,Y., Kamada, T., Matsuoka,Y., et al., 1997. Clinical experience of heavy ion irradiation synchronous with respiration. Proceedings of the XIIth ICCR, Salt Lake City, pp. 176–177.

Ozawa, S., Kase, Y., Yamashita, H., et al., 2013. QA Guideline for Particle Beam Therapy Equipment, Proceedings of the Third International Conference on Real-time Tumor-tracking Radiation Therapy with 4D Molecular Imaging Technique, p.50 Sapporo, Japan, 7- 8 February, 2012.

Paganetti, H.. 2003. Significance and implementation of RBE variations in proton beam therapy. Tech. Canc. Res. Treat. 2, 413–426.

Palm, A., Johansson, K.A., 2007. A review of the impact of photon and proton external beam radiotherapy treatment modalities on the dose distribution in field and out-of-field; implications for the long-term morbidity of cancer survivors. Acta Oncologica 46, 462–473.

Pampfer, S., Streffer, C., 1988. Prenatal death and malformations after irradiation of mouse zygotes with neutrons or X-rays. Teratology 37, 599–607.

Pedroni, E., Bacher, R., Blattmann, H., et. al, 1995. The 200-MeV proton therapy project at the Paul Scherrer Institute. Conceptual design and practical realization. Med. Phys. 22, 37–53.

Pedroni, E., Scheib, S., Böhringer, T., et al., 2005. Experimental characterization and physical modeling of the dose distribution of scanned pencil beams. Phys. Med. Biol. 50, 541–561.

Parodi, K., Bortfeld, T., Enghardt, W., et al., 2008. PET imaging for treatment verification of ion therapy: Implementation and experience at GSI Darmstadt and MGH Boston. Nucl. Instr. Meth. Phys. Res. A591, 282–286.

Pelowitz, D.B. (Ed.), 2008. MCNPX User's Manual, Version 2.6.0, Los Alamos National Laboratory Report LA-CP-07-1473.

Perin, B., Walker, A., Mackay, R., 2003. A model to calculate the induced dose rate around an 18MV ELEKTA linear accelerator. Phys. Med. Biol. 48, N75-N81.

Podgorsak, E.B., 2005. Radiation Oncology Physics: A Handbook for Teachers and Students. International Atomic Energy Agency.

Polf, J.C., Newhauser, W.D., 2005. Calculations of neutron dose equivalent exposures from range-modulated proton therapy beams. Phys. Med. Biol. 50, 3859–3873.

Preston, D.L., Ron, E., Tokuoka, S., et al., 2007. Solid cancer incidence in atomic bomb survivors. Radiat. Res. 168, 1–64.

Preston, D.L., Cullings, H., Suyama, A., et al., 2008. Solid cancer incidence in atomic bomb survivors exposed in utero or as young children. J. Natl. Cancer Inst. 100, 428–436.

RPC, 2012. Guidelines for the Use of Proton Radiation Therapy in NCI-Sponsored Cooperative Group Clinical Trials, April 12, 2012. http://rpc.mdanderson.org/RPC/home.htm

Sachs, R.K., Brenner, D.J., 2005. Solid tumor risks after high doses of ionizing radiation. Proc. Natl. Acad. Sci. U S A 102, 13040–13045.

Sakama, M., Kanai, T., Fukumura, A., et al., 2009. Evaluation of w values for carbon beams in air using a graphite calorimeter. Phys. Med. Biol. 54, 1111–1130.

Sawyer, L.J., Whittle, S.A., Matthews, E.S., et al., 2009. Estimation of organ and effective doses resulting from cone beam CT imaging for radiotherapy treatment planning. Br. J. Radiol. 82, 577–584.

Schmid, E., Schlegel, D., Guldbakke, S., et al., 2003. RBE of nearly monoenergetic neutrons at energies of 36 keV-14.6 MeV for induction of dicentrics in human lymphocytes. Radiat. Environ. Biophys. 42, 87–94.

Schneider, U., Agosteo, S., Pedroni, E., et al., 2002. Secondary neutron dose during proton therapy using spot scanning. Int. J. Radiat. Oncol. Biol. Phys. 53, 244–251.

Schneider, U., Lomax, A., Besserer, J., et al., 2007. The Impact of Dose Escalation on Secondary Cancer Risk after Radiotherapy of Prostate Cancer. Int. J. Radiat Oncology Biol. Phys. 68, 892–897.

Schneider, U., Lomax, A., Timmermann, B., 2008. Second cancers in children treated with modern radiotherapy techniques. Radiother. Oncol. 89, 135–140.

Scholz, M., Kellerer, A.M., Kraft-Weyrather, W., et al., 1997. Computation of cell survival in heavy ion beams for therapy. The model and its approximation. Radiat. Environ. Biophys. 36, 59–66.

Schonfeld, S.J., Tsareva, Y.V., Preston, D.L., et al., 2012. Cancer mortality following in utero exposure among offspring of female Mayak Worker Cohort members. Radiat. Res. 178, 160–165.

Schulze-Rath, R., Hammer, G.P., Blettner, M., 2008. Are pre- or postnatal diagnostic X-rays a risk factor for childhood cancer? A systematic review. Radiat. Environ. Biophys. 47, 301–312.

Scott, B.R., 1993. Early occurring and continuing effects. In: Modification of models resulting from addition of effects of exposure to alpha-emitting nuclides. Washington, D.C., Nuclear Regulatory Commission, NUREG/CR-4214, Rev 1, Part II, Addendum 2 (LMF-136).

Scott, B.R., Hahn, F.F., 1989. Early occurring and continuing effects models for nuclear power plant accident consequence analysis. Low-LET radiation. Washington DC, Nuclear Regulatory Commission, NUREG/CR-4214 (SAND85-7185) Rev. 1, Part II.

Shin, D., Yoon, M., Kwak, J., et al., 2009. Secondary Neutron Doses for Several Beam Configurations for Proton Therapy. Int. J. Radiat. Oncol. Biol. Phys. 74, 260–265.

Shrimpton, P.C., Jones, D.G., Hillier, M.C., et al., 1991. Survey of CT Practice in the UK. Part 2: Dosimetric aspects. NRPB Report R249. Chilton, UK.

Sihver, L., Tsao, C.H., Silverberg, R., et al., 1993. Total reaction and partial cross section calculations in proton-nucleus ($Z_t \leq 26$) and nucleus-nucleus reactions (Z_p and $Z_t \leq 26$). Phys. Rev. C47, 1455–1236.

Silari, M., 2001. Special radiation protection aspects of medical accelerators. Radiat. Prot. Dosim. 96, 381–392.

Slater, J.M., 1995. Future direction of clinical ion beam radiation. In: Linz, U. (Ed.), Ion Beam in Tumor Therapy. Chapman & Hall. London, pp.163-168.

Soarers, H.P., Kumar, A., Daniels, S., et al., 2005. Evaluation of new treatments in radiation oncology: are the better than standard treatments? JAMA 293, 970–978.

Stovall, M., Blackwell, C.R., Cundiff, J., et al., 1995. Fetal dose from radiotherapy with photon beams (AAPM Report No.50.). Med. Phys. 22, 63–82.

Suit, H., Goldberg, S., Niemierko. A,, et al., 2007. Secondary carcinogenesis in patients treated with radiation: a review of data on radiation-induced cancers in human, non-human primate, canine and rodent subjects. Radiat. Res. 167, 12–42.

Sullivan, A.H., 1992. A Guide to Radiation and Radioactivity Levels near High Energy Particle Accelerators, p137, Nuclear Technology Publishing, Kent, England.

Sutherland, B.M., Bennett, P.V., Schenk, H., et al., 2001. Clustered DNA damages induced by high and low LET radiation, including heavy ions. Phys. Med. 17 Suppl 1, 202–204.

Taddei, P.J., Fontenot, J.D., Zheng, Y., et al., 2008. Reducing stray radiation dose to patients receiving passively scattered proton radiotherapy for prostate cancer. Phys. Med. Biol. 53, 2131–2147.

Taddei, P.J., Mirkovic, D., Fontenot, J.D., et al., 2009. Stray radiation dose and second cancer risk for a pediatric patient receiving craniospinal irradiation with proton beams. Phys. Med. Biol. 54, 2259–2275.

Tapiovaara, M., Siiskonen, T., 2008. PCXMC: A PC-based Monte Carlo program for calculating patient doses in medical X-ray examinations (2nd Ed.). Report STUK-A231. Radiation and Nuclear Safety Authority. Helsinki, Finland.

Tayama, R., Fujita, Y., Tadokoro, M, et al., 2006. Measurement of neutron dose distribution for a passive scattering nozzle at the Proton Medical Research Center. Nucl. Instr. Meth. Phys. Res. A564, 532–536.

Tobias, C.A., Benton, E.V., Capp, M.P., et. al., 1977. Particle radiography and autoactivation. Int. J. Radiat. Oncol. Biol. Phys. 3, 35–44.

Tobias, C.A., Roberts, J.E., Lawrence, J.H., et al., 1956. Irradiation of hypophysectomy and related studies using 340-MeV protons and 190-MeV deuterons. Peaceful uses Atom. Energy 10, 95–106.

Torikoshi, M., Minohara, S., Kanematsu, N., et al., 2007. Irradiation system for HIMAC. J. Radiat. Res. 48, A15–A25.

Tsuji, H., Yanagi, T., Ishikawa, H., et al., 2005. Hypofractionated radiotherapy with carbon ion beams for prostate cancer. Int. J. Radiat. Oncol. Biol. Phys. 63, 1153-1160.

Tsujii, H., Kamada, T., Baba, M., et al., 2008. Clinical advantages of carbon-ion radiotherapy. New J. Phys. 10, 075009.

Tsujii, H., Akagi, T., Akahane K., et al., 2009. Research on radiation protection in the application of new technologies for proton and heavy ion radiotherapy. Jpn. J. Med. Phys. 28, 172–206.

Tsujii, H., Kamada, T., 2012. A review of update clinical results of carbon ion radiotherapy. Jpn. J. Clin. Oncol. 42, 670–685.

UNSCEAR, 1988. Sources, Effects and Risks of Ionizing Radiation. 1988 Report to the General Assembly with Annexes, United Nations, New York.

UNSCEAR, 1993. Report to the General Assembly, Annex I, Late deterministic effects of radiation in children. United Nations, New York, NY.

UNSCEAR, 2008. Report to the General Assembly with Annexes. United Nations, New York, NY.

UNSCEAR, 2013. Sources, Effects and Risks of Ionizing Radiation. UNSCEAR 2013 Report to the General Assembly with Annexes, Volume II Scientific Annes B: Effects of Radiation Exposure of Children. United Nations, New York, NY.

Van der Giessen, P. H., 1996. A simple and generally applicable method to estimate the peripheral dose in radiation teletherapy with high energy X-rays or gamma radiation. Int. J. Radiat. Oncol. Biol. Phys. 35, 1059–1068.

Vanhavere, F., Huyskens, D., Struelens, L., 2004. Peripheral neutron and gamma doses in radiotherapy with an 18 MV linear accelerator. Radiat. Prot. Dosim. 110, 607–612.

WHO, 2008. Radiotherapy Risk Profile. WHO/IER/PSP/2008.12, World Health Organization.

Withers, H.R., Taylor, J.M.G., Maciejewski, B., 1988. Treatment volume and tissue tolerance. Int. J. Radiat. Oncol. Biol. Phys, 14, 751–759.

Wong, J.W., Sharpe, M.B., Jaffray, D.A., et al. 1999. The use of active breathing control (ABC) to reduce margin for breathing motion. Int. J. Radiat. Oncol. Biol. Phys. 44, 911–919.

Wroe, A., Rosenfeld, A., Schulte, R., 2007. Out-of-field dose equivalents delivered by proton therapy of prostate cancer. Med. Phys. 34, 3449–3456.

Wroe, A., Clasie, B., Kooy, H., et al., 2009. Out-of-field dose equivalents delivered by passively scattered therapeutic proton beams for clinically relevant field configurations. Int. J. Radiat. Oncol. Biol. Phys. 73, 306–313.

Xu, X.G., Bednarz, B., Paganetti, H., 2008. A review of dosimetry studies on external-beam radiation treatment with respect to second cancer induction. Phys. Med. Biol. 53, R193–R241.

Yan, X., Titt, U., Koehler, A.M., et al., 2002. Measurement of neutron dose equivalent to proton therapy patients outside of the proton radiation field. Nucl. Instr. Meth. Phys. Res. A476, 429–434.

Yang, T.C., Craise, L.M., Mei, M.T. et al., 1985. Neoplastic cell transformation by heavy charged particles. Radiat. Res. 104, S177–S187.

Yang, T.C., Mei, M., George, K.A., et al.. 1996. DNA damage and repair in oncogenic transformation by heavy ion radiation. Adv. Space Res. 18, 149–158.

Yashima, H., Uwamino, Y., Iwase, H., et al., 2004a. Cross sections for the production of residual nuclides by high-energy heavy ions. Nucl. Instr. Meth. Phys. Res. B226, 243–263.

Yashima, H., Uwamino, Y., Iwase, H., et al., 2003. Measurement and calculation of radioactivities of spallation products by high-energy heavy ions. Radiochim. Acta 91, 689–696.

Yashima, H., Uwamino, Y., Sugita, H., et al., 2002. Projectile dependence of radioactive spallation products induced in copper by high-energy heavy ions. Phys. Rev. C66, 044607.

Yashima, H., Uwamino, Y., Sugita, H., et al., 2004b. Induced radioactivity in Cu targets produced by high-energy heavy ions and the corresponding estimated photon dose rates. Radiat. Prot. Dosim. 112, 195–208.

Yonai, S., Matsufuji, N., Kanai, T., et al., 2008. Measurement of neutron ambient dose equivalent in passive carbon-ion and proton radiotherapies. Med. Phys. 35, 4782–4792.

Yonai, S., Matsufuji, N., Kanai, T., 2009. Monte Carlo study on secondary neutron in passive carbon-ion radiotherapy: Identification of the main source and reduction in the secondary neutron dose. Med. Phys. 36, 4830–4839.

Yonai, S., Kase, Y., Matsufuji, N., et al., 2010. Measurement of absorbed dose, quality factor and dose equivalent in water phantom outside of the irradiation field in passive carbon-ion and proton radiotherapies. Med. Phys. 37, 4046–4055.

Zacharatou Jarlskog, C., Lee, C., Bolch, W.E., et al., 2008. Assessment of organ specific neutron equivalent doses in proton therapy using computational whole-body age-dependent voxel phantoms. Phys. Med. Biol. 53, 693–717.

Zacharatou Jarlskog, C., Paganetti, H., 2008. Risk of developing second cancer from neutron dose in proton therapy as function of field characteristics, organ, and patient age. Int. J. Radiat. Oncol. Biol. Phys. 72, 228–235.

Zankl, M., Panzer, W., Petoussi-Henss, N., et al., 1995. Organ doses for children from computed tomographic examinations. Radiat. Prot. Dosim. 57, 393–396.

Zheng, Y., Newhauser, W., Fontenot, J., et al., 2007. Monte Carlo study of neutron dose equivalent during passive scattering proton therapy. Phys. Med. Biol. 52, 4481–4496.